Groundwater modelling of a coastal semi-arid hydrogeological system

Dissertation

Doctoral thesis approved in fulfilment of the requirements

for the degree of Doktor-Ingenieur(Dr.-Ing.) at the

Department of Material and Earth Sciences

Institute for Applied Geosciences

Technische Universität Darmstadt

TECHNISCHE
UNIVERSITÄT
DARMSTADT

Submitted by

Christos Pouliaris, M.Sc.

born on 05.04.1987 in Athens, Greece

Date of thesis submission: 14.03.2019
Date of examination: 10.10.2019

Thesis approved by

Supervisor Prof. Dr. Christoph Schüth
Co-Supervisor Prof. Dr.-Ing. Andreas Kallioras

Darmstadt, 22th October 2019

D17

Board of Examiners

Head:	Prof. Dr. Hans-Joachim Kleebe
Supervisor:	Prof. Dr. Christoph Schüth
Co-Supervisor:	Prof. Dr.-Ing. Andreas Kallioras
Examiner:	Prof. Dr.-Ing. Boris Lehmann
Examiner:	Prof. Dr.-Ing. Jochen Hack

Darmstadt 10. October2019

Pouliaris, Christos: Groundwater modelling of a coastal semi-arid hydrogeological system
Darmstadt, Technische Universität Darmstadt,
Year thesis published in TUprints 2019
URN: urn:nbn:de:tuda-tuprints-91953
Date of the viva voce 10.10.19

Christos Pouliaris
Matriculation Number: 2661256

Doctoral Thesis
Title: "Groundwater modelling of a coastal semi-arid hydrogeological system"

Submitted: 12 November 2019

Supervisor: Prof. Dr. Christoph Schüth

Co-Supervisor: Prof. Dr.-Ing. Andreas Kallioras

Declaration

I hereby declare that the presented dissertation is based on original research and is the result of my own work. I certify that this dissertation contains no material which has been accepted for the award of any other degree in my name, in any university or other tertiary institution and, to the best of my knowledge and belief, contains no material previously published or written by another person, except where due reference has been made in the text.

Darmstadt, at 21 November 2019

Contents

List of Figures

List of Tables

Abstract

The present study involved the development of a groundwater flow model for the evaluation of different MAR scenarios at the coastal plain of Lavrio, Greece.

In the initial steps of the study, an identification of the principal elements of the hydrological cycle and their interrelation was performed, using extended literature review and a series of activities in the field. The main hydrological processes taking place were identified and data that would later be used at the groundwater flow model building were collected.

Following that, a groundwater flow model was built for the coastal hydrosystem of Lavrio. The data collected in the previous step was used as an input. The primary goal of the model was to have a qualitative, at least, estimation of the dynamics between the two aquifer systems that are present in the area and the adjacent sea. The sensitivity analysis of the model was thoroughly done and drove to a robust parameter estimation process.

In the final step, a model that focused on the karstic aquifer was built. Elements that characterize the karstic system of Lavrio were additionally collected and implemented in the previous model. A sensitivity analysis of the different parts of the different components of the aquifer was performed in order to identify the parts of the model that play a significant role in the model performance. The aim of the model was to pinpoint these essentials and propose a new methodology for obtaining such data.

The work was done under the umbrella of the MARSOL FP7 Project (Managed Aquifer Recharge as SOLution to Water Scarcity and Drought, Grant No. , 2013-2016) and parts of this work can be found in the following list of publications:

Papers in International Journals (peer-reviewed)

- **Pouliaris C.**, Perdikaki M., Foglia L., Schüth C., Kallioras A. 2018. Hydrodynamic analysis of a Mediterranean aquifer system with the use of hydrochemical and isotopical analysis as supporting tools, Environmental Earth Sciences, 77 (6), 237, https://doi.org/10.1007/s12665-018-7418-2

Papers in International Conferences (peer-reviewed)

- **Pouliaris C.**, Perdikaki M., Vasileiou E., Foglia L., Apostolopoulos G., Schüth C., Kallioras A. 2015. Conceptual hydrogeological model of a coastal hydrogeological system in the Mediterranean Basin, 13th Conference of the Greek Hydrotechnical Association , Athens, Greece, pp. 313-319 [in Greek]**.**
- Perdikaki M., **Pouliaris C.,** Stathopoulos N., Vasileiou E., Schüth C., Kallioras A. 2014. Application of GALDIT vulnerability index for the coastal phreatic aquifer of Thoricos, Greece, 10th International Hydrogeological Congress of Greece, Thessaloniki, Greece

Poster presentations

- Mitropapas A., **Pouliaris C.,** Apostolopoulos G., Vasileiou E., Schüth C., Vienken T., Dietrich P., Kallioras A. 2016. Conceptual hydrogeological model of a coastal hydrosystem in the Mediterranean, Geophysical Research Abstracts Vol. 18, EGU 2016-17174, EGU General Assembly 2016, Vienna, Austria.
- **Pouliaris C.,** Perdikaki M., Karalemas N., Apostolopoulos G., Foglia L., Kallioras A., Schüth C. 2015. Characterization of a coastal karstic system in the Mediterranean region, 42th Congress of the International Association of Hydrogeologists, Rome, Italy.
- **Pouliaris C.,** Schumann P., Danneberg N. C., Foglia L., Kallioras A., Schüth C. 2015. Conceptual model of a coastal hydrosystem in a semi-arid environment subjected to the climate change: The case of Lavrion, Greece, Geophysical Research Abstracts Vol. 17, EGU 2015-12729, EGU General Assembly 2015, Vienna, Austria.

Acknowledgments

Having reached at a point where a work that took a fair amount of time has come to an end, it is inevitable to look back and make an overall evaluation. Such long processes are always a mixture of good and bad days, along with correct and false decisions. Self motivation, along with the aid from other people is the driving force that can keep someone moving. To these people I have to express my gratitude now that this manuscript is submitted.

To Christoph Schüth, for having the willingness to provide advice and solutions in problems of every nature. His support throughout the whole period of this study has been critical and for that I am grateful.

To Andreas Kallioras, for always having faith in me and for providing both scientific and, most of all, ethical guidance. The present work is certainly something that would be a lot more difficult without his mentoring.

To Laura Foglia, for always having the time and the ideas to help during this long period of research. Her contribution has been critical and for this I am thankful.

I would also like to thank Matthias Hinderer and Jochen Hack for participating in the committee.

I would also like to thank all my colleagues, both from the Technical University of Darmstadt and the National Technical University of Athens for their support during my studies. Working with all those people has been a privilege and an honor for me.

Finally, finishing this long process would not b easy without the support of my family throughout all these years.

1 Introduction

The present study, focusing in Lavrio, Greece, includes an extended literature review, collection of primary data the field, monitoring of physical and chemical parameters, evaluation of existing and recorded data, aquifer characterization and various modelling applications. The conceptual structure, results and general output of the study is presented and discussed in the following sections.

1.1 Background of the study

Coastal areas have been inhabited since the beginning of known history by humans due to the favourable climatic conditions (milder winters and lower precipitation), the availability of resources (fishery, agriculture etc.) and other environmental parameters (e.g. easier to build infrastructure etc.). The primary resource needed for every kind of activity, of course, is fresh water. Its availability has always been of paramount importance, since assuring the fresh water resources in an area provided a reliable building ground for every other activity. In coastal areas the primary fresh water resource is groundwater, with rivers also a possibility in regions where the capacity of the surface water network is sufficient for the coverage of at least a fraction of the fresh water demand. The need for high quality water in large volumes for the various water uses has added much stress to the water bodies (Custodio, 2010). Agriculture has invariably had the highest demand in fresh water, contributing in the growth of local societies, but with the accompanied drawback of the depletion of the groundwater reserves due to bad planning. The development of modern cities has also caused a disturbance in the hydrological cycle due to the introduction of relatively impervious surfaces in a large extend. However, the installation of water distribution networks (drinking water and wastewater) in large cities has also proven to be an unexpected source of recharge for groundwater due to network losses. This figure has had positive effects in the groundwater quantity in the case when the losses originated from the drinking water distribution network and negative results in the groundwater quality when the source was the wastewater network.

An additional component to the hydrological cycle in the coastal areas is, of course, the sea. Seawater intrusion has been a major issue in those areas, with the main reason being the poorly planned (if any) water resources management scheme in regional scale. In most cases, the demand for fresh water has led the people working in agriculture to built private wells/drills in close proximity with each other and without having any protection zones around their infrastructure. This resulted in the overexploitation of the aquifers and the drop of the water table. Consequently, the seawater has

intruded the aquifer systems and saline water has been mixed with fresh water. The result is in many cases permanent, since the remediation of such areas is a rather complicatedtask, both in terms of the physical system (time needed for the system to respond) and financial feasibility. In the end, the situation that is shaped leads people to start importing water from other regions to cover drinking, agricultural and commercial needs, else a water shortage is created, lowering the growth rate potential that a region has due to out - flowing funds.

1.2 Aquifer types and their characteristics

In general, aquifers are categorized depending on the characteristics of the water flow. The main categories are the granular, fractured and karstic aquifers. The karstic aquifers are the evolution of fractured aquifers, where the process of karstification took place, ending up in an environment where the water flows primarily in preferential flow paths (fractures/conduits) of various open areas. With the exception of karstic aquifers, the other types of aquifers cannot fall in between those categories.

Apart from the type of flow, the aquifers are also categorized depending on the hydraulic pressure regime, which, on a second level, also affects the type of flow. Aquifers can be characterized either as confined, when there is an impermeable layer covering the permeable aquifer layer, or unconfined when the confining layer does not exist and a free (i.e. not restricted by a top layer) piezometric surface, called water table, is formed. Aquifers with mixed characteristics of the aforementioned two also exist and are called leaky aquifers.

1.2.1 Granular aquifers

The granular aquifers, built of material with various grain sizes and chemical composition, are the ones that were, in principal, mainly exploited. This trend is a result of both practical and technical reasons. Hand dug wells were easier to build in this type of aquifers when the need for digging very deep was not necessary, while the lack of tools and technical knowledge to exploit the other types of aquifers may have contributed to the reasons why granular aquifers have been favoured for a long time. Groundwater flow in the saturated zone is well described, while many exploration and investigation methods have been developed and optimized in the context of granular aquifers. The flow is considered to be undisturbed and, in general, laminar due to the fact that these aquifers are conceptualized as being homogeneous and isotropic, at least at a regional scale. The overexploitation

of such aquifers has eventually led to the need to explore and exploit other types of aquifers, such as karstic aquifers.

1.2.2 Karstic aquifers

Karstic aquifers have different characteristics than the granular ones. The crucial factor that plays a determinant role in the way the water moves in the aquifer is the level of karstification. This factor is actually very hard to approach and estimate, since it is affected by a great number of other parameters (climatic conditions, chemical composition of rain, regional tectonic regime etc.) and it is site specific, making it very hard to have a general rule or method to evaluate the level of karstification. The formations at which the karstic aquifers are naturally developed have a primary network of fractures that form preferential pathways for groundwater. Furthermore, the karstification results in the widening of those fissure/fractures and the formation of conduits where the flow conditions are more similar to that of a pipe (either open or closed, depending on the amount of water that is in the pipe). The interconnection between all those preferential flow pathways, along with the interexchange relationship with the water that is in the matrix of the formation, create a complex flow environment (Figure 1-1) that is very difficult both to comprehend and to put in mathematical equations. On occasions, the response of such an aquifer is very irregular (Pouliaris et al., 2018) and great approximations have to be taken when studying such systems. High groundwater flow velocities that could easily reach hundreds of meters per day have also been recorded (Binet et al., 2017), while low storage times are also a typical feature. These characteristics push the limits of the validity of Darcy's law, where all the groundwater flow theory is based, making karstic systems very difficult to approach theoretically. Nevertheless, the karstic aquifers are considered to be a reliable source since the storage capacity can be quite large, although these aquifers certainly have a high vulnerability and can be easily contaminated.

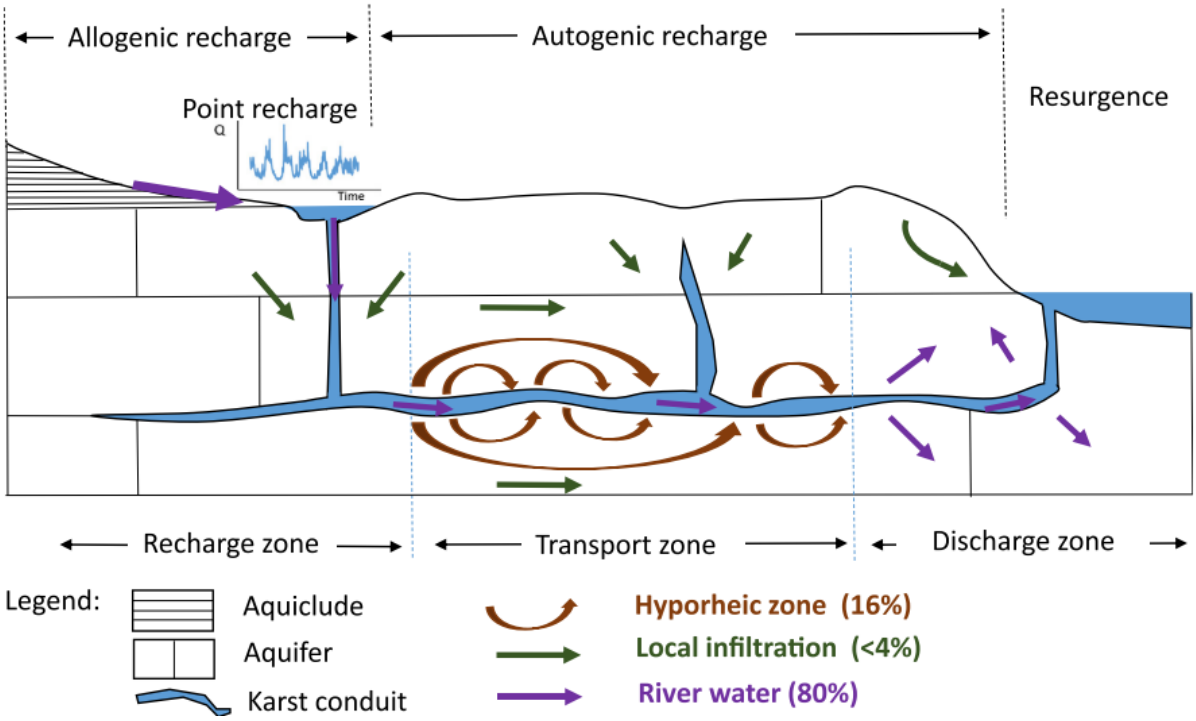

Figure 1-1: Conceptual model of groundwater flow within a coastal karstic aquifer (Binet et al., 2017).

1.3 Modelling of groundwater flow in aquifers

Research involving modelling applications in coastal areas has become more and more utilized throughout the years in order to assess the groundwater resources management and exploitation (Javadi et al., 2015), especially under the prism of the continuous growth of technology and computational capacity, which has been a major step forward in modelling applications. Many of those studies have been based on the use of the MODFLOW code, or at least on one of the versions of MODFLOW, since it has been already available since 1988 (McDonald and Harbaugh, 1988). MODFLOW 2005 (Harbaugh, 2005) has been a long lasting version of the code and has been heavily utilized, even later, when other versions became available (LGR, CFP, FMP etc.).

The majority of modelling applications have, in general, been done for granular aquifers (e.g. in El Yaouti et al., 2008; Kallioras et al., 2010; Cobaner et al., 2012; De Filippis et al., 2016). The reasons for this are many; the coastal aquifers have been heavily utilized, as mentioned before, and the need to have a conceptualization of such systems has been vital when strategic plans for water recourses management became necessary. However, one of the main reasons is that MODFLOW is a code that uses the mathematical equation of the saturated flow in porous media, also assuming that the water has constant density (Harbaugh, 2005). Later, flow in the unsaturated zone has also been implemented in MODFLOW, making the code capable of involving another major component of

subsurface hydrology. Heterogeneity, both in the vertical and the horizontal direction, can be added to the model, although, especially in the case of horizontal heterogeneity, this is quite rare due to common lack of high resolution spatial data for the various aquifers.

1.3.1 Overall approaches in modelling of coastal hydrosystems

The process of seawater intrusion has been modelled mainly using three approaches. The first one (Bakker et al., 2013) simulates a sharp interface between the fresh and saline water (Figure 1-2). This method can definitely give a good approximation of the dynamics of this interface but it is based on a strong simplification of the physical system, since, in the natural system, there is actually a transition zone between the fresh and the saline water. This approach is still used today (e.g. Chang and Yeh, 2010; Szymkiewicz et al., 2018) and it may be useful in models where the seawater intrusion has to be somehow integrated in the simulation, but the process is not modelled explicitly.

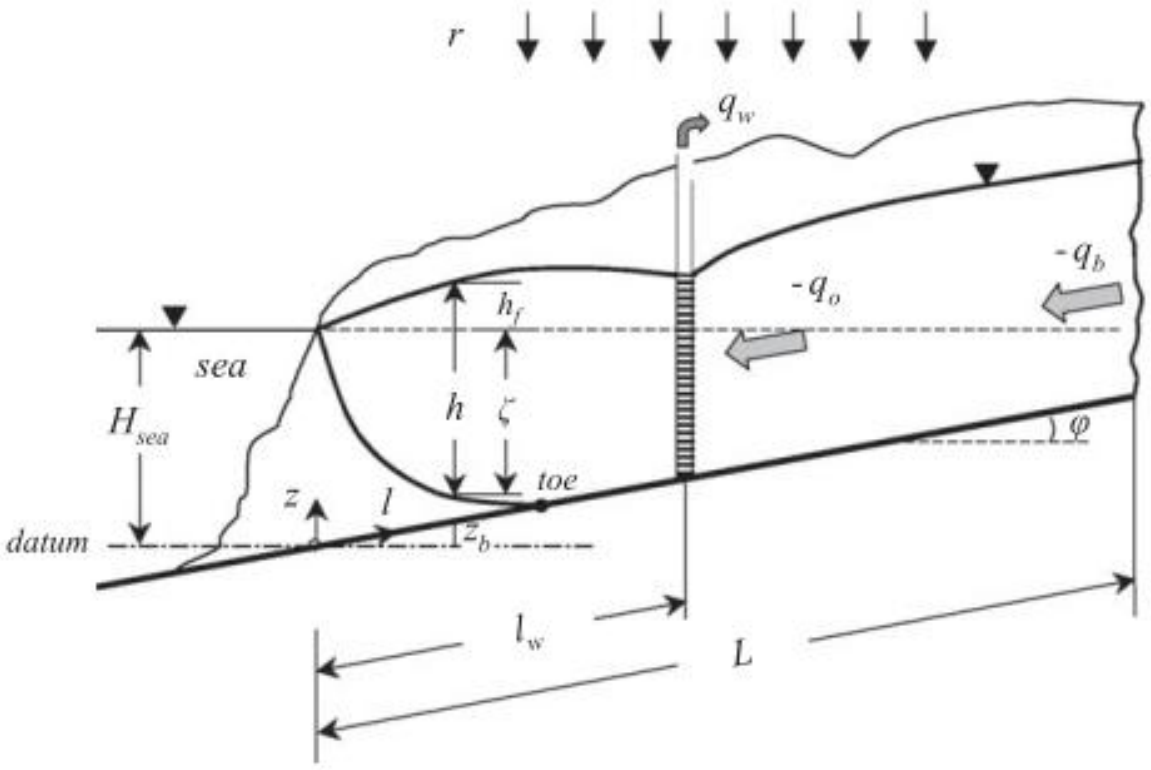

Figure 1-2: Conceptual model of seawater intrusion, using the sharp interface approach, in coastal aquifers, where pumping is involved (Koussis et al. 2012).

In the second approach (Langevin et al., 2008) the difference is that the density of the fresh and the saline water is taken into account when solving the groundwater flow equation(Shoemaker, 2004; Qahman and Larabi, 2006; Lin et al., 2009; Langevin and Zygnerski, 2013; Romanazzi et al., 2015; De

Filippis et al., 2016; Siarkos and Latinopoulos, 2016), making this approach a more sophisticated one, yet difficult to handle due to high non linearity, especially when many of the hydrosystems' components are implemented (Figure 1-3). However, this is considered to be the most scientifically accurate way to simulate seawater intrusion in coastal aquifers (Kourakos and Mantoglou, 2015).

The last approach is based on analytical solutions of the problem (Mantoglou, 2003; Kacimov and Sherif, 2006; Koussis et al., 2012). These models can vary in terms of the level of complexity and the way they are built is non standard, making them useful probably only in specific sites. Analysing further this type of approach is far from the scope of the present study.

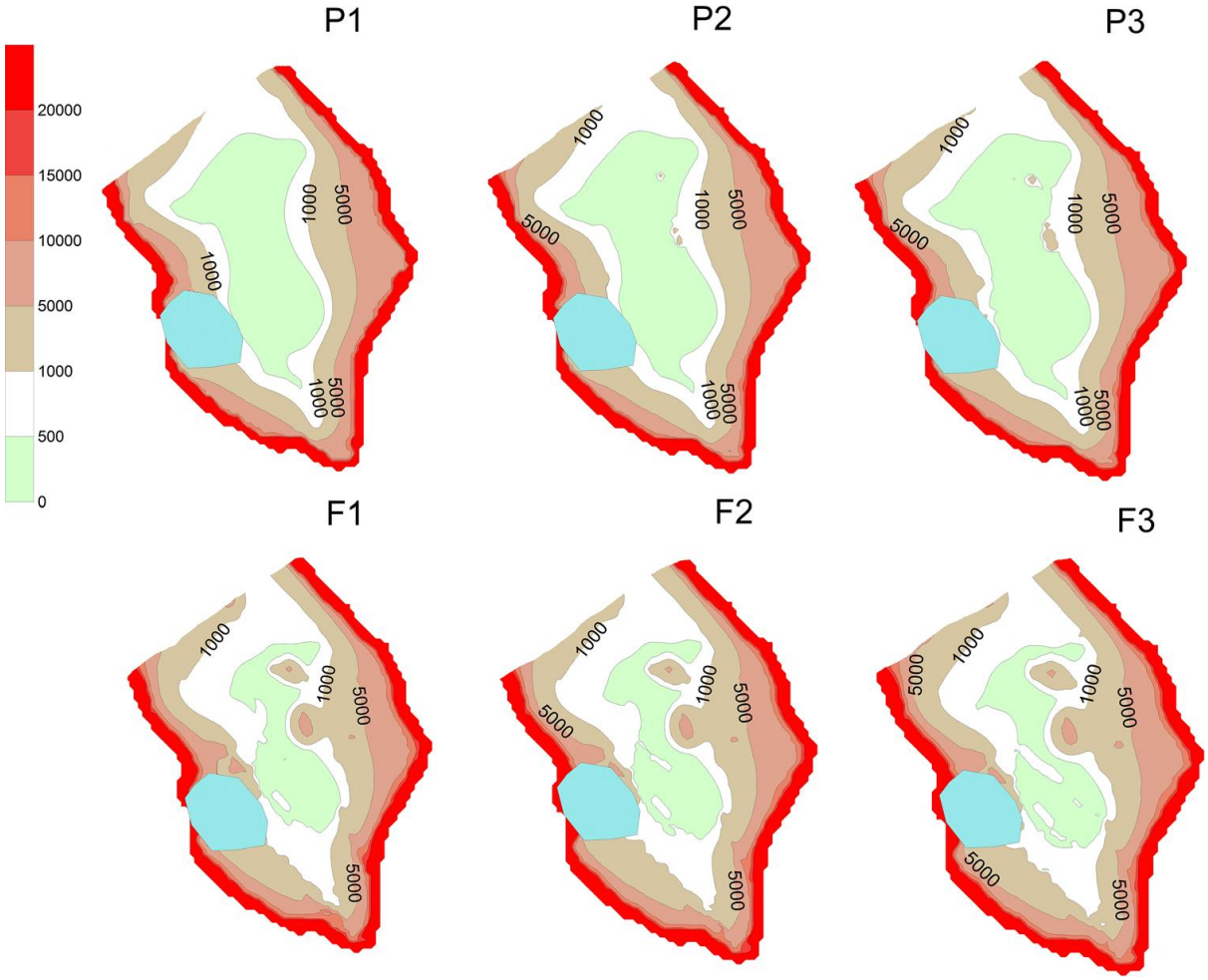

Figure 1-3: Past (P1-P3) and future (F1-F3) salinity maps for different exploitation scenarios of a coastal aquifer (Romanazzi et al., 2015, the values presented are in mg/l).

1.3.2 Modelling of flow in karstic aquifers

Modelling activities have also been held in coastal karstic aquifers. A major differentiation of those aquifers is that the principal components of the hydrological cycle (runoff, infiltration and evapotranspiration) have much different contribution than in the granular aquifers. The recharge assessment in such aquifers is one of the most important parameters since the percentage of precipitation that actually reaches the water table is very high, unlike runoff, which is practically zero when no surface water network is developed in karstic regions. Environmental isotopes have been used on some occasions (Aquilina et al., 2005; Barbieri et al., 2005; Praamsma et al., 2009; Binet et al., 2017) to investigate groundwater recharge, while other methods, such as geophysical investigations (Chalikakis et al., 2011) and even combinations of existing methodologies (Guardiola-Albert et al., 2014) have also been utilized. Balance models have also been used in the opposite direction, i.e. to approximate the recharge in the karstic aquifer, either in large (Hartmann et al., 2015) or regional scale (Fleury et al., 2007; Andreo et al., 2008; Hartmann et al., 2013).

The groundwater flow conditions, as described above, become even more complicated when seawater is also involved. Efforts to have a well defined method to assess the flow conditions in the karstic aquifer (Figure 1-4 a and b), with the fracture/conduit network included, have been made (Worthington, 2009; Geyer et al., 2013; Jeannin et al., 2013; Oehlmann et al., 2013; Malard et al., 2015), but their requirements in input data make them difficult to use. Methods to delineate the fracture networks and implement them into the models were also developed (Figure 1-5), but more global applications of those approaches are not yet available. For that reason, traditional MODFLOW approaches in karstic aquifers have been used in the literature (Panagopoulos, 2012; Abusaada and Sauter, 2013), even in combination with other mathematical codes (Rozos and Koutsoyiannis, 2006). Some modelling applications also involve the impact of climate change along with the seawater intrusion process (Romanazzi et al., 2015), while there are studies that also introduce the flow in conduits along with seawater intrusion modelling (Xu et al., 2018).

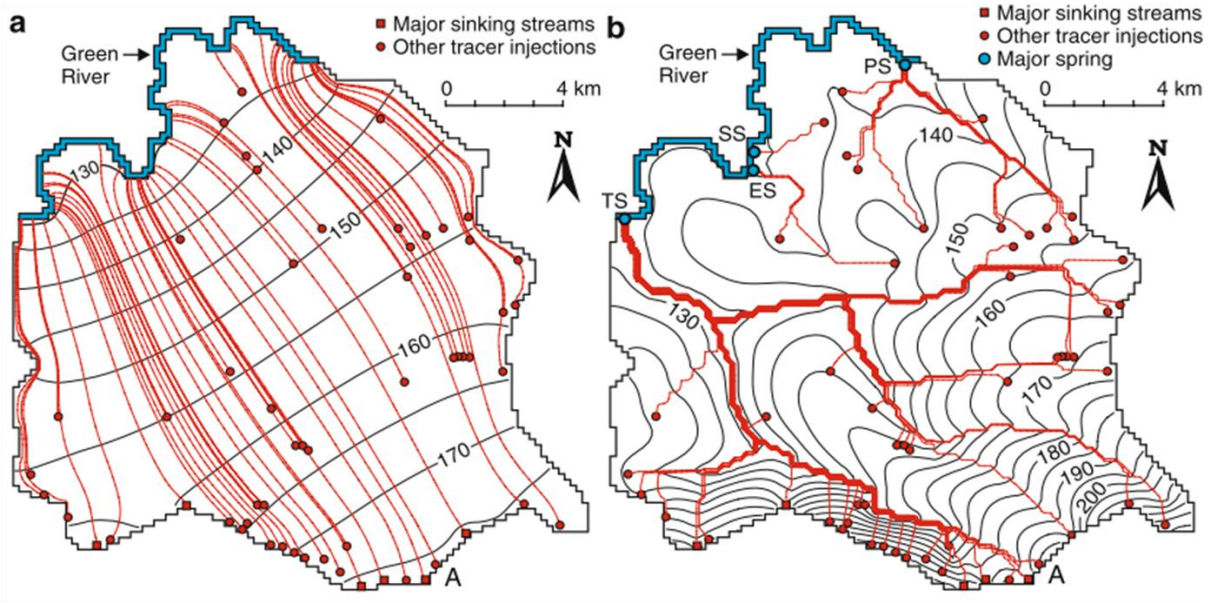

Figure 1-4: Comparison of simulated hydraulic heads using a) a conventional MODFLOW approach and b) high hydraulic conductivity zones (Worthington, 2009).

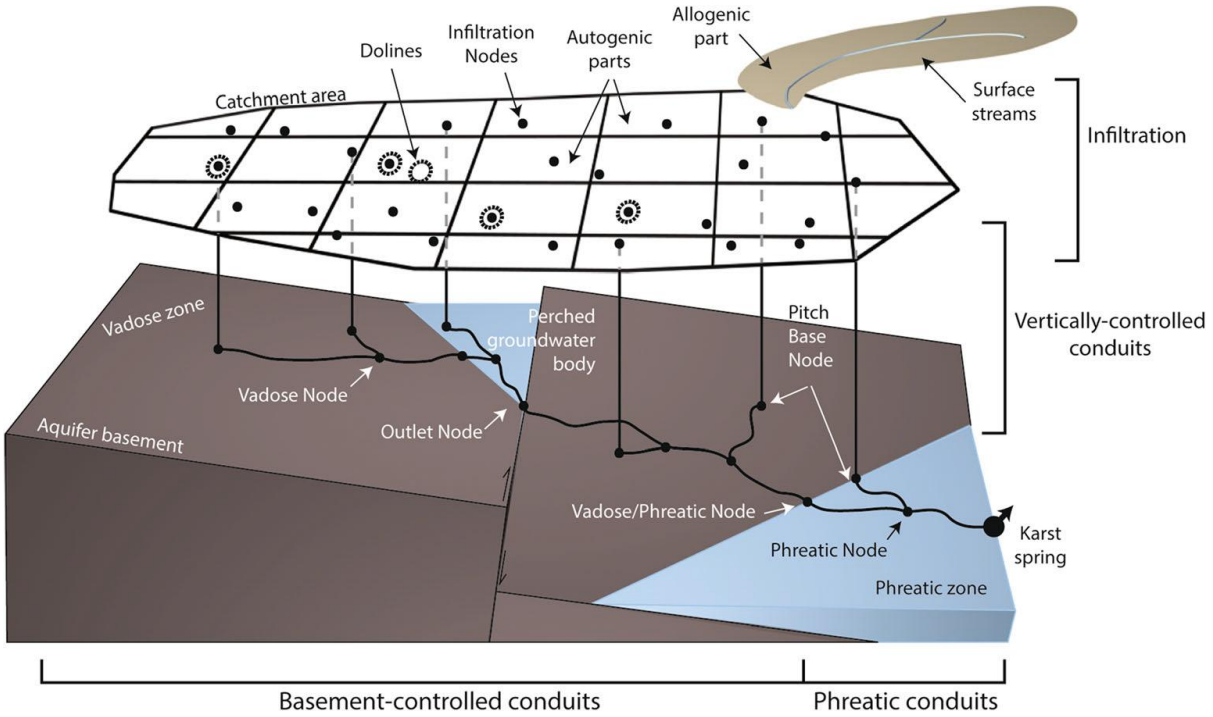

Figure 1-5: Integration of a karstic conduit network to a groundwater flow model using the KARSYS method (Malard et al., 2015).

1.3.3 Boundary conditions at the coast

The general trend in the literature, for a long period of time, is that the boundary condition at the coast is represented using a constant head boundary. This could be a simplification since the seawater level is constantly changing and this has an effect on the hydrodynamics of the coastal system (Figure 1-6). However, such changes have been implemented in the models in case studies where the seawater level fluctuation is monitored (El Yaouti et al., 2008 using MODFLOW, Amir et al., 2013; Sefelnasr and Sherif, 2014 using FEFLOW).

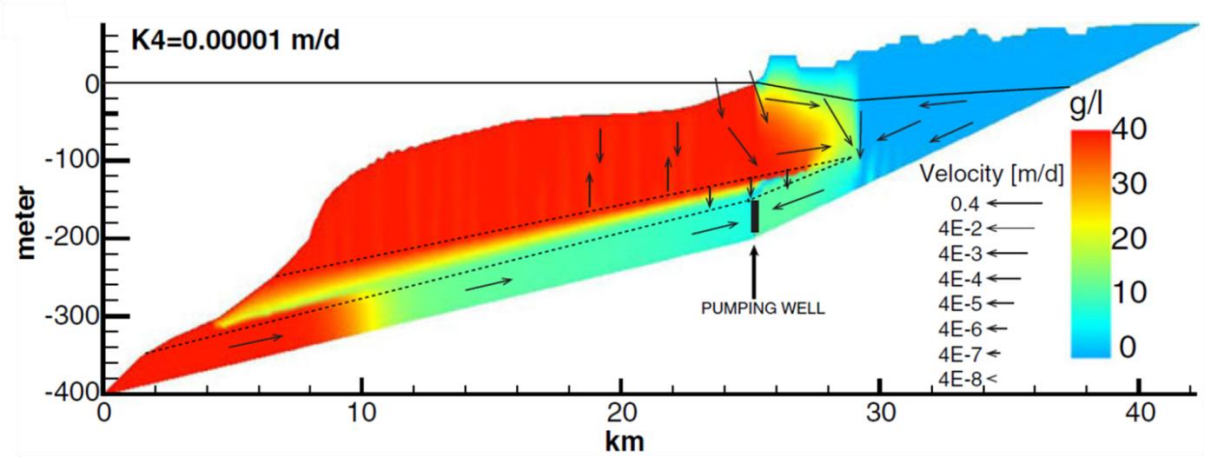

Figure 1-6: Simulation results of pumping in a coastal aquifer system (Amir et al., 2013).

The constant head boundary condition has been extensively used over time in numerous studies (Shoemaker, 2004; Qahman and Larabi, 2006; Datta et al., 2009; Lin et al., 2009; Langevin and Zygnerski, 2013; Lu et al., 2015; Romanazzi et al., 2015; De Filippis et al., 2016; Siarkos and Latinopoulos, 2016 just to name a few). This general trend has found some alternatives recently, where the long established way of treatment for the coastal boundary as an undeniable 0 m constant head at the coast, is disputed. The need to have a better representation of the natural system has led to the need of different approaches for different sites. Examples involve the use of alternative heads for the various layers of the aquifers that are in contact with the sea (De Filippis et al., 2017), or the use of general head, rather than a constant head, boundary condition representing the coast (Hanson et al., 2014).

As it seems, the better understanding of the conceptual model of an area leads to the need of a more complex representation of the coastal boundary. This might be even more enhanced at sites where there is also submarine groundwater discharge (Figure 1-7) since the groundwater flow model inevitably has to be expanded towards the sea. However, the implication of many different

components with high detail into a groundwater flow model in the initial stages can lead to impracticalities. In that case, any biased results can be affected by the later developed need to both have a successfully running simulation and handle the amount of information produced by the models.

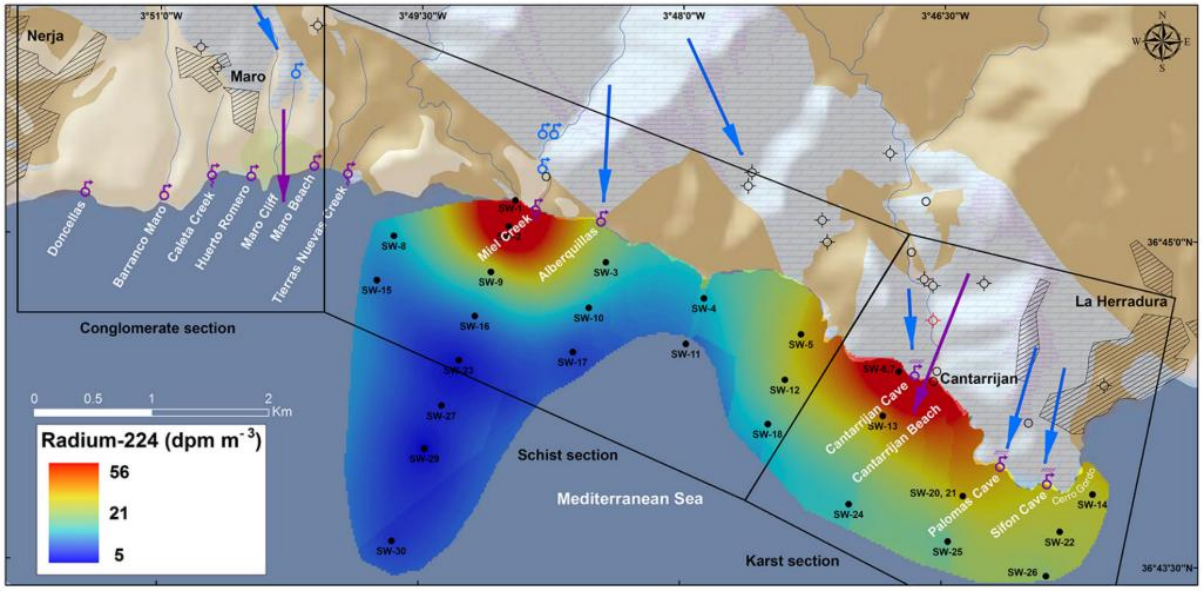

Figure 1-7: Point submarine discharge identified from radium concentrations in seawater (Montiel et al., 2018).

1.3.4 Codes available for simulating groundwater flow

Apart from MODFLOW, the code FEFLOW (Diersch, 2005) has been used in numerous occasions, some of them also dealing with coastal aquifers and seawater intrusion (e.g. in Gossel et al., 2010; Amir et al., 2013; Sefelnasr and Sherif, 2014; Levanon et al., 2017). The codes' main difference is the way the analysis of the flow equation is developed spatially; MODFLOW uses a finite difference approach while FEFLOW a finite element approach. Both have been heavily used in comparison with other codes that either do or do not have an explicit representation of the karstic features (Table 1). MODFLOW still dominates the field though, partly because of the long establishment and the continuous support and development provided by the USGS. Still, advantages and disadvantages do exist in all codes, but this is an issue that is not within the scope of the present study.

Table 1: Available codes for simulating flow in karstic aquifers (apart from MODFLOW).

Code	Reference	Explicit karstic representation
OpenGeoSys	Kolditz et al., 2015	No
KARSTAQUIFER	Kaufmann, 2016	Yes
COMSOL Multiphysics	COMSOL, 2018	No
CAVE	Liedl et al., 2003	Yes

Other codes that have been used for karstic aquifer flow modelling and are based on MODFLOW 2005 include MODFLOW DCM (Sun et al., 2005), MODFLOW CFP (Shoemaker et al., 2007) and MODFLOW NLFP (Mayaud et al., 2015). The approaches differ in the representation of the karstic processes. The codes either use a dual conductivity approach for the conduits and the formation matrix (DCM), or assess the non linearity of the flow by using Forchheimer's equation (NLFP) or explicitly introduce the large karstic conduits as linear elements (CFP). Although with the use of such codes the special characteristics of the flow can be determined and incorporated in the models, the increased complexity and, in many cases, lack of those characteristics can prevent modellers from using them. Finally, in large scales, these local differentiations from the general flow patterns are usually neglected, resulting on a simplification that, on the other hand, may well serve the purpose that the model has been developed for.

2 The wider area of Lavrio and its regional characteristics

2.1 Description of the study area

The city of Lavrio is located in the southeast coast of the Attica peninsula (Greece), within the wider area of Lavreotiki (Figure 2-1). The study area has an extent of approximately 60 km^2, with a Mediterranean climate. In the past the area around Lavrio has been extensively mined, with the focus being around silver and lead. This exploitation has already started from the Neolithic period and it seized only in 1865, when the company that had the last factory shut down.

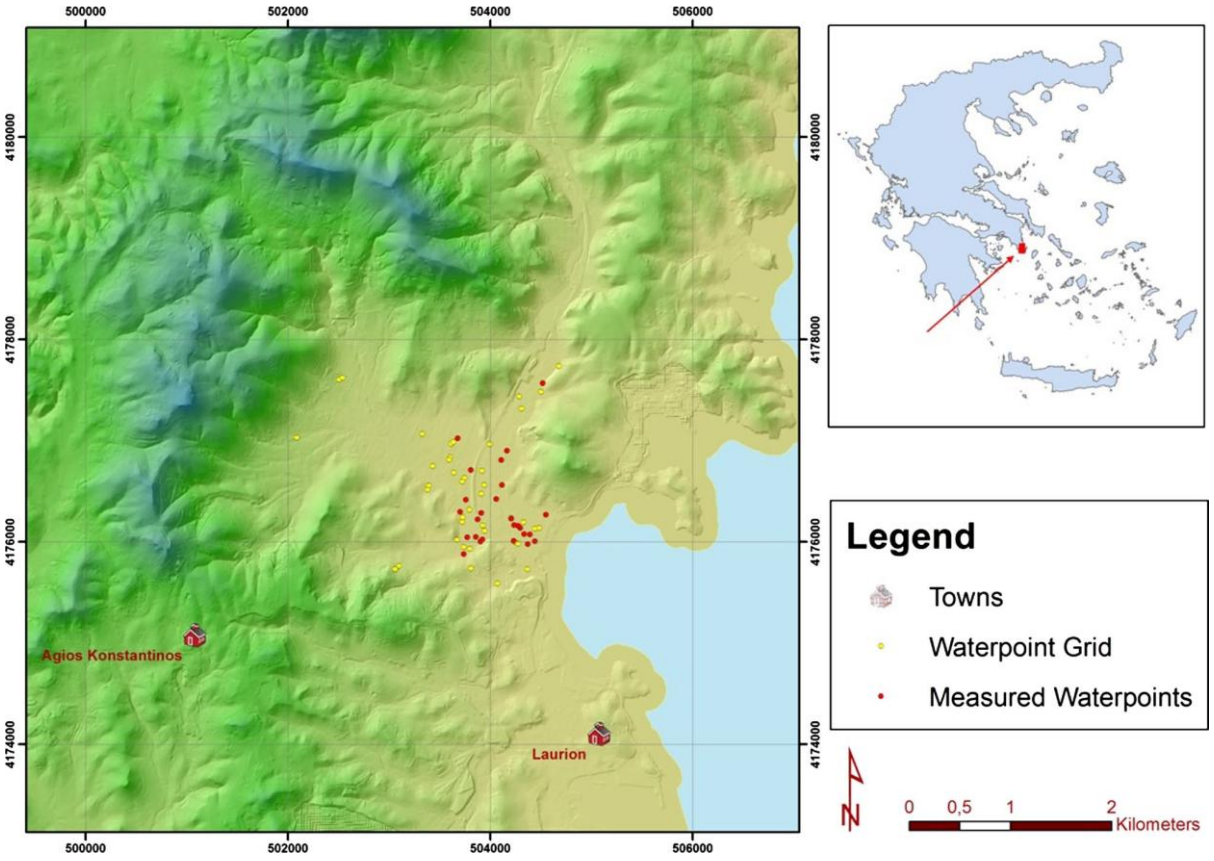

Figure 2-1: Geographical location of the study area.

The interest around groundwater resources management in the area is high, since there are many stresses in the system, with the main groundwater demand coming from agriculture and drinking water supply. In the past, the karstic aquifer has been exploited for drinking water purposes, while the irrigation demand has been covered by the alluvial aquifer until 1984. The increase of the population, though, along with the expansion of human activities increased the demand for drinking

water. The intensive pumping resulted in depletion of the water reservoirs and, eventually, to the effect of seawater intrusion in both aquifers. This had also bilateral effects, because water from other external sources had to be used, increasing the cost of agricultural activities and, inevitably, the cost of the products produced. Given that, the remediation of the aquifers around Lavrio would improve the ecosystemical services provided by the aquifers, having a positive effect, not only on the environment but also on the financial growth of the area.

2.1.1 Climatic data for the study area

The only meteorological station that is in the area vicinity is the Lavrio Port Meteorological Station (LPMT, National Observatory of Athens) and has daily available data since 01/10/2008 (Figure 2-2). Another set of data has been acquired from the Public Power Corporation S.A., which operated a station in the area during the period 1970 - 1996.

The mean annual temperature, according to this data, is 19.1 °C, although the values vary from 38.7 °C in August to 1.4 °C in February. This results in having mild winters and hot dry summers in Lavrio. Regarding the precipitation, the annual average is 377 mm, but this figure also varies throughout the years (e.g. the 257 mm for 2010 and the 496 mm for 2015). The major rain events are not evenly distributed in the year, with most rain falling between October and April, and the summer period being almost entirely dry. In both datasets, a general lowering of precipitation is identified as the general trend (Figure 2-3), marking the fact that the availability of freshwater is, overall, becoming lower. This has also a straight effect to the amount of groundwater that is exploited. The evapotranspiration, as in other parts of the country (Paparrizos et al., 2014) reaches its maximum during the period between May and September, when there is also the highest water demand. Evapotranspiration can also be enhanced due to the high wind speed (Allen et al. 1998), which in the case of Lavrio can reach up to 40 km/h Centre for Renewable Energy Sources and Saving, 2001). Researchers have categorized the climate of the whole Attica peninsula as semi-arid (Bajocco et al. 2012; Kargas et al. 2012; Nastos et al. 2013; Moussoulis et al. 2015), making the management of water resources in the area an issue of paramount importance.

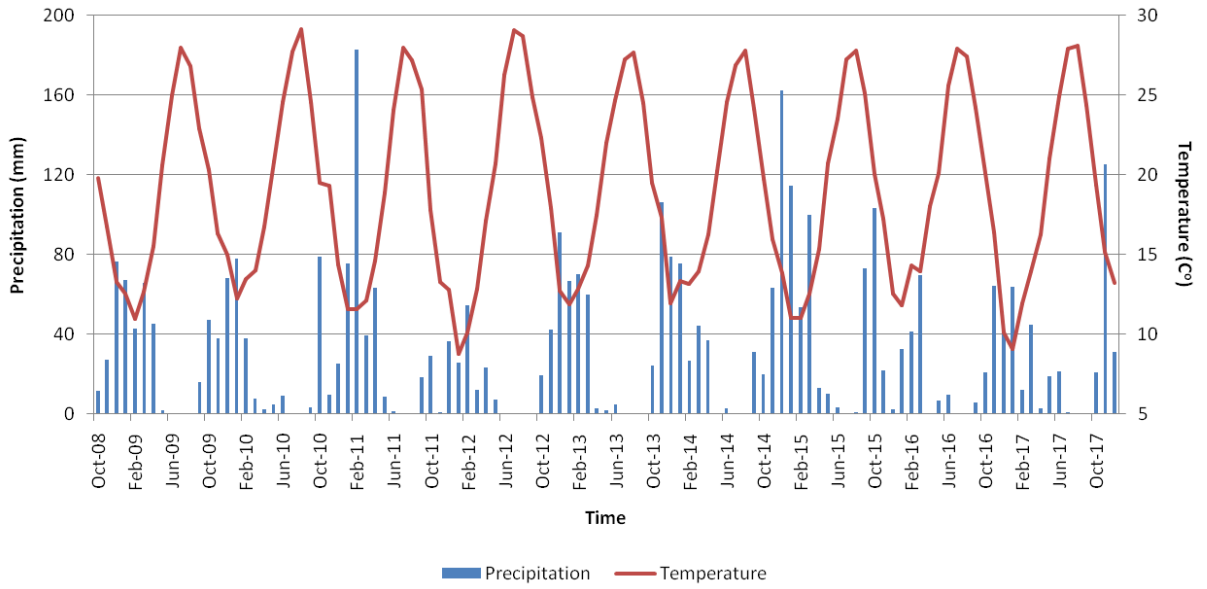

Figure 2-2: Meteorological data taken from the meteorological station at the port of Lavrio.

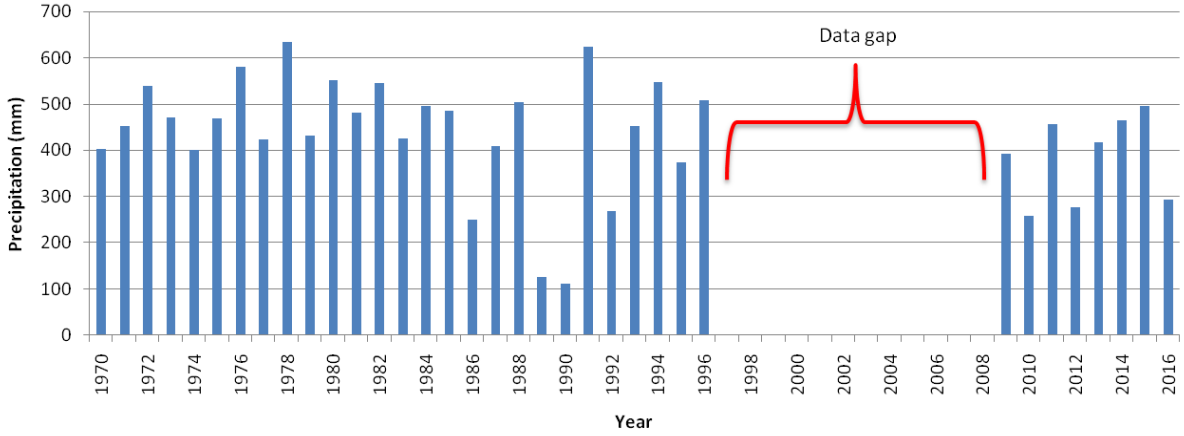

Figure 2-3: Precipitation graph that summarizes rain data from both meteorological stations.

2.1.2 Geological setting

The geological structure of the wider Lavrio area has been an area of research for many decades, due to the fact that the ore deposits present in the area were of great importance and mining activities have been active even since the classical times (Kakavogiannis, 2005). Despite these efforts, a final widely accepted theory on the geological evolution of the Lavrio area is not reached, with researchers having conflicting views on important aspects of the topic. Ongoing study of the area is taking into account these opposite views (e.g. Scheffer et al., 2015 and references therein. Here, a summary of the geological structure is presented in order to define the general setting. The nomenclature used in many of the studies (Marinos and Petrascheck, 1956; Stamatis et al., 2001; Skarpelis, 2007; Baziotis, 2008; Skarpelis et al., 2008; Baziotis et al., 2009; Liati et al., 2009; Baziotis

and Mposkos, 2011; Berger et al., 2013; Liati et al., 2013) is utilized, while the structure is based on these references and the geological maps published by the Institute of Geological and Mineral Exploration (IGME, 2003; 2007, Figure 2-4), and on field observations that took place during the MARSOL project related field work.

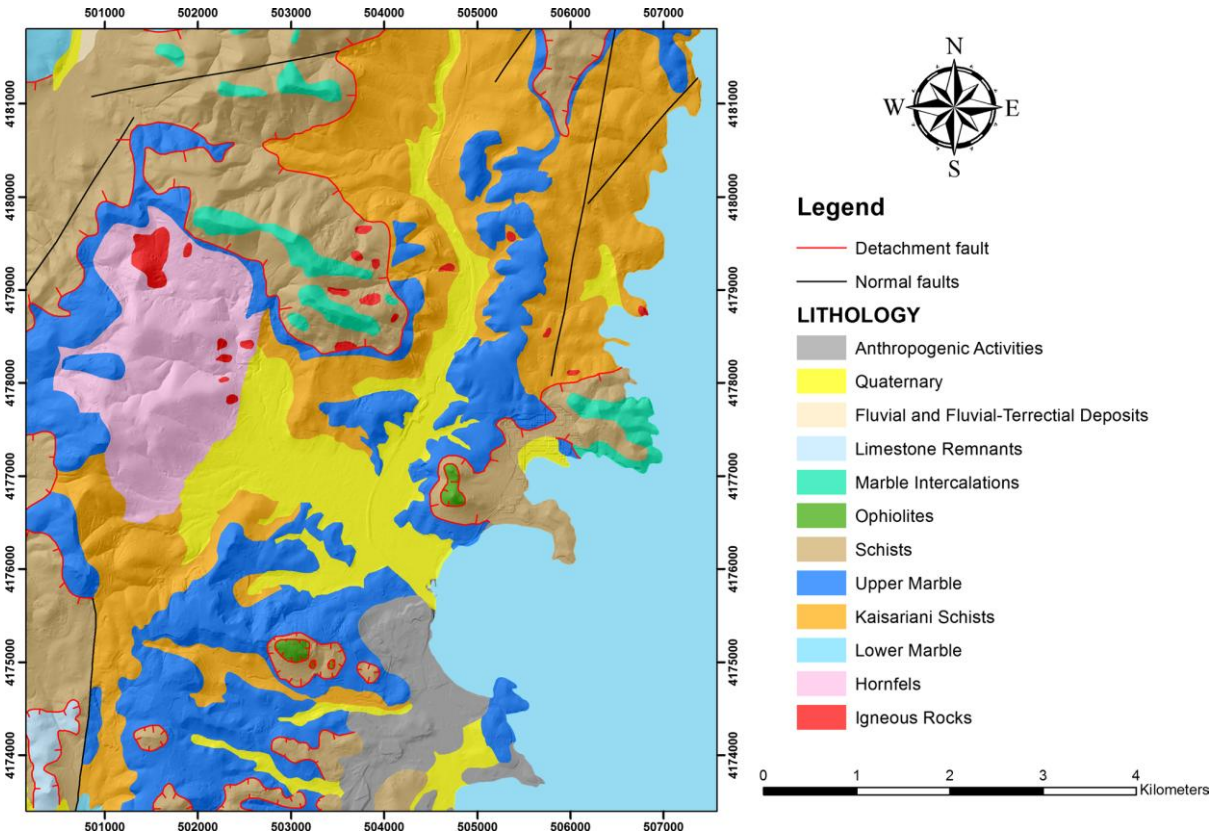

Figure 2-4: Geological map of the study area (based on IGME 2003; 2007, with modifications).

The study area constitutes of three major geological groups; the Lower Unit, the Upper Unit, and the Neogene — Quaternary deposits. The Lower Tectonic Unit (LTU, also found in the literature as the Kamariza Unit) in Lavrio is represented by three layers. At the bottom, the Lower Marble formation is a 400 m thick sequence of marble (IGME, 2003), mainly present at the southwestern part of the area. Above it there is a thick sequence of schists, named either Kaisariani or Kamariza schists in the literature. On the top of the LTU there is the Upper Marble formation which is a highly karstified and, at the same time, mylonitized marble. For the LTU there is also the theory that there is just one marble formation that is above the Kaisariani schists and that the folding patterns and/or normal faulting are responsible for having the marble below and above the schists (Avdis, 1990; Photiades and Carras, 2001; Baziotis, 2008).

The Upper Tectonic Unit (UTU, also described as the Lavrio Unit) consists of phengite – chlorite - epidote schists that are mainly metapelites and metasandstones, forming blueschists and greenschists (Baziotis et al., 2009) with some marble intercalations. Some small metabasalt bodies are also present in the UTU (Baziotis et al., 2009). Locally, above the UTU, limestone remnants of Upper Jurassic age are found, with this formation being assigned to the non - metamorphic (Photiades and Carras, 2001; Scheffer et al., 2015) Sub-Pelagonian Tectonic Unit.

On top of the stratigraphic column, recent alluvial deposits are covering both the LTU and UTU. The alluvial deposits are of Neogene - Quaternary age (Alexakis, 2011) and are consisted mainly of silty material. Adjacent and into the small streams that are present in the area, the material becomes coarser. The thickness of the formation varies from a few meters up to around 20 m in the central part of the alluvial valley.

An igneous intrusion is also present in the area. The intrusion is in the LTU and it is a granodiorite, with the intrusion time being approximately 15 - 9 Ma (Baziotis, 2008; Skarpelis et al., 2008). The main minerals that characterize the intrusion are quartz, plagioclase, K-feldspar and biotite, while minerals like zircon and apatite are also present (Voudouris et al., 2008). Dykes also originate from the intrusive body, which is placed approximately 4 km below the surface (Tsokas et al., 1998), and are spread throughout the area. This intrusion is the source of the Pb-Zn-Ag rich ore deposits in the area. The metalliferous minerals are pyrite, sphalerite, galena, and tetrahedrite - tennantite (the latter two Ag rich), but other sulphuric salts (e.g. pyrargite, lillianite) are present (Voudouris et al., 2008; Skarpelis and Argyraki, 2009). The ore is found in skarn, veins or skarn-free carbonite replacement (Voudouris et al., 2008). The age of the intrusion is 8.34 ± 0.2 Ma (Liati et al., 2009).

The contact between the LTU and the UTU and its nature is one of the key points where there is a big controversy between scientists. The contact is undoubtedly tectonic, but the debate on its kinetics is still ongoing. Some researchers support that the contact is a thrust fault while the majority interprets the contact as a thrust fault that has evolved to a low angle extensional detachment fault under the present tectonic regime in the Aegean (Scheffer et al., 2015 and references therein). Other normal faults are also present in UTU and not in the LTU (IGME, 2003; 2007; Scheffer et al., 2015).

2.2 Field investigations in the alluvial plain

During the MARSOL project, a series of field investigations were done in order to have a more complete idea of the spatial extend and depth of the alluvial plain in Lavrio. Additionally, the aim was also to improve the monitoring network and scheme by installing new monitoring points. This was done because the concept of the project involved the scenario of using the alluvial aquifer at a Soil Aquifer Treatment (SAT) system. The investigations combined geophysical surveys along specified paths and drilling activities.

2.2.1 Geophysical surveys

The investigations that took place in Lavrio aimed at acquiring some information about the thickness of the alluvial formation in various locations. The method used was the Electrical Resistivity Tomography (ERT) method using a pole - dipole configuration. Apparent resistivity was measured in 8 profiles that were spread across the alluvial valley (Figure 2-5).

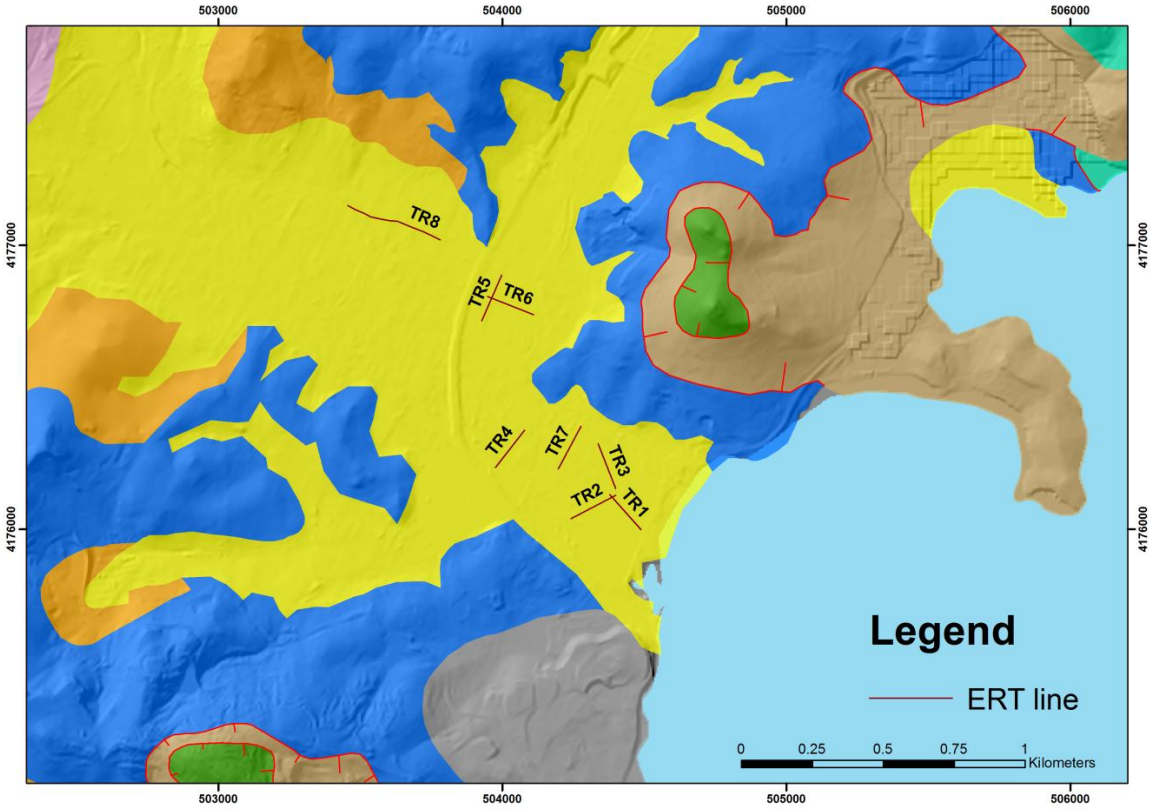

Figure 2-5: Locations of the electrical resistivity tomography (ERT) lines in the alluvial plain.

The results of the interpretation (Figure 2-6) give an insight about the geological structure and the thickness of the formations in the subsurface. In general, the thickness of the alluvial formation closer to the coast, as seen in the cross sections, is approximately 14 m (TR1, TR2 and TR3). The thickest part of the alluvium is in the center of the valley (TR4 and TR7), where the thickness varies up to 20 m in the deepest part. Although quite robust as a method, the results of the ERT can be a subject of discussion in the case of Lavrio because they are expected to be highly affected by the fact that the groundwater in the aquifer is saline, so measurements of resistivity can include a certain amount of noise in them. Nevertheless, the results of ERT have been of major importance when the next step (i.e. the planning of the Geoprobe campaign) was scheduled.

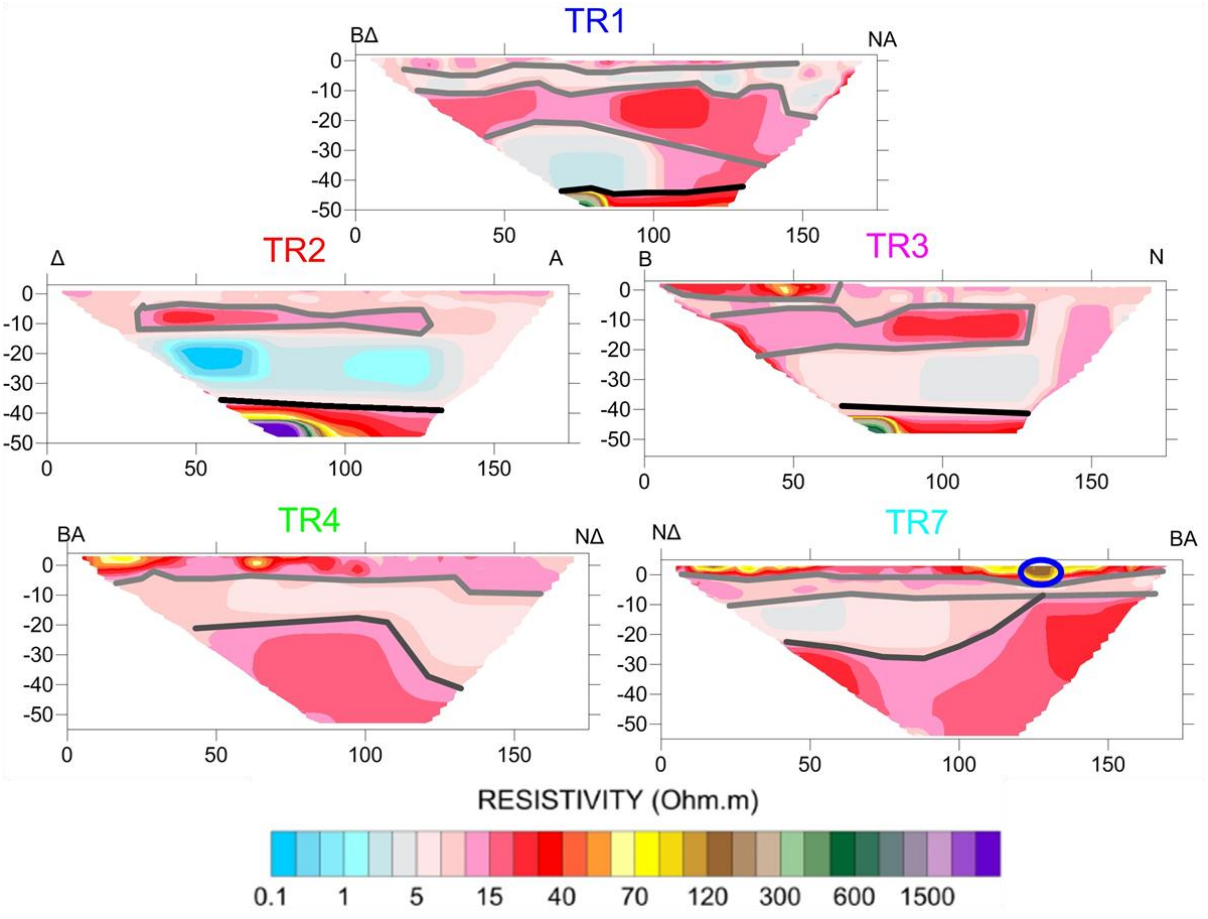

Figure 2-6: Results of the ERT survey (Apostolopoulos et al., 2014) for selected locations. The blue circle in TR7 shows what is believed to be a paleoriver.

2.2.2 Geoprobe drilling campaign

Another part of the field investigations that took place in Lavrio was done with the aid of the Helmholtz Centre of for Environmental Research (UFZ, Department of Monitoring and Exploration

Technologies), a partner in the MARSOL project. This involved the installation of piezometers in the alluvial plain in order to establish a tailored monitoring system. The need for that has also risen by the fact that the hand dug wells and drills located during the field survey were clustered closer to the coast (where the water table is closer to the surface), while elsewhere there were fewer points where measurements could be taken.

The investigations were done using the Geoprobe direct push drilling machine (Figure 2-7). The sequence involved an initial investigation to do the electrical conductivity (EC) profiling and then the installation of the piezometer was performed.

Figure 2-7: The Geoprobe direct push drill was used to install the piezometers and perform the electrical conductivity profiles

Finally, EC loggings were performed and piezometers were installed at 11 points within the alluvial valley (Figure 2-8). The points were chosen in order to have a good spatial distribution and ease of access for the drilling machine. The depth at which the Geoprobe can reach depends mainly of the hardness and the consolidation level of the formations that are about to be drilled. The drilled depth is considered to be the alluvial formation thickness in the case of Lavrio because below that, either the marble or schist formations can be found. These metamorphic formations are quite hard and cannot be penetrated by the Geoprobe, so approximating the drilling depth as the alluvial thickness is a reasonable assumption.

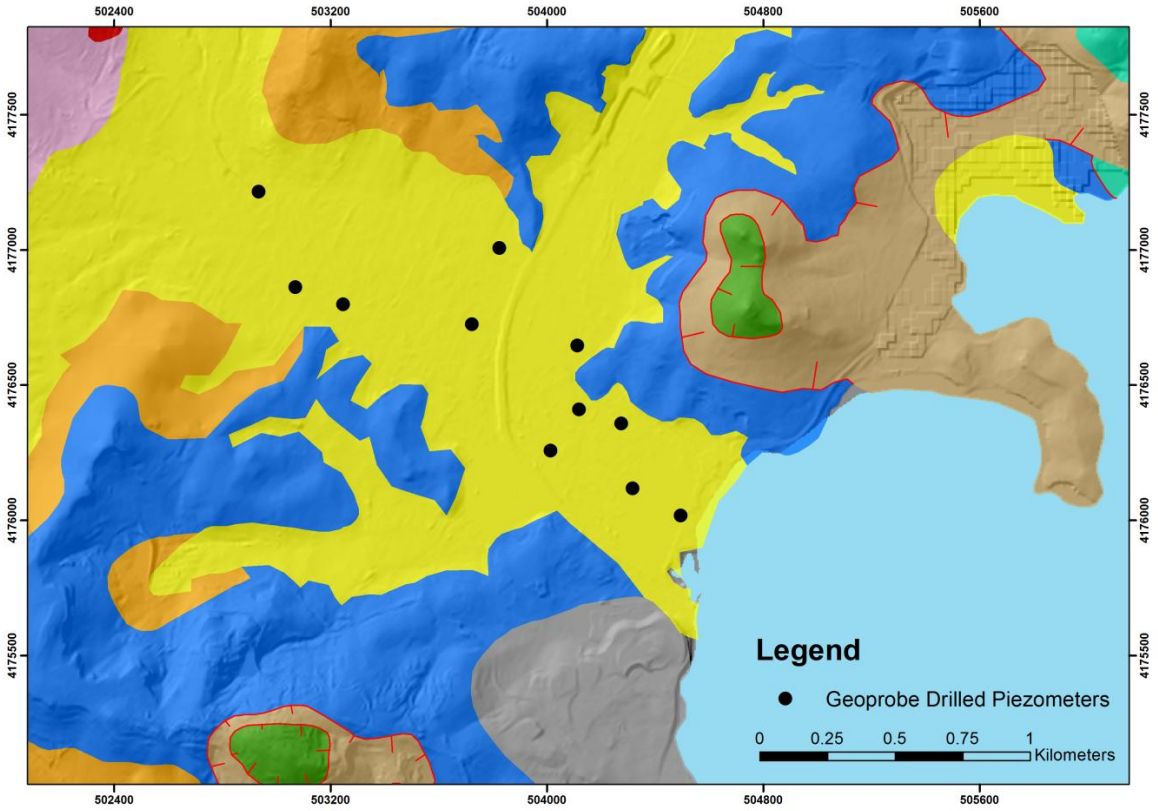

Figure 2-8: Points in the alluvial plain where the Geoprobe has installed piezometers.

The monitoring of the EC has also given some insight to the variety of the grain sizes in the alluvial formation (Figure 2-9). The general trend noticed is that there is a coarser sub-layer at the top of the formation that then transits into a finer sub-layer that extends deeper down until the formation bottom. However, it should be mentioned that the measurements are expected to be affected by the fact that the groundwater present in the aquifer has high salinity. Nevertheless, the EC loggings can give a good approximation to the lithostratigraphy of the alluvial plain.

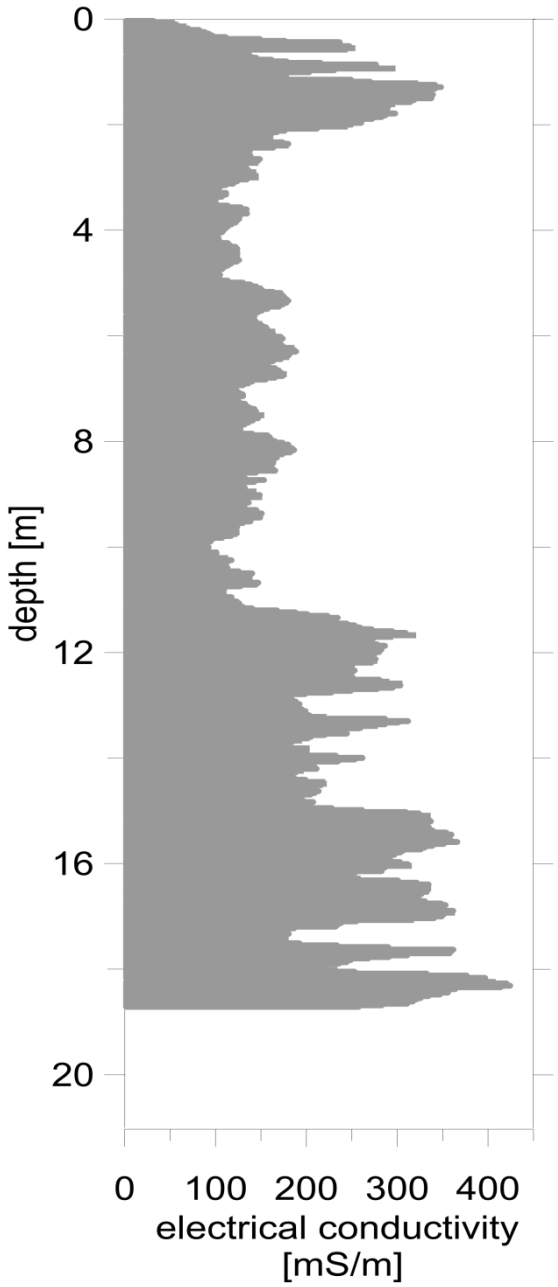

Figure 2-9: Electrical conductivity (EC) logging for one of the points in Lavrio. The changes in the values denote the transition from a coarser band (until almost 11 m depth) to a finer band until the bottom of the drill (around 18.5 m).

2.3 **Regional hydrology**

The identification of the hydrological processes taking place in a system, along with the interconnection between the system components, is of paramount importance when any kind of planning takes place. Having the base of the geological knowledge, the aquifer characteristics need to be defined in order to be able to produce a conceptual model that is representing the physical system adequately.

2.3.1 Aquifer system analysis

The background information regarding the groundwater resources in the study area has been scarce in the literature. The only available published research in the alluvial aquifer has been by Stamatis et al., (2001), where some information about the groundwater quality could be found. On the basis of that, a series of field campaigns were used to obtain data and conceive the hydrological conceptual model of the area. A monitoring network, derived from a large number of points of interest that were collected through field campaigns, literature review and other databases (Figure 2-10), was developed and used for acquiring hydraulic head data from dug wells and piezometers in the alluvial aquifer and a few drills in the karstic aquifer. The network used in order to have the optimal coverage of the study area.

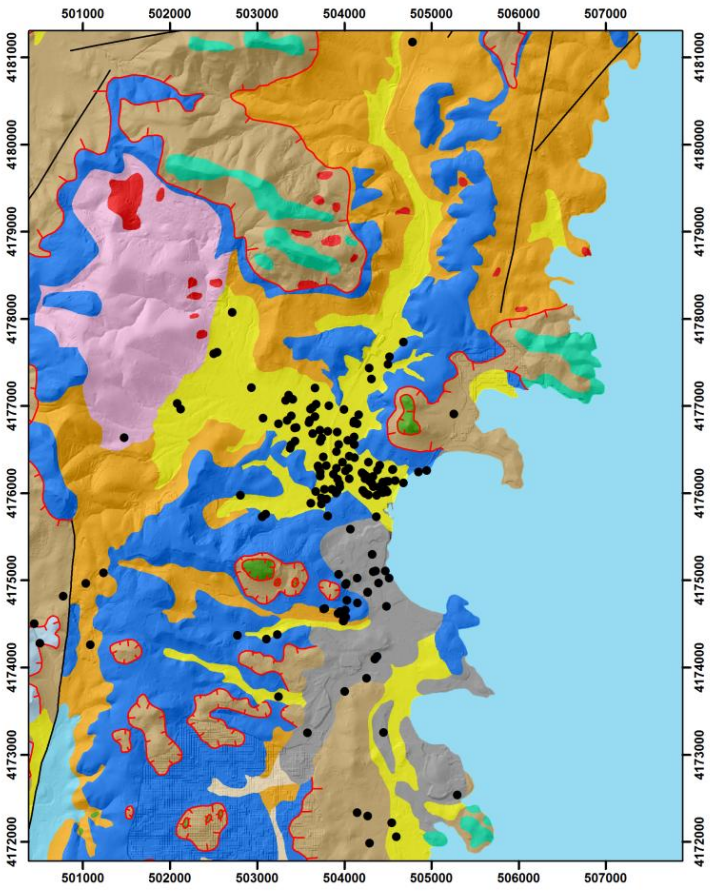

Figure 2-10: Map with all the locations where information was collected.

Regarding the surface water, in the study area the surface water network is poorly developed. The main stream course is the Keratea – Lavrio wadi which originates from the area of Keratea in the north, flows initially in an eastward direction that then changes to southward before it finally

discharges into the Thoricos Bay (Alexakis, 2011). The reason for this change in the stream direction is probably an effect coming from the tectonic regime of the area (Pavlopoulos, 1997). This stream has an ephemeral character, with flash floods occurring periodically when the precipitation is high, rapid and intense. The stream is dry for the most time of the year and this result in having no information about the behaviour of this stream due to the lack of measurements.

In the study area there are two aquifer systems that are developed within different geological formations. The characteristics of the two aquifers are presented, along with the hydraulic connection that exists between them, but also with the adjacent sea.

The upper aquifer, which is developed in Quaternary deposits, is a granular aquifer. The general flow direction is towards the southeast and it discharges to the Thoricos Bay in the east. The thickness of the alluvial formation that hosts the aquifer is from practically zero at the sides of the valley (where the geological boundary is) until up to 20 m at the center. Water from is aquifer is used to cover part of the small scale irrigation demand in the area. The pumping period is from April till September, although pumping rates are expected to have been lowered due to the quality deterioration of the groundwater.

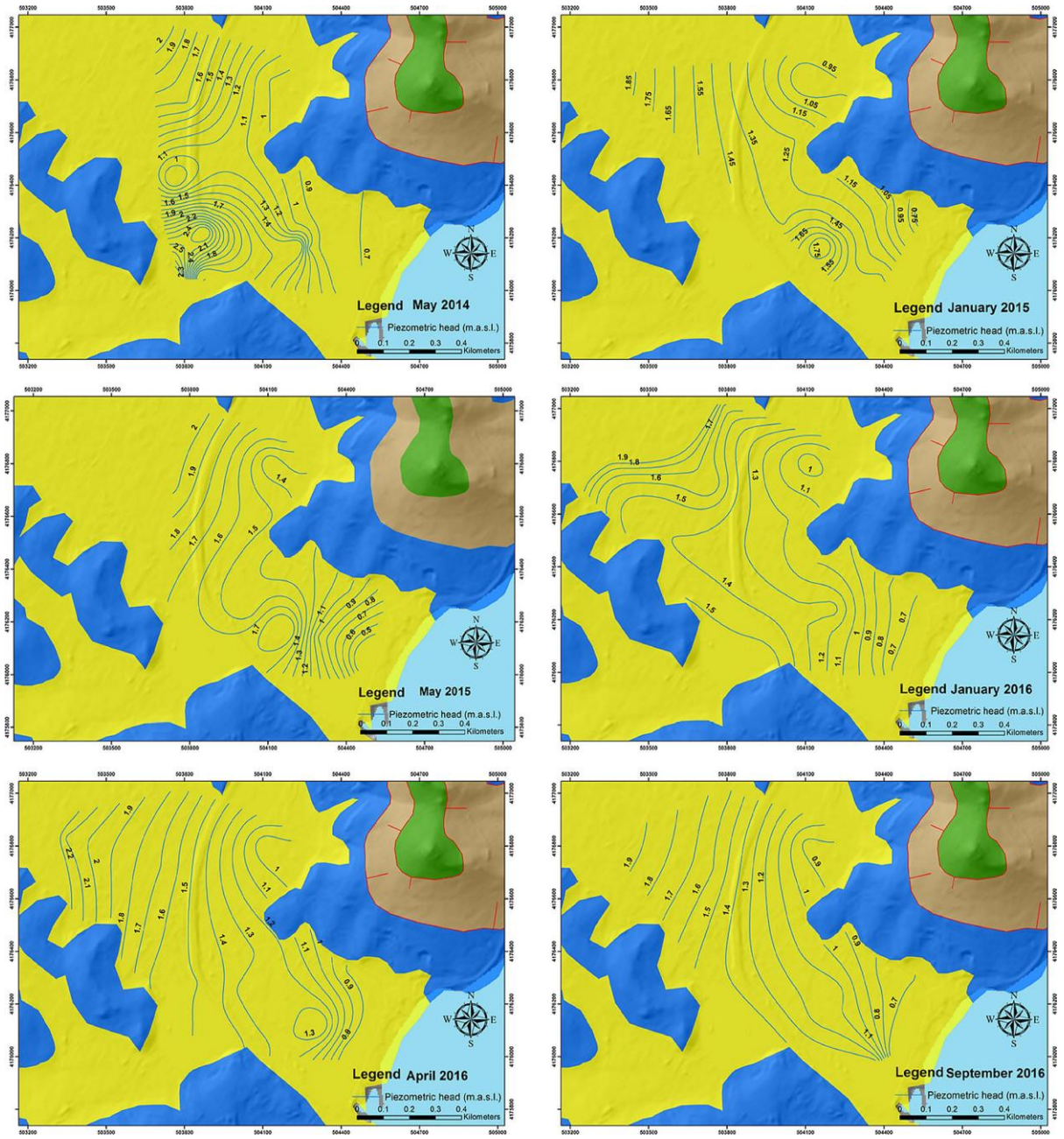

Figure 2-11: Piezometric maps of the alluvial aquifer during the field campaigns (May 2014–September 2016), covering wet and dry periods of the hydrological year.

The lower aquifer is a karstic aquifer developed in the Upper Marble Formation of the LTU. This aquifer has been used for drinking water supply for the city of Lavrio in the past but the decline in the groundwater quality due to seawater intrusion has led to the abandonment of the source. Yet water coming from that source is still used, in smaller amounts, for other purposes (e.g. irrigation of green areas). The thickness of the formation is variable and in the literature values of 150-200 m are reported (IGME, 2003; 2007). In the area around Lavrio a thickness of 50 m is considered to be a minimum, a figure that is taken from drill loggings, at points where this formation was drilled.

However, these drills only partially penetrated the formation (Koumantakis et al., 2000). The main inflow in the aquifer is recharge from the precipitation while the aquifer discharges to the sea either as diffused flow or as point discharges which have, nevertheless, small discharge rates. The exchange with the alluvial aquifer is also a part of the water balance that, in the case of the karstic aquifer, is thought to be only a small fraction of the total equilibrium.

2.3.2 Hydrogeological boundaries of the aquifers

The hydrogeological boundaries of the aquifers had to be defined in order be able to have an accurate representation of the hydrological system. In the case of the alluvial aquifer this is relatively straightforward since the hydrogeological boundaries coincide with the geological formation boundaries. In the case of the karstic aquifer though, defining such a boundary is a task that requires a more sophisticated approach. Assuming that the hydrogeological (subsurface) boundary is identical to the hydrological (surface) boundary is also an approach that could be taken. This assumption could be true in some cases but, as a general rule, it can lead to results that can vary from a minor simplification of the flow conditions to an extreme underestimation of the volumes that are exchanged between the karstic and the adjacent systems.

In the case of the karstic system in Lavrio, the fact that the marble is above a schist formation is the first important attribute. This means that the marble is hydraulically isolated from the other formations that potentially have hydrogeological significance (e.g. the Lower Marble formation). The second attribute that defines the hydrogeological boundaries is the folding patterns in the area. The combination of the two attributes delineates the hydrogeological basin of the karstic aquifer. In the northern part of the study area, the boundary was defined relatively close to the entrance of the alluvial plain (Figure 2-12 a). The fold can clearly separate the boundary of the northern section (not flowing into the study area) and the southern section (that is part of the hydrogeological equilibrium in the area). In the west, the karstic aquifer is clearly isolated from other formations that have a potential to host groundwater with the intermediate schist formation (Kaisariani schists). In the southern part, using the folding patterns was not as easy as in the north, so in that case, a different consideration had to be done. The marble formation in this area can be found in much higher altitudes and, at the same time, the thickness of the formation becomes very small. Under these circumstances, an approximation can be made and the hydrogeological boundary of the karstic aquifer in the south is defined at the point that the formation has the smallest thickness (Figure 2-12 b).

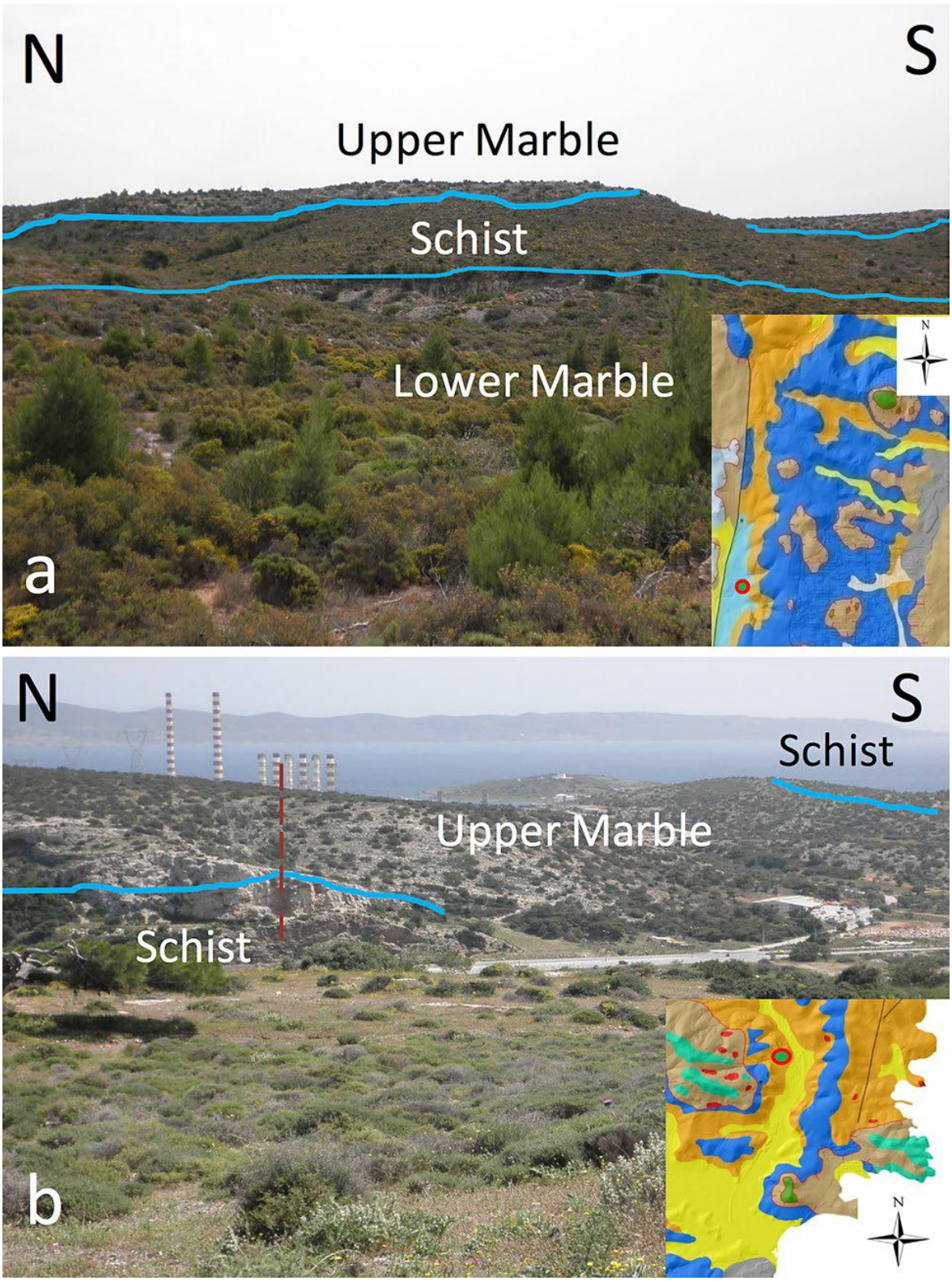

Figure 2-12: Boundaries of the hydrogeological basin as defined in the southern (a) and northern (b) part of the study area.

2.3.3 Hydrological behaviour of the karstic aquifer

The response of the karstic aquifer to precipitation events shows a relatively irregular behaviour (Figure 2-13). The drill, for which the hydraulic head data is presented, is located at a point that the marble formation outcrops and the meteorological station are approximately 1.5 km away, so a straight comparison is possible. The aquifer shows a rapid response to rain events that are approximately 40 mm/day but rain events that have a smaller precipitation height have to accumulate in order to be able to record a response in the hydraulic head. The time that is required in order to have a response recorded in the aquifer, when the events are smaller than 40 mm/day, is from 2 to 10 days approximately. Finally, the water temperature showed minor fluctuations, with a mean value of 21.7 °C in the winter and 22.3 °C in the summer. As a result, the water temperature is considered not to be a suitable parameter to trace the rain events that contribute significantly to groundwater recharge, at least in the case of Lavrio.

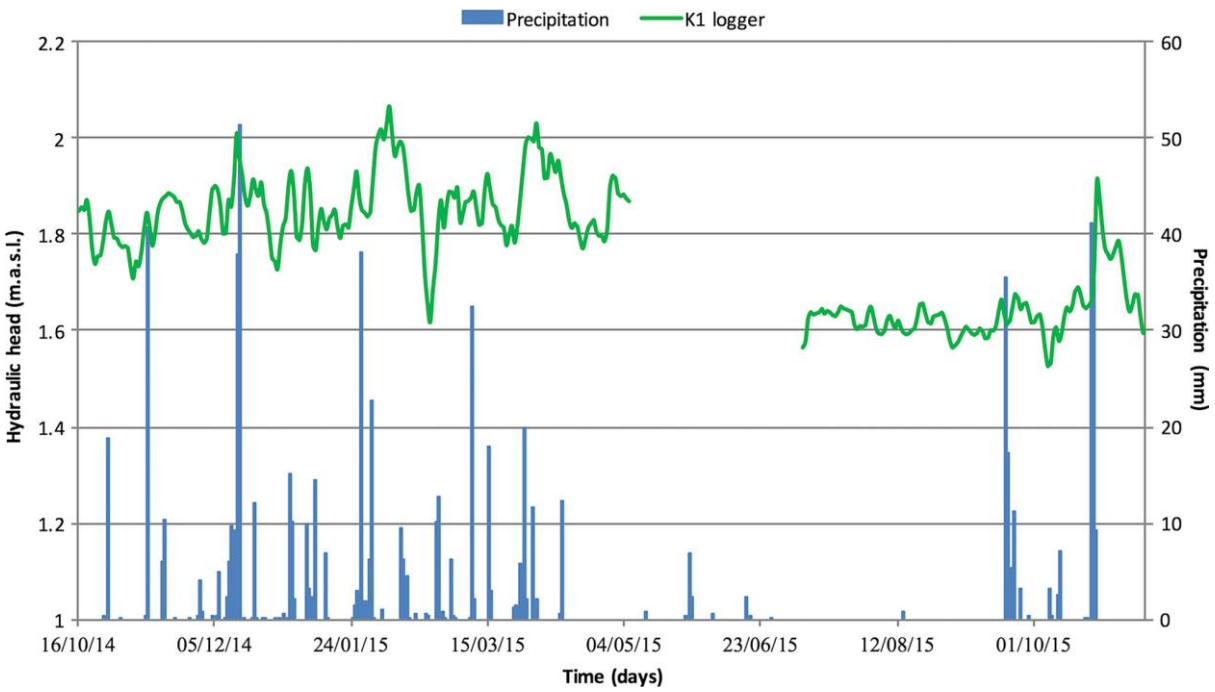

Figure 2-13: Hydraulic head fluctuations at a monitoring well drilled in the karstic aquifer (point K1).

2.3.4 Hydraulic properties of the aquifers

For the completion of the conceptual model of the study area, an estimation of the hydraulic parameters of the two aquifers had to be made. The approaches used in the two occasions differed, depending on the availability of appropriate data.

For the karstic aquifer, a series of pumping test data from a previous study (Koumantakis et al., 2000) were acquired and re-evaluated. For the managing of the data and the evaluation, the AQTESOLV 4.5 PROFESSIONAL software, distributed by HydroSOLVE Inc., was used. From the available analytical solutions, the one that was considered to be representative and appropriate to use in a karstic aquifer, is the one by Barker (1988).

The solution by Barker is developed for dual porosity aquifers (i.e. flow in the matrix and in fractures) and it is considered to be better than other methods that are used more widely (e.g. the Theis and Cooper – Jacob approximations) to interpret the pumping test results from the karstic aquifer (although, strictly speaking, the karstic aquifers have a different behaviour than the fractured aquifers). The solution, interestingly enough, also accounts for well storage and well skin effect, while the type of flow (one, two or three dimensional, Figure 2-14) is important for the final results. The output of the analysis using the Barker solution includes hydraulic parameter values for both matrix (Km and Ssm) and fracture (Kf and Sf).

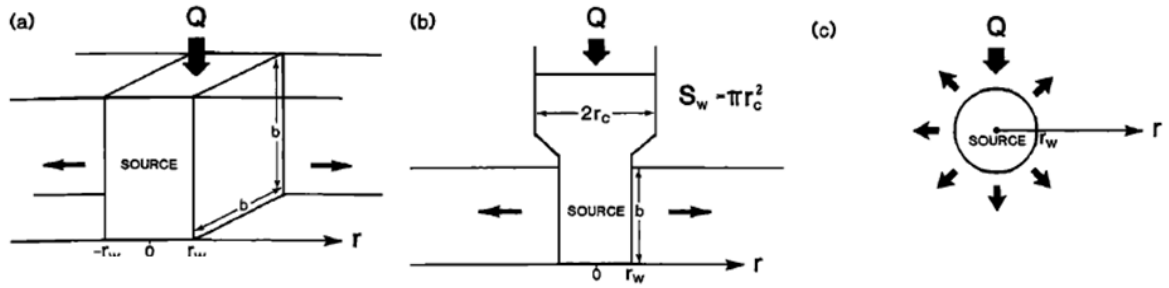

Figure 2-14: Graphical representation of the flow in one (a, planar flow), two (b, cylindrical flow) and three (c, spherical flow) dimensions (Barker, 1988).

Analyzing the available data, the fracture hydraulic conductivity (Kf) was found to vary between 30 and 310 m/day, while the matrix hydraulic conductivity (Km) varied between 1.2 X 10^{-5} and 0.46 m/day. Regarding the storage parameters, the fracture storage coefficient (Sf) was estimated between 2.29 X 10^{-7} and 7.598 X 10^{-5} while the matrix specific storativity (Ssm) between 1.8 X 10^{-4} and 0.0581 m^{-1}.

While processing the original data another interesting feature about the flow in the aquifer occurred. As seen in the time-drawdown graph (Figure 2-15b), during the time of the pumping test, after some drawdown had been achieved there was a rapid recovery of the water table. This sudden entry of water in the system could possibly be explained as follows; the difference in hydraulic head that was caused between the aquifer and the drill (due to pumping) mobilized water that was previously inert

and this water emerged in the drill. In steady state conditions (i.e. without the affection from pumping), this water is stored in fractures or small cavities in the karstified aquifer and can me mobilized at occasions (e.g. large head differences, either positive or negative with respect to the immobile water, in small areas). The flow regime of such water cannot be, of course, estimated or predicted but the knowledge that this inert water is stored in the aquifer is still important.

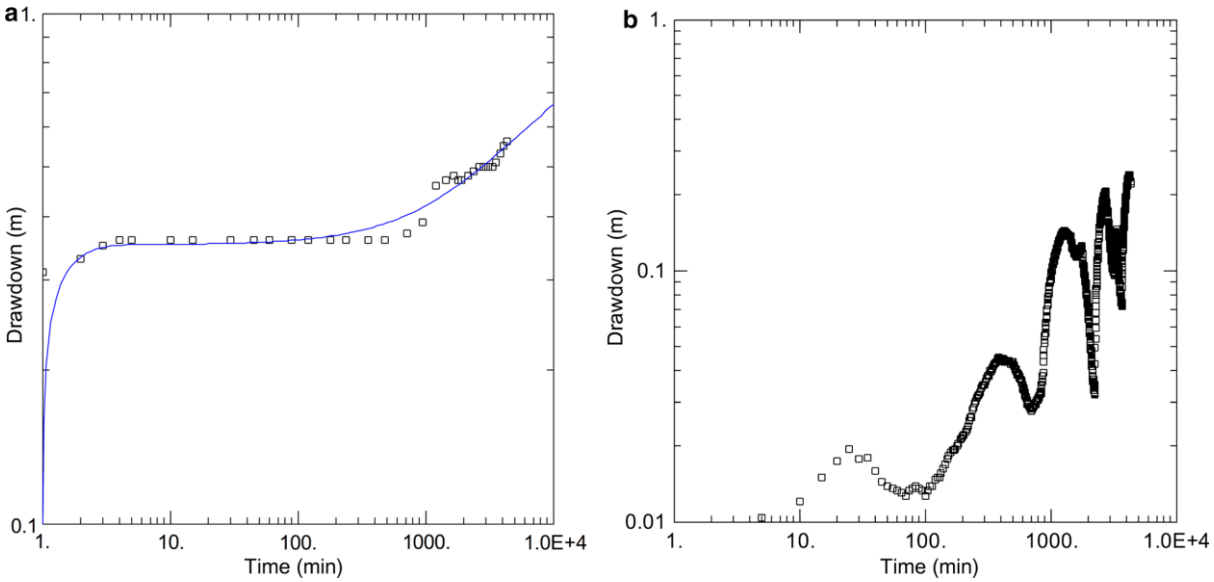

Figure 2-15: Pumping test data a) used for the determination of hydraulic properties in the karstic aquifer and b) results showing the result of previously immobile water entering the system.

A dataset similar to the one available for the karstic aquifer was, unfortunately, not available for the alluvial one. To get an estimate of the hydraulic properties of that aquifer, a series of infiltration tests, spread along the extent of the aquifer, were performed (Figure 2-16). A double ring infiltrometer was used and the method used was the falling head test method. This method provides a flow regime that can lead to a safer estimation of the infiltration rates because the water only flows vertically and there are no losses from the inner ring (which is used for the measurement) to the sides of the ring. The locations of the tests were chosen in order to ensure the supply of water that is necessary for the test and also ensure a good spatial distribution of the measurement points. Each test was carried out until the infiltration rate was stabilized. The tests lasted about 30 minutes on average. As an output, an approximation to the vertical hydraulic conductivity under saturated conditions is acquired. The mean value for all the tests was 1.5 m/day (Table 2).

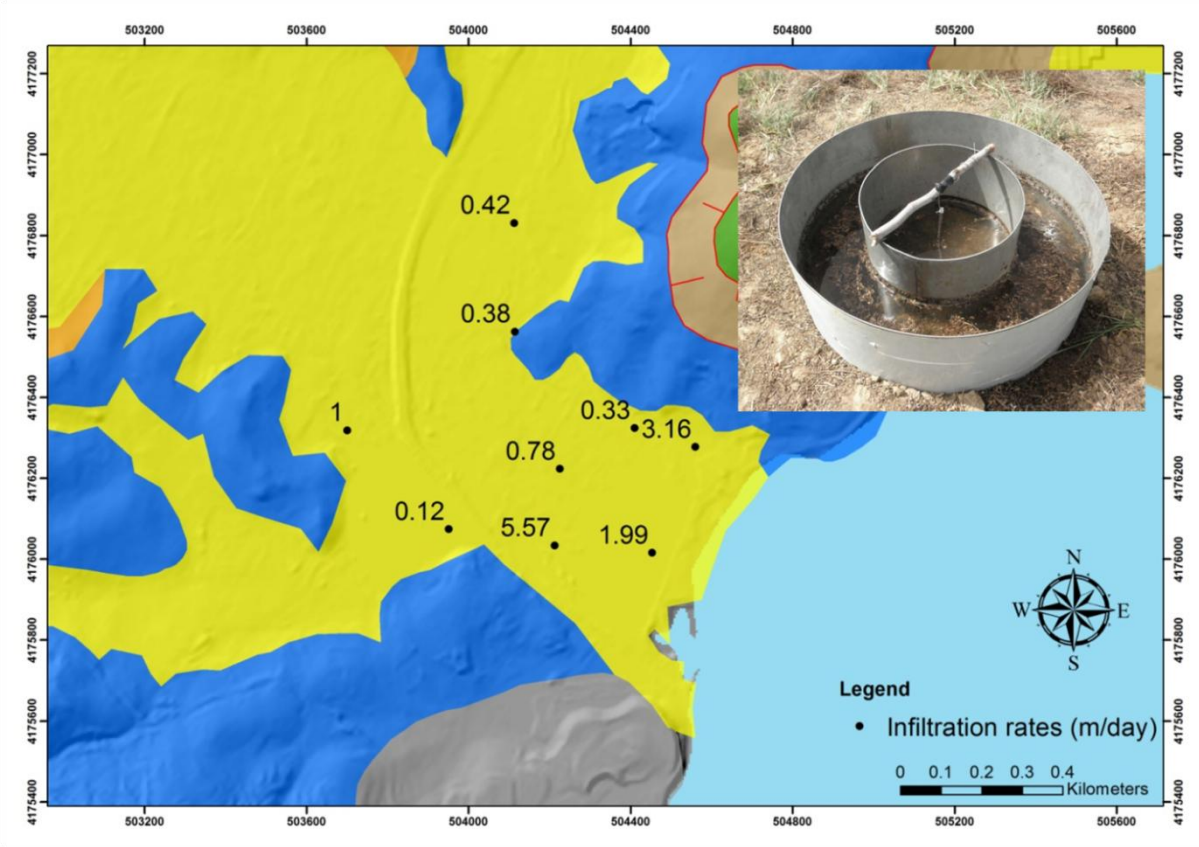

Figure 2-16: Points in the alluvial plain where the infiltration tests took place. The tests were done using the double ring infiltrometer (inlayed photo).

Table 2: Summary of the results from the interpretation of hydraulic test data for the two aquifers.

Property	Granular Aquifer	Karstic Aquifer
Hydraulic conductivity (m/day)	1.5 (mean verticalconductivity)	30 to 310 (fractures), 1.2 X 10^{-5} to 0.46 (matrix)
Storage coefficient	-	2.29 X 10^{-7} to 7.598 X 10^{-5}(fractures; storage coefficient), 1.8 X 10^{-4} to 0.0581 m^{-1}(matrix,specific storage)

2.3.5 Aquifer interconnection

The hydraulic connection between the two aquifers and the main stream in the area is a field that needs clarification in order to be able to have an accurate approximation of the natural system. The general trend is that the karstic aquifer contributes to the alluvial one. This figure is clearer in the southern part of the alluvial valley. In the northern part, on the other hand, the flow regime is,

generally, more complex, with the hydrological units of the area (alluvial and karstic aquifer, surface water, sea) being in tight hydraulic connection within a very small area.

Taking the piezometric data under consideration, the general tendency is for the water to move from the alluvial aquifer to the karstic one, as mentioned before, although the seawater influence could interfere with that mechanism. Figure 2-17 shows the comparison of the hydraulic heads of two points that each one is in a different aquifer (MSW11 is in the alluvial aquifer while D8 is in the karstic one). The difference in the hydraulic head is approximately 0.34 m and the head is higher in the alluvial aquifer that the karstic aquifer, having a relatively stable difference, so, at least for the dry period of the year, results show that the alluvial aquifer feeds the karstic aquifer. Finally, the response of the two aquifers in the rain events is consistent, something which also reflects, to some extent, how rapid the recharge is in both aquifers, at least in the northern part of the study area. This last point is also supported by the fact that the water table is relatively shallow in both cases.

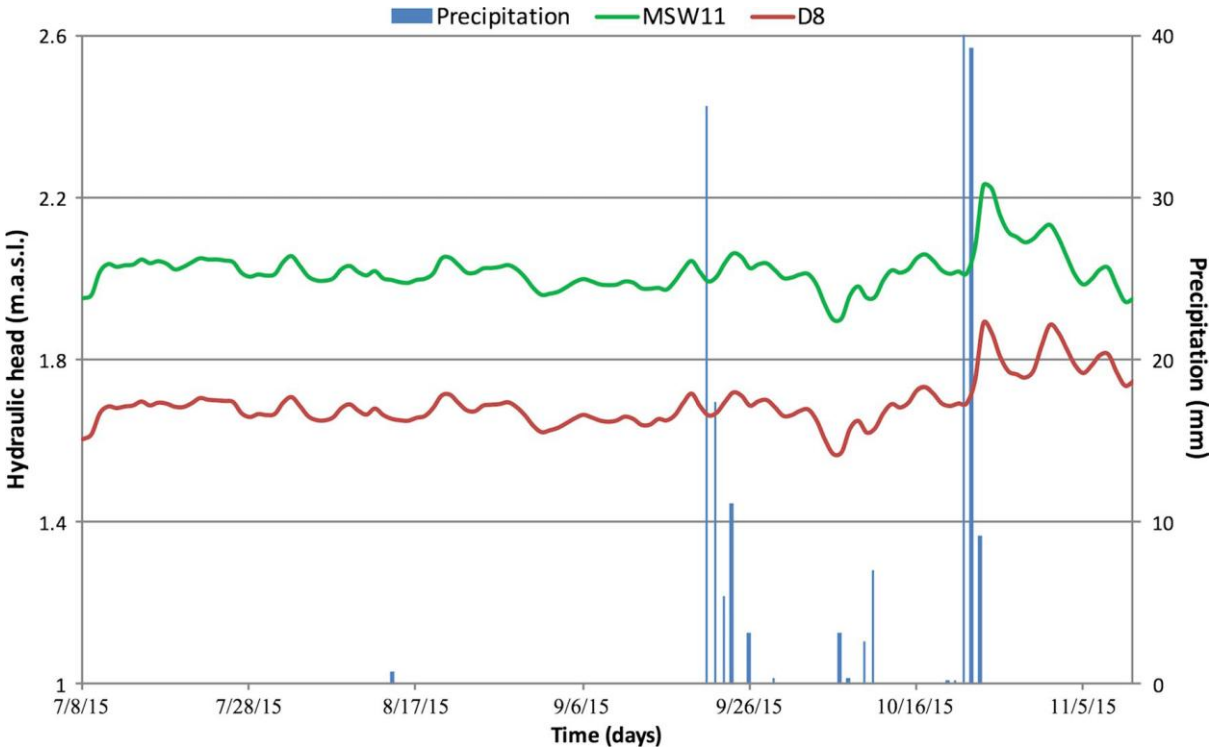

Figure 2-17: Comparison of the hydraulic heads in the karstic (D8) and the alluvial (MSW11) aquifers.

After considering all the available information for the aquifers and the flow regime, the conceptual model of the study area could be established (Figure 2-18). The base of both aquifers is the Kaisariani schist formation. Although locally the schist has been weathered and mechanically reworked, the formation can be safely considered a relatively impermeable base. Nevertheless, in areas located in

higher altitudes a few hand dug wells were found. These wells are considered to have been used in the past, during the time the ore exploitation was still active, and the purpose of those wells was probably double; at first hand to collect whatever water could be stored in the weathered mantle of the schist and at second to store water that was transferred there using other means (e.g. animals).

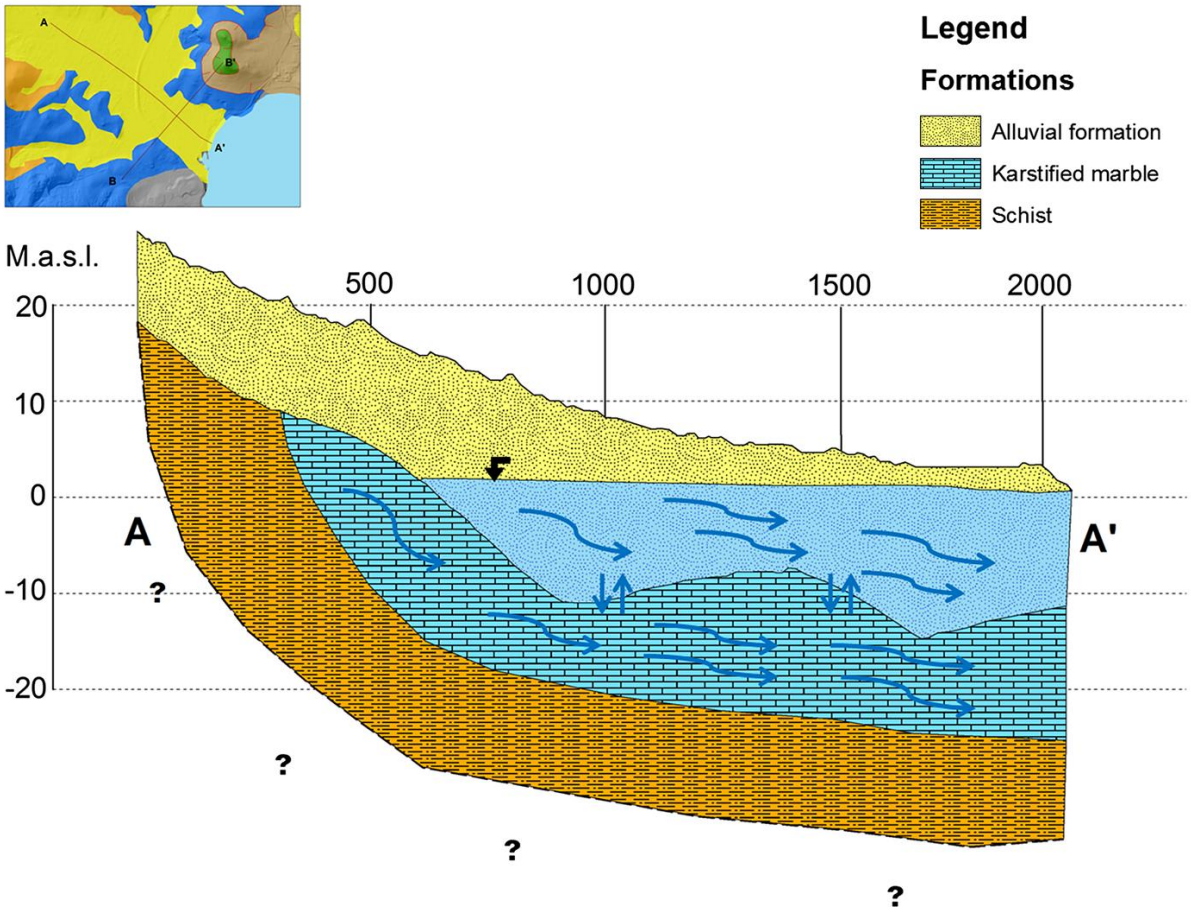

Figure 2-18: Hydrogeological cross section of the coastal part of the Lavrio hydrosystem in NW–SE direction.

Depending on the location, the sequence of the impermeable schist and the alluvial formation may be interrupted by the presence of the marble formation (where that karstic aquifer is formed). The exchange of water between the aquifers is a process that takes place throughout the whole hydrological year. The sea also has a major role, especially during the time that water is pumped out of the alluvial aquifer.

2.4 **Recharge estimation**

As mentioned before, the basic inflow to both aquifers is the recharge coming from precipitation. For that reason, an estimation of the amount of water that reaches the water table had to be done, in

order to support the model activities that were to follow. The method that was selected was the water level fluctuation method (Healy and Cook 2002; Scanlon et al. 2002). The changes in the hydraulic heads recorded at specific locations are used on the method, along with values for the specific yield of the respected aquifer and the precipitation height at the same period of time.

In the case of the alluvial aquifer, consisted mainly of silty soils, a value of 0.19 is used for the specific yield, as suggested by the method developers (Healy and Cook, 2002). The mean change in the hydraulic heads in the alluvial aquifer is 0.32 m and, at the same period, the precipitation recorded was 391 mm so the estimated recharge for the alluvial aquifer is 15.53 % of the precipitation rate.

For the karstic aquifer, using the same method may produce uncertainties, since the groundwater flow is in both the matrix and the karstic conduits, so the flow does not have a specific pattern. This can be very important in the case that water that infiltrates is not directed into the drill, on the contrary, it is stored in cavities, as mentioned earlier (§ 2.3.4). Nevertheless, the chosen method can still be used in such an aquifer to get a first estimation of the rechargesince, generally speaking, it only takes under consideration the amount of water that reaches the water table. The specific storativity for the matrix of the karstic aquifer, as seen in the analysis of the pumping test data, is 0.001661 m^{-1} and with a minimum thickness of 50 m and a specific yield of 5 % for such aquifers (Ford and Williams, 2007), the estimated recharge is 38 % of the precipitation amount. The figure may seem high but in such areas, where the is practically no surface runoff and the karstification gives a path for water to further infiltrate into the subsurface, recharge can be a substantial amount of the precipitation.

2.5 Hydrochemical identity of groundwater

The chemical characteristics of the groundwater in Lavrio have also been identified using water sample analyses performed in the lab. These analyses confirmed the seawater intrusion effect and the deterioration of groundwater quality in both aquifers (Figure 2-19). As seen from the spatial distribution of chloride ions in the alluvial aquifer, the effect is more extensive there. The higher precipitation and lower (practically zero) pumping rates from the aquifer are definitely parameters that affect this result. During the wet period of the year the concentrations are still considerably high yet lower that the ones in the dry period. Concentration values that are at the same range have also been reported in earlier studies (Stamatis et al., 2001; Alexakis, 2002), also showing that the general trend has not changed for more than 15 years.

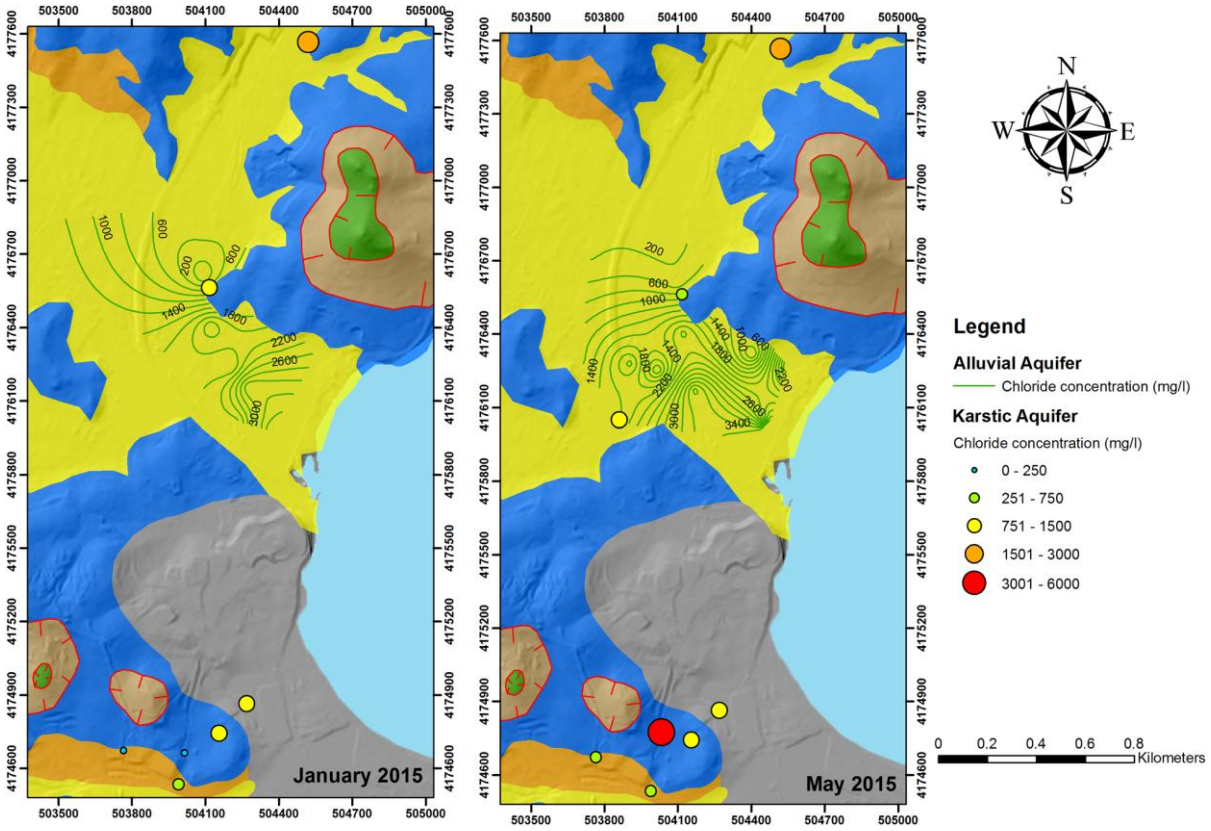

Figure 2-19: Spatial distribution of chloride ions for both aquifers.

The effect of seawater intrusion is clear in the hydrochemical signature of the samples taken in field campaigns (Figure 2-20a and b), providing an extended insight to the process that cannot be identified just from piezometric data. However, the fact that the piezometric heads are at all occasions above the sea level means that there is a steady hydraulic gradient towards the sea and that the seawater intrusion that is recorded in the groundwater is probably passive, i.e. seawater intrusion has happened in the past and what is recorded today is remnants of that effect. The flow regime in the karstic aquifers is much more complex than in the alluvial aquifers and changes can become rapidly, leading to the conclusion that there is possibility that the seawater enters the karstic aquifer first and then passes to the alluvial aquifer. This is also related to the general state of the hydraulic connection that has also been discussed previously in the present study.

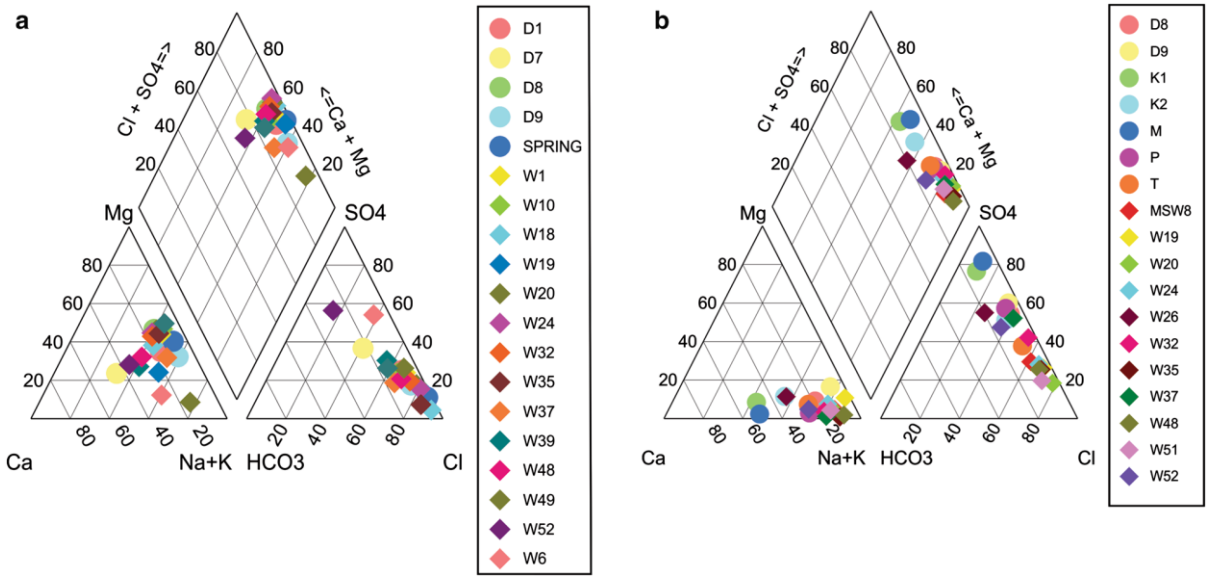

Figure 2-20: Piper diagrams for the groundwater samples collected a) prior to the irrigation period of 2014 and b) prior to the irrigation period of 2015.

Having a record of the sea level fluctuation in the area would also aid the better understanding of the processes taking place since, as seen in other studies (e.g. in Hanson et al., 2014), even small changes can have a substantial effect on the hydrodynamics of the system.

The chemical types at which the groundwater can be classified (Figure 2-21) once more show that there is a clear affection from seawater. The dominant type in the area is the Na – Cl type, followed by the Na – Ca – Cl type that is probably originating from interactions between the seawater and clay minerals that are present in the alluvial aquifer. HCO_3 and Mg ions can also be found in groundwater further from the coast, showing enrichment from the adjacent carbonate and schist formations.

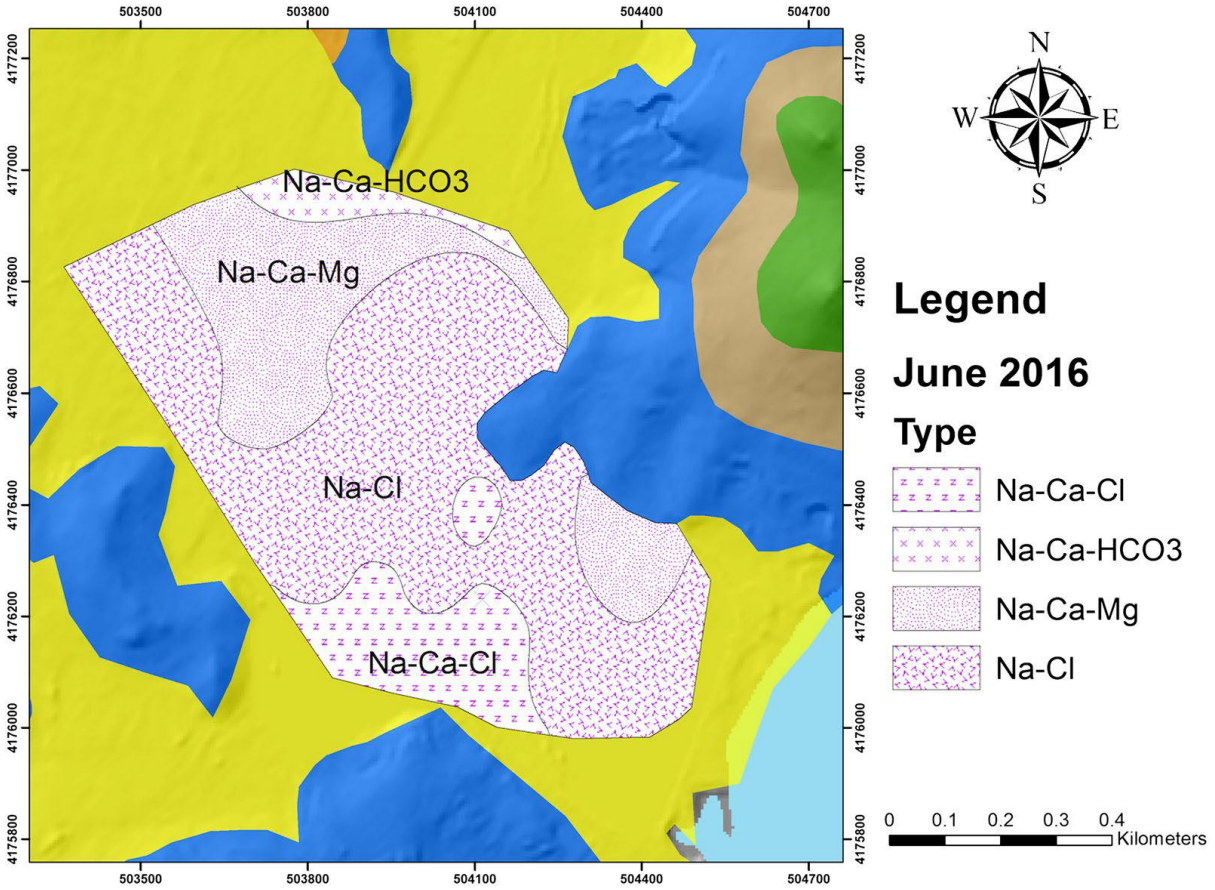

Figure 2-21: Spatial variation of the chemical composition types of groundwater samples.

The isotopic signature of the samples was also determined. Stable isotopes ($\delta^{18}O$ and $\delta^{2}H$) can be used to depict the seasonal changes and the effect of evaporation has in groundwater. The results (Figure 2-22) are plotted along with meteoric lines from other locations (Gat, 1971; Matiatos, 2010; IAEA, 2016) that are, despite that, relevant to the Lavrio case because there are certain similarities (e.g. proximity, similar hydrological and climatic conditions etc.). As seen, samples taken from open wells in the alluvial aquifer show a fluctuation in their isotopic signal while the ones from the karstic aquifer have smaller variations. The samples from the karstic aquifer plot on a certain meteoric line related to the process of rainwater infiltration, which appears to be occurring at a relatively fast rate. This is a reasonable result, since the hydraulic parameters in that particular aquifer have a very high value. The evaporation effect can be seen more clearly in the samples that are taken from the large diameter wells (~ 1 m) of the alluvial aquifer.

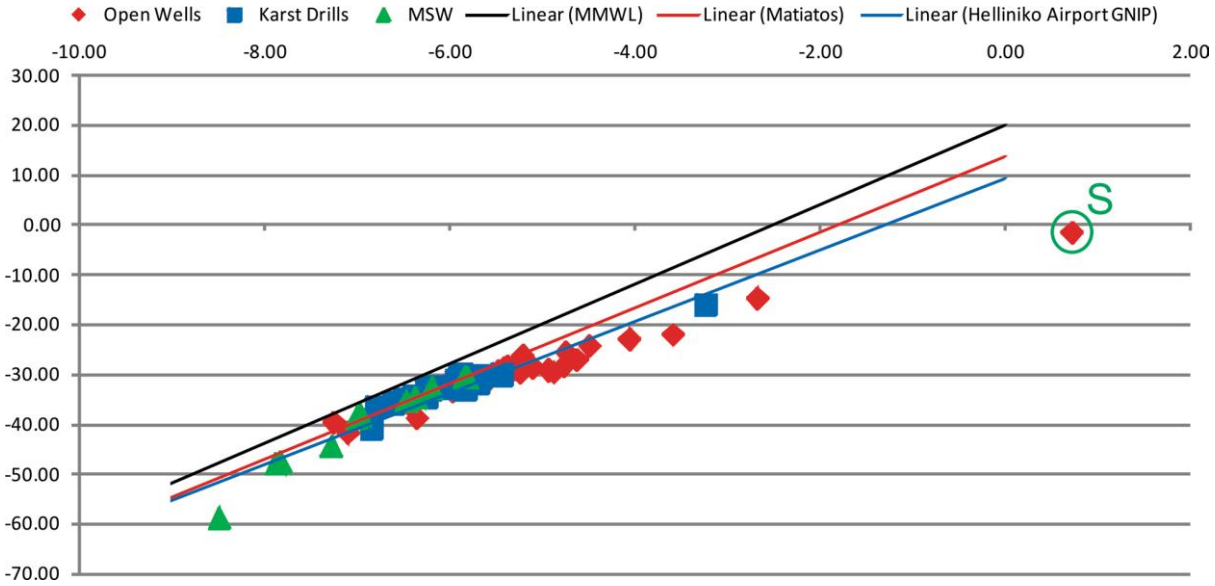

Figure 2-22: Isotopic signatures for the GW samples based on different sources. Relevant meteoric lines are also plotted.

3 Integrated hydrogeological model

The modelling activities that were performed in Lavrio are divided in two parts. In the first part, a conventional groundwater flow model was developed and used to test how different boundary conditions representing the coast perform. In the second part, a different model, focusing on the processes taking place in the karstic aquifer is developed. The aim is to evaluate the effect a variety of parameters of that model have on the simulation results, in order to have a guide on which parameters are important to include in the simulations when similar assessments are made.

3.1 Principals and concepts of the MODFLOW 2005 code

All the modelling activities in this part of the study were performed using the MODFLOW 2005 code (Harbaugh, 2005). This code uses the finite difference approach to simulate flow in the aquifer. The approximations that are taken into account are that the groundwater has constant density and that the (porous) aquifer material is homogeneous. The equation of flow that is solved is (Eq. 1):

$$\frac{\partial}{\partial_x}\left(K_{xx}\frac{\partial h}{\partial x}\right)+\frac{\partial}{\partial_y}\left(K_{yy}\frac{\partial h}{\partial y}\right)+\frac{\partial}{\partial_z}\left(K_{zz}\frac{\partial h}{\partial z}\right)+W=S_s\frac{\partial h}{\partial t} \qquad \text{Eq. 1}$$

where Kxx, Kyy, and Kzz are values of hydraulic conductivity along the x, y, and z coordinate axes (L/T), h is the potentiometric head (L), W is a volumetric flux per unit volume representing sources and/or sinks of water, SS is the specific storage of the porous material (L-1) and t is time (T). Because of the fact that such equations are rarely solved using analytical solutions (Harbaugh, 2005), the equation is solved using iterations, with different values used for the hydraulic head and the equation being solved until the convergence criteria are met. These criteria are primarily the head changes from one time step to the next and flux changes between grid cells (Figure 3-1). The various boundary conditions used in each layer provide the inputs (source) and output (sink) terms in the numerical model and are specified for each time step.

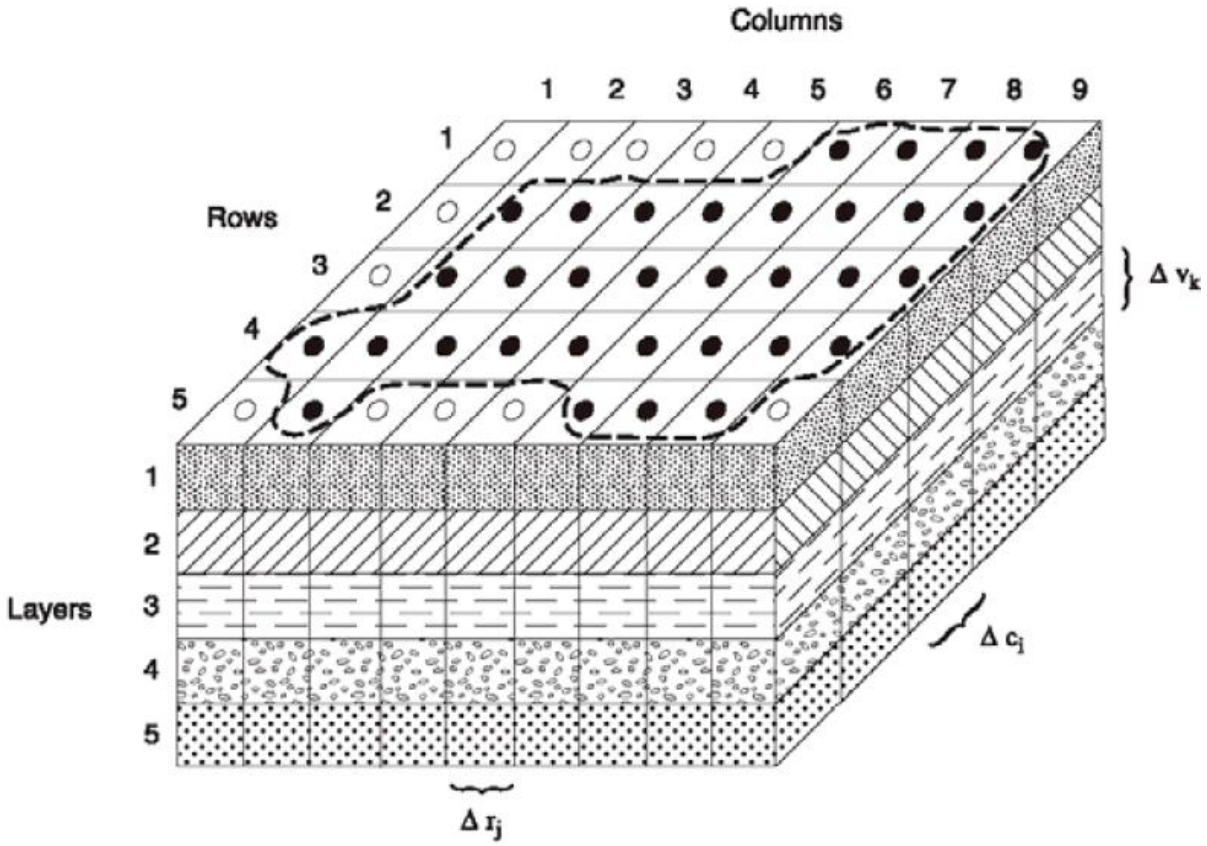

Figure 3-1: Example of a grid representing a layered aquifer system (Harbaugh, 2005). The various layers are represented (Layer 1-5) while the cells can be either active (black dots) or inactive (white dots).

3.2 Model setup

The model was developed following a series of sequential steps. These steps are presented the order that they were made. For the model development process, presentation and documentation, a general guide the USGS was followed (Reilly and Harbaugh, 2004). This guide is recommended when similar modelling activities are reported.

3.2.1 Spatial discretization

The area covered by the model is approximately 60 km^2. The area is discretized in a grid that has a 50 m X 50 m length. The cells that each layer has are 23661, so 70983 in total, with 14460 being active (in all three layers). The cell size is considered to be adequate for representing the study area in detail, especially the part that is closer to the coast, where many of the observation points are located and, thus, finer discretization is necessary.

The topographic relief of the study area is taken from the National Cadastre and Mapping Agency S.A. and are in the form of a Digital Elevation Model (DEM) that has a 5 m X 5 m discretization. This was resampled using GIS and a grid that matches the desired cell size was created. The elevations for the rest of the layer were derived as described below for each layer.

3.2.2 Vertical discretization

The layers included in the model are three, with each one representing a specific geological formation; the alluvial formation at the top, the Upper Marble formation and the Kaisariani Schists formation respectively. In the first two layers aquifers are formed, while that last one is their base. The characteristics of each layer are the following:

- Alluvial aquifer layer: The aquifer developed in the alluvial formation is a granular aquifer and it has been the main source of water for irrigation in the past. The spatial extend of the aquifer coincides with the geological boundary of the formation. The thickness of the layer is taken from the drilling in various locations that was extrapolated using geostatistical methods (kriging). Depths from the drilling for the installation of piezometers in Lavrio were provided by the UFZ and an approximation was made, since the drilling length was taken as being the total thickness of the alluvial formation. In the boundaries of the formation, a minimum thickness of 3 m was assigned inorder to avoid numerical problems during the simulation. The aquifer is simulated as Convertible (i.e. unconfined).
- Karstic aquifer layer: Within the Upper Marble formation a karstic aquifer is developed. The aquifer is highly heterogeneous and, as a result, the flow regime is complex. The boundaries of the hydrogeological basin of that aquifer are defined at field scale in order to have an accurate representation of the natural system. The thickness assigned in the layer is 60 m which, for the Lavrio area, is considered to be an average. This aquifer is also simulated as Convertible (i.e. unconfined).
- Schist base layer: The Kaisariani Schist formation is the base of both aquifers, apart from the areas where the alluvial aquifer is directly above the karstic one. The hydraulic properties assigned in this layer are very poor, especially when compared to the parameters of the karstic aquifer. The thickness of the layer is 40 m and is simulated as Confined.

An important characteristic of the model is that the two aquifers are in direct hydraulic contact with each other, but also with the sea. The relation between them is clarified only in part and it would not

be easily done through conventional monitoring techniques. For that reason, clarifying this relation is included at the aims of this model.

3.2.3 MODFLOW 2005 packages

For the model development, the following MODFLOW 2005 packages were used:

- Layer Property Flow package (LPF): The package is used to set up the hydraulic parameters of the layers of the model (Table 3).

Table 3: Parameters as listed in the LPF file and used in the model.

Parameter	Abbreviation	Details
Horizontal hydraulic conductivity	K_A	Alluvial layer. The vertical is taken as 1/10 of the horizontal one.
\\	K_S	Schist layer. The vertical is taken as 1/10 of the horizontal one.
Specific storage	SS_A	Alluvial layer. Default values are used because of its minor importance in the solution.
\\	SS_K	Karstic layer. Default values are used because of its minor importance in the solution.
\\	SS_S	Schist layer. Default values are used because of its minor importance in the solution.
Specific yield	SY_A	Alluvial layer. Single value for the entire aquifer.
\\	SY_K	Karstic layer. Single value for the entire aquifer.
Horizontal hydraulic conductivity zone	K_K_N	Zone for the part of the karstic aquifer that is north of the alluvial valley.The vertical is taken as 1/10 of the horizontal one.
\\	K_K_M	Zone for the part of the karstic aquifer that is covered by the alluvial valley.The vertical is taken as 1/10 of the horizontal one.
\\	K_K_S	Zone for the part of the karstic aquifer that is south of the alluvial valley.The vertical is taken as 1/10 of the horizontal one.

- Stream Flow Routing package (SFR): That specific package is used for the simulation of the main stream in the area that comes from the north. The streams are, as mentioned before, dry during the period of the simulation, so this package is used as a proxy to evaluate the model simulation results. The SFR package is favoured compared to the River (RIV) package because it can simulate a volumetric stream discharge in contrast with the RIV that simulates a flux between the aquifer and the river segment. The stream generally has similar characteristics throughout its whole length. The parameters that are essential for the SFR package take the following values (Table 4):

Table 4: Parameters related to the SFR package.

Parameter	Value	Details
Reach length (RCHLEN)	Object length	-
Streambed top (STRTOP)	(Model top + Alluvium bottom)/2	-
Stream slope (SLOPE)	0.017 m/m	Slope of 1°
Streambed thickness (STRTHICK)	1 m	Maximum estimate
Streambed Kv (STRHC1)	0.00001 m/day	Estimate
Stage calculation (ICALC)	Rectangular channel	Better approximation in our case
Stream width (WIDTH)	5 m	Mean width
Channel roughness (ROUGHCH)	0.03	Chow, 1959

- Gage package (GAGE): The Gage package is used along with the SFR package for extracting the results (stream stage, volumetric discharge etc.) from the simulation of the stream at a specific observation point.
- Well package (WEL): The Well package is used instead of the Recharge (RCH) package for the inflow from precipitation in each aquifer. It is also used for the simulation of the irrigation pumping from the alluvial aquifer. The rates used are estimated using the water level fluctuation method presented in § 2.4. The parameters used for that package are the following (Table 5):

Table 5: Parameters used in the WEL package.

Parameter	Abbreviation	Details
Recharge	R_A	Recharge homogeneously divided in the alluvial aquifer.
Recharge	R_K	Recharge homogeneously divided in the parts of the karstic aquifer that outcrop.
Discharge	Pump	Negative, representing pumping from the alluvial aquifer.

- Head observation package (HOB): This package is simply used for the importing and exporting of hydraulic head observations and simulated heads of the model.

The model developed also includes the main outflow component, which is the boundary condition representing the coast. At this point there is a differentiation and two models were tested. The differentiation is only at the boundary condition and, as a result, how the coast interacts with the aquifers:

- The first model developed with the use of the time variant specified head package (CHD). The starting and ending heads are 0 m for the entire simulation and the boundary condition is assigned in both aquifers.
- The second model is developed using the general head boundary package (GHB). The difference with the CHD package is that the GHB also has a conductance factor that regulates the amount of water the boundary can exchange with the aquifers (Table 6). The initial value chosen is two orders on magnitude lower than the hydraulic conductivities of the adjacent aquifers.

Table 6: Paraemeters used when the GHB package is assigned to the coast.

Parameter	Abbreviation	Details
Boundary conductance	GHB_A	Connection between the alluvial aquifer and the sea.
Boundary conductance	GHB_K_M	Connection between the northern part of the karstic aquifer and the sea.
Boundary conductance	GHB_K_S	Connection between the southern part of the karstic aquifer and the sea.

The background behind the use of two different boundary conditions for the coast is the awareness that the CHD can provide (or absorb) unlimited amount of water to the model. The GHB, on the other hand, is more strict and can be regulated to provide a better representation of the connection between the sea and the aquifer system. Having a reasonable estimation for the boundary condition conductance is, however, unrealistic, yet this is the reason why it should be carefully handled during the sensitivity analysis and parameter estimation processes.

3.2.4 Temporal discretization

The period simulated by the model is two years, from January 2014 to December 2015. The time step used in the model is daily, mainly to be able to see rapid changes in the aquifers. Each stress period corresponds to a month. One more steady state stress period is added in the beginning of the simulation in order to stabilize the initial conditions and make the rest of the simulation run more smoothly. The remaining stress periods are all transient, so the storage effects are also included in the model.

3.2.5 Solver options

The availability of solvers in MODFLOW 2005 is quite large (PCG, GMG, SIP etc.), so for each problem a different solver might be more suitable than the other. In this model the Preconditioned Conjugate Gradient (PCG) solver is used because of its robustness and efficient performance. The options used in the solver (Table 7) are presented:

Table 7: Convergence criteria and options used in the PCG package.

Parameter	Value
Head change criteria (HCLOSE)	0.1 m
Flux criteria (RCLOSE)	0.1 m^3/day
Maximum outer iterations (MXITER)	1000
Maximum inner iterations (ITER1)	1000
Matrix preconditioning method (NPCOND)	Modified incomplete Cholesky

The most important features of the solver are the closure criteria for the hydraulic head and the volumetric fluxes (HCLOSE and RCLOSE). These had to be slightly adjusted in order to achieve convergence in the initial steady state step for the karstic aquifer. Nevertheless, the values chosen for the closure criteria are considered to be reasonable for this kind of system.

3.3 Hydraulic parameters values of the model layers

The hydraulic parameters of the simulated aquifers certainly are the most important parameters that are included in the model. In the model developed for the Lavrio area, two distinct aquifers with different characteristics are simulated. Their impermeable basement is also represented in the model.

The data availability for the alluvial aquifer was scarce so a literature review was done, focusing on areas with similar characteristics. In Greece, alluvial aquifers such as the one in Lavrio are quite typical, so some information was has been acquired (Table 8).

Table 8: Table with information acquired from the literature review.

Region	Transmissivity (m^2/day)	Storage coefficient (-/-)	Source
Piros basin	10.28 – 27.56	-	Voudouris et al., 1997
Glafkos basin	39.05 – 48.73	-	Voudouris et al., 1997
Greece (review)	0.1 – 100	10^{-5} - 10^{-2}	Daskalaki and Voudouris, 2008
Rhodope	71.7 – 751.68	$1.55 * 10^{-5}$ - $1.18 * 10^{-3}$	Petalas et al., 2009

The lack of literature data for the study area led to the need for an estimation of the hydraulic properties of the alluvial aquifer. This was achieved with the use of double ring infiltration tests, which gave an estimate of 1.5 m/day for the vertical hydraulic conductivity (as presented in § 2.3.4). The range though varied so the parameters had to be included in the sensitivity analysis in order to evaluate the effect on the model results.

The data availability for the karstic aquifer had been more due to the acquisition of a series of pumping test results that were re-evaluated and interpreted to get an estimate for the hydraulic properties of the karstic aquifer (§ 2.3.4 of the present study).

Having already an understanding about the conceptual model and the hydraulic properties and connections in the system, a set of initial parameters had to be chosen for the model (Table 9). In the first model runs, small changes were done in those parameters in order to have a model that had an acceptable performance and could be used in the following steps. Sequentially, the sensitivity analysis and parameter estimation processes steps were performed.

Table 9: Starting values for the hydraulic parameters of the model (hydraulic conductivity values are in m/day, conductance values are in m^2/day, specific yield values are dimensionless).

Aquifer	Parameter	Abbreviation used	Starting value
Alluvial	Hydraulic conductivity	K_A	1.5
Alluvial	Specific yield	SY_A	0.1
Karstic	Hydraulic conductivity (north sector)	K_K_N	15
Karstic	Hydraulic conductivity (middle sector)	K_K_M	15
Karstic	Hydraulic conductivity (south sector)	K_K_S	40
Karstic	Specific yield	SY_K	0.08
Alluvial	GHB conductance	GHB_A	1.5
Karstic	GHB conductance (middle sector)	GHB_K_M	1.5
Karstic	GHB conductance (south sector)	GHB_K_S	4

For the karstic aquifer the domain was divided into three different hydraulic conductivity zones (Figure 3-2), in order to have a better understanding about how the different sectors of the karstic aquifer affect the flow in the model. For that reason, the zones where chosen as to represent the area that underlies the alluvial plain (K_K_M) and the areas north and south of the alluvial plain (K_K_N and K_K_S respectively).

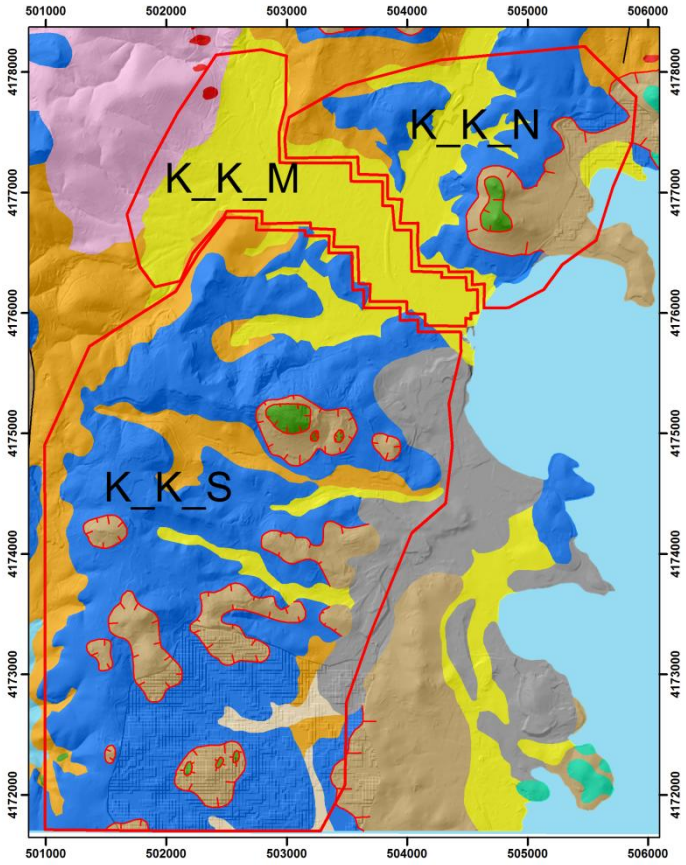

Figure 3-2: Conductivity zones in the karstic aquifer (K_K_N the conductivity in the northern sector, K_K_M the conductivity in the mid sector and K_K_S the conductivity in the southern sector).

The schist layer, which is the basement of both aquifers, was also represented with relatively poor hydraulic properties in the model (conductivity of 0.001 m/day). A value of $10^{-5}m^{-1}$ was chosen for the specific storage of all layers because the contribution to the final storage is expected to be insignificant, as it is for unconfined aquifers.

3.4 Importing observations into the model

The observations were imported into the model using the HOB package, as mentioned above. The time steps that correspond to the days that the measurements took place were chosen and hydraulic head data were implemented. In the case of the data taken for the karstic aquifer using pressure transducers every 15 minutes, a daily average was used as an observation.

3.4.1 Hydraulic head and stream discharge observations

The calibration of the groundwater flow models is done using hydraulic head observations at various locations in the aquifer. The model performance is evaluated when the observed and the simulated results are compared. The volumetric discharge at specific points in streams and/or rivers or between different elements of the model could also be used if available.

In the present study it was not possible to have stream flow measurements since the main stream is dry for the most time of the wet period of the year and completely dry during the dry period. This, at a first level, could pass as a problem for the model. However, this is not necessarily, since no flow observations can also be used in the model and the sensitivity analysis of the model for evaluation. Hydraulic head data were collected through field campaigns for the alluvial aquifer while for the karstic one a number of pressure transducers were installed in order to record the response of the aquifer to the precipitation events. The way the karstic system behaves hydraulically would be a key point in the evaluation of the model.

An important feature of the measurements is that they are gathered within a very small area close to the coast (Figure 3-3). This is because the other parts of the study area are in much higher altitudes where drilling for groundwater would not be sufficient or economically feasible. For this reason, extra measuring points were installed during the Geoprobe MARSOL campaign (§2.2.2). Nevertheless, the area closer to the coast is, in any case, more important for the model than the other regions in the edges of the study area, due to the fact that all the rapid changes are expected to be at this area.

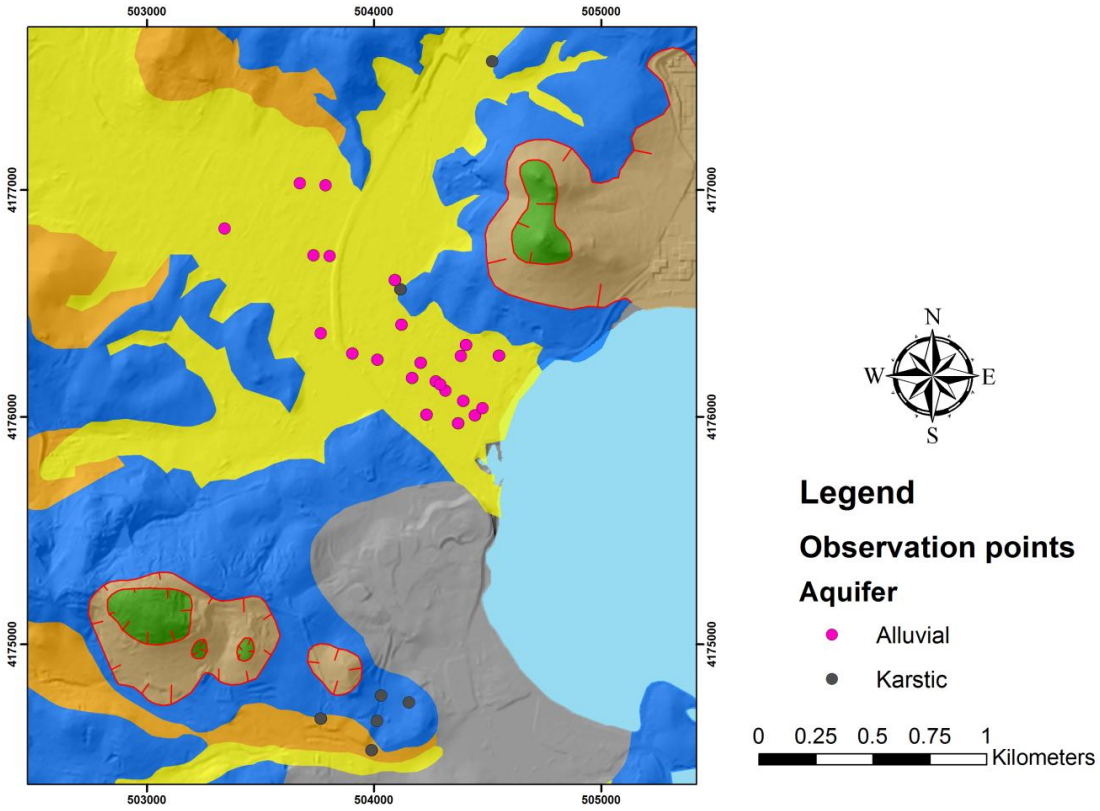

Figure 3-3: Locations of the observation points of the two aquifers.

The total number of observations that are included in the model is 243. The same observations are used for both the sensitivity analysis and the parameter estimation. The number of measurements that are in the alluvial aquifer are 110, while and the remaining 134 for the karstic one. The total number of observations in each aquifer is not much different, thus preventing the results of the sensitivity analysis from having bias towards the parameters of either aquifer. For the stream in the area there are no observations since it is dry for the most part of the hydrological year, so artificial records were introduced into the model for the evaluation of this component of the hydrological cycle. The zero flux measurements were located at a point close to the northern part of the alluvial valley where there was no water observed throughout the whole monitoring period.

3.4.2 Data quality

One of the main requirements when proceeding to modelling activities is a set of trustworthy hydraulic head observations. On many occasions though, data is provided from external sources, without being properly transcribed into some kind of database. Additionally, the conditions under

which these data was acquired are usually not well recorded, adding uncertainty right from the first step of model building.

In the case of Lavrio, the majority of data used were collected with own efforts and under conditions known to the modeller. Data from other sources has also been available, with those data being pre-processed before being used in the models. For that reason, the information that is used as an input to the Lavrio groundwater flow model is considered to be of very good quality. In general, it is desirable that the modeller has an active role to the methodologies that are used when taking information that are going to be used for modelling. This can optimize the routine of data collection and improve the model structure and the use of the acquired data.

3.5 Sensitivity analysis methods for the evaluation of the models

The sensitivity analysis of the model has been an inseparable part of the modelling activities. The method used is based on the comparison of the heads simulated by the model with the observations done in the field. This is done using a statistical approach (explained below). The head observations either come from field campaigns and have a seasonal frequency, or from equipment placed at specific points of interest. The equipment used was a number of pressure transducers that measure hydraulic pressure (along with temperature) with an interval of 15 minutes.

3.5.1 Weights assignment

In each type of observations a weight has to be assigned to represent the level of confidence for each hydraulic head measurement. All kinds of potential errors that can accumulate at the process of measuring have to be considered when assigning weights. Potential errors can originate from malfunctions of the equipment used, lack of experience of the personnel taking the measurements, mistakes when transferring the data from one format to the other (e.g. from hand written notes to the computer etc.).

The hydraulic head measurements taken in Lavrio were subjected to errors that the original DEM had, so the absolute altitudes of the wells and drills had to be corrected using differential GPS measurements. The accuracy of the differential GPS was lower than 5 cm in most cases, which is definitely within an acceptable range. The measurements in Lavrio were done by experienced personnel in the case of the open wells and with pressure transducers in the case of drills in the

karstic aquifer. Therefore, the measurements are considered to have very good quality and the cumulative error would not, in any case, exceed the value of 10 cm.

The statistics used in the sensitivity analysis (and later in the parameter estimation) is the standard deviation (σ), meaning that the measurement cumulative error could not be more than 10 cm. The weight is calculated using Eq. 2.

$$\omega_{ii} = \frac{1}{\sigma^2} \qquad \text{Eq. 2}$$

where ω_{ii} is the assigned weight and σ the standard deviation of the measurement.

3.5.2 Sensitivity analysis basic concepts

The sensitivity analysis of the models was performed using the UCODE 2014 code (Poeter et al., 2014). The code can be used for the parameter estimation also and its usability is not limited in groundwater flow models but can be expanded in other types of models. The code uses a number of statistical indicators to quantify the sensitivity of each model parameter by comparing changes in the hydraulic heads and the volumetric flows that are simulated with different parameters set. Each time, the hydraulic heads and volumetric flows are compared to the relevant observed values that are used in the model. The outputs are used in order to make the selection of the parameters that are most important and are going to be used in the parameter estimation process. The use of such a powerful mathematical tool should be done with care in order to avoid misinterpretation of the results and, eventually, unrealistic modelling approach to the physical system. Further information on the code, its structure and useful guidelines on model building, can be found in the literature (Poeter et al., 2005; 2014; Hill and Tiedman, 2007).

One of the strong advantages of UCODE 2014 is the fact that the user can perform sensitivity analysis to as many parameters desired. In comparison, when using the more traditional trial and error method, the modeller has to select in prior the parameters that are expected to have high sensitivity and perform the sensitivity analysis. In that way, the sensitivity analysis may not be able to include many or all of the available parameters due to lack of flexibility or inability to explore the parameter value acceptable limits. This characteristic can be of vital importance in the case of very complex models with a large number of parameters. In addition, parameters that may initially be considered

having low importance can be overseen by the user, so the code results can highlight the parameters that are most important for the modeller. Finally, the way the sensitivities are produced makes the choice for the parameters that are going to be used in the parameter estimation more defendable due to the statistical methodology that is followed.

The results of the sensitivity analysis are presented in the following section. Before the sensitivity analysis run, a manual calibration step was necessary in order to achieve smaller residuals and have more credibility in the results of the sensitivity. This step can also significantly reduce the time and computational effort needed in the parameter estimation process.

3.5.3 Scaled sensitivities

The chosen method for the sensitivity analysis is the use of the fit independent statistics. The method has the advantage of not requiring the initial model results to be extremely accurate while the results can be directly evaluated and used in the parameter estimation. However, having initial results that are not completely unrealistic is still helpful for the simulation. More information about the fit independent statistics can also be found in Hill and Tiedman (2007).

3.5.3.1 Dimensionless and composite scaled sensitivities

One of the main indicators used in the sensitivity analysis is the dimensionless scaled sensitivity (DSS), which is a measure that reflects how effective a change in a specific parameter is to the model. The comparison is with the initial parameter value and the perturbed value that is used in the specific iteration. The DSS is calculated using the Eq. 3:

$$dss_{ij} = \left(\frac{\partial y'_i}{\partial b_j} \right) \left| b_i \right| \omega_{ii}^{1/2} \qquad \text{Eq. 3}$$

where y'_i is a simulated value, b_j the jth parameter, the $\left(\frac{\partial y'_i}{\partial b_j}\right)$ derivative is the "sensitivity" of the ith observation to the jth parameter, b is a vector containing that parameter values and ω_{ii} is the weight that is assigned to the ith observation (Hill and Tiedman, 2007). When summing all the DSS for a single parameter the scaled sensitivity (CSS) is calculated. This indicator is mainly used for the selection of the parameters that are the model is mostly sensitive to.

3.5.3.2 Parameter correlation coefficient

The correlation between different parameters is one of the most important aspects of the sensitivity analysis since highly correlated parameters cannot be estimated independently. In that case, when used in the parameter estimation, one of them should be assigned with a fixed value when the other is estimated and vies versa. The choice of which parameter to fix can be taken in combination with the CSS i.e. if two parameters have high correlation coefficient, the parameter with low sensitivity could be fixed when the parameter with high sensitivity is estimated. The parameter correlation coefficient (PCC) is calculated using Eq. 4:

$$\mathrm{Cov}\{b\}_{jk}/\left[\mathrm{Var}\{b\}_{jj}\ \mathrm{Var}\{b\}_{kk}\right] \qquad \text{Eq. 4}$$

where $\mathrm{Cov}\{b\}_{jk}$ is the covariance between two parameters and $\mathrm{Var}\{b\}_{jj}, \mathrm{Var}\{b\}_{kk}$ the variances of each parameter (Hill and Tiedman, 2007).

For the UCODE 2014 to be able to estimate a pair of values independently, their PCC is suggested to be below 0.95 (Hill and Tiedman, 2007). When parameters with higher PCC are used, a justification on the reasons why this option is chosen should be presented.

3.6 Sensitivity analysis of the tested models

The main part of the evaluation of the sensitivity analysis includes the presentation of the results and the comparison of the level of sensitivity and the correlation between various parameters.

3.6.1 The CHD model

The sensitivity run for the CHD model included all the available parameters and the results are presented. The parameters that highly affect the model results are primarily the ones related to the karstic aquifer (Figure 3-4). The values for R_K and SY_K, along with the pumping from the alluvial aquifer (Pump), have the highest CSS values. The R_A, K_K_S, K_K_N and SY_A parameters are the ones that follow. Most information for the parameters is coming from the observations that are in the northern part of the alluvial valley (Karstic) and the ones within the alluvial aquifer (Alluvial). The fact that there is small contribution from the observations in the alluvial aquifer to the parameters related to the karstic aquifer and vies versa is an interesting result that means that the aquifers may

have hydraulic interconnection, but the fluxes from the alluvial aquifer to the karstic one are probably small.

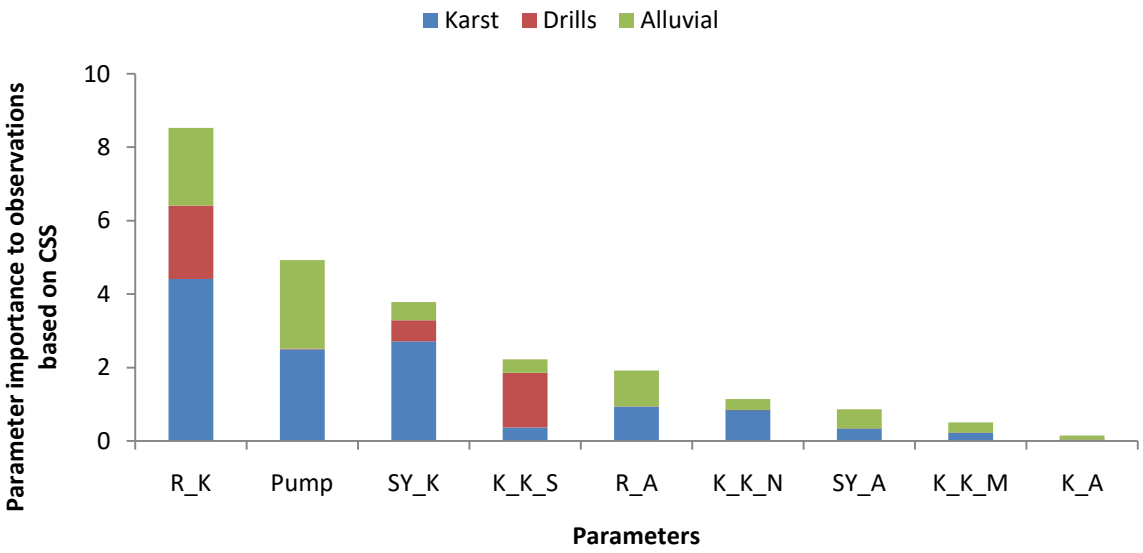

Figure 3-4: Parameter CSS for the CHD model. Observations are categorized in order to be able to portray the quantified amount of affection of each observations group to each model parameter.

The combination of the PCC and CSS give greater understanding to the model parameters interrelations. There are two parameter sets (R_K and K_K_N, R_K and K_K_S) that are entirely correlated (PCC of 1.0). There also four other parameters that are highly correlated with SY_K (K_K_N, K_K_S and R_K have a PCC of 0.99 with SY_K, Pump has a PCC of 0.98 with SY_K). The Pump parameter is also highly correlated with the parameters K_K_N, K_K_S, R_K (0.98) and SY_A (0.97).

The outputs of the sensitivity analysis show that the parameters related to the recharge are the ones that mostly affect the model. The specific yield of the karstic aquifer has also much higher sensitivity that the one of the alluvial aquifer. This is in direct connection with the fact that the hydraulic conductivities are much higher in the karstic aquifer, so any change in those parameters has much higher effect in both aquifer systems than changing the hydraulic parameters in the alluvial aquifer. Finally, the specific storage for all aquifer has no sensitivity, which is a reasonable result, since the contribution of the specific storage is minor in the unconfined aquifers, such as the ones simulated in this model.

3.6.2 The GHB model

The process for the sensitivity analysis of the GHB model was similar to the one for the CHD, in order to have results that are comparative. The results have some significant differences that are presented in the following section.

For the GHB model (Figure 3-5), two of the values of the karstic aquifer (R_K and SY_K), along with the pumping for irrigation from the alluvial aquifer (Pump) have the highest CSS. R_A, SY_A, GHB_K_S and K_K_N are following, with smaller CSS. The remaining parameters (K_A, GHB_A, K_S, K_K_S, K_K_M and GHB_K_M) have insignificant sensitivities.

These results make the choice of the parameters that are going to be used in the parameter estimation process much more straightforward. Furthermore, there is more contribution from all the observation groups in this model, so in principal, a more representative parameter estimation is expected since more information is used by the code.

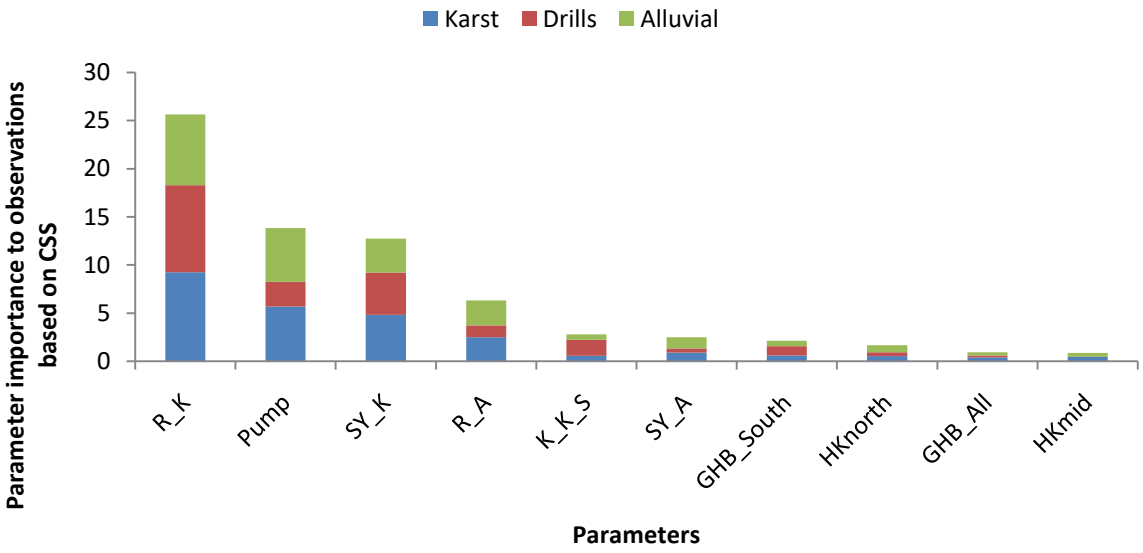

Figure 3-5: Parameter CSS for the GHB model. As seen, there are some similarities to the parameters that have the highest sensitivities with the CHD model. Also, the parameters related to the GHB boundary do not show very high CSS.

When looking at the correlation between the different parameters, the highest one is 0.98 between SY_K and R_K (positive correlation). GHB_A and GHB_K_M with 0.91 (negative correlation) and K_S

with GHB_A with 0.88 (negative correlation) are the ones that follow, with the rest of the parameters not showing any correlation whatsoever.

As in the case of the CHD model, the parameters that highly affect the results of the GHB model are the ones related to the karstic aquifer. Assigning the GHB boundary condition in the sea introduces the GHB conductance in the sensitivity analysis, but it does not have a very high sensitivity, although being the main output of the model. PCC values are also lower that the suggested 0.95, except on just one parameter pair, so using them in different parameter estimation runs would overpass this issue. Lastly, there is a distinct difference between the parameters with the highest CSS and the rest, so it is easier to select the parameters that are going to be used in the parameter estimation.

3.6.3 Comparison of the sensitivity analyses of the two models

Through the analysis of the sensitivity analysis results, some of the key components of the two models tested can be highlighted. In general, it is clear that the parameters that are related to the karstic aquifer are the ones that have the highest impact in both models. Having the observations in such a small area may have some influence in the sensitivity analysis process but this is not expected to produce non realistic results. The low sensitivity of the parameters related to the alluvial aquifer shows that the karstic aquifer dominates the hydrological processes at the Lavrio hydrosystem. This is the reason why changes in the karstic aquifer parameters affect the observations in the alluvial aquifer more that when these changes are done in the parameters of the alluvial aquifer.

3.7 Parameter estimation process and final results of the models

Having the results of the sensitivity analysis allowed to proceed to the parameters estimation. As mentioned before, UCODE 2014 is once more used at this point. Results are presented in the following sections.

3.7.1 Parameter estimation

After the first model runs, a manual calibration was introduced as a first step to produce the initial results. This step was considered to be necessary in order to avoid computational instabilities when moving to the parameter estimation. After a relative acceptable residuals level was reached (up to 5 m on average), the automatic parameter estimation followed in steps that each time differed in the parameters used. The chosen parameters had to have high CSS, in order to be able to achieve a

better state of the model after the estimation, and low PCC, in order to get meaningful results for the parameters combination used in the estimation.

3.7.2 The CHD model results

The sequence followed at the parameter estimation process, along with the initial and final values are presented. The first parameter chosen is R_K, since it is the most sensitive parameter. The estimated value was more than two times higher than the initial one. The specific yield for the two aquifers followed, with that run having no convergence because the changes in the simulated heads were very high and the closure criteria of UCODE 2014 were not met. This is reasonable, since even small changes in the specific yield can end up in large differences in the simulated heads and fluxes. For that reason, constrains between sensible values in the selected parameters can be assigned in order for the parameter values to not be able to reach unrealistic numbers. Small increments in the perturbation of the values in successive iterations were also assigned. Eventually, SY_A varied a lot, ending up in having the lowest residuals with the initial value, while SY_K remained quite stable. An iteration using K_K_S and R_A followed, were K_K_S was reduced by 50 % while R_A increased by a factor of 3. R_K was used one more time in the end together with R_A, with the first increasing further and the latter remaining relatively stable. Eventually, the sum of squared weighted residuals (SSWR, Table 10) did not improved dramatically.

Table 10: Results of the parameter estimation for the CHD model.

Parameter	Starting Value	Estimated value	Initial SSWR	Final SSWR
R_K	30 %	69.71 %	59387	51503
SY_A	0.2	0.12		
SY_K	0.08	0.15		
K_K_S	15 m/day	7.78 m/day		
R_A	15 %	45 %		

3.7.3 The GHB model results

The process of parameter estimation for the GHB model was quite similar with the one for CHD model, with the main difference being that there are a few more parameters to use. The Pump parameter was intentionally overseen in the parameter estimation process, although it has a high sensitivity, due to the fact that the estimate of the pumping rates can be assumed to be accurate

and, in the end, adjusting the pumping rates to fit the model is not a method was considered to be appropriate.

Since the parameters related to the karstic aquifer are the ones that have the highest sensitivities, those were used in the first parameter estimation step. The use of K_K_S, R_K and GHB_K_S led to a substantial improvement to the model performance already from the first step. The following runs were, eventually, used only to make the model as representative of the physical system as it was possible. Nevertheless, there were parameters (e.g. K_K_N) that were fluctuating a lot and having a good estimate using the code was not feasible. Those were estimated last so that the other parameters have their final values before. After the termination of the process, the sum of squared weighted residuals was significantly improved (Table 11).

Table 11: Results of the parameter estimation for the GHB model.

Parameter	Starting Value	Estimated value	Initial SSWR	Final SSWR
K_K_S	40 m/day	181.7 m/day	17754	3441
GHB_K_S	1.5 m^2/day	4.67m^2/day		
R_K	30 %	45.5 %		
K_K_N	15 m/day	141.3 m/day		
SY_A	0.1	0.2		
SY_K	0.08	0.11		
R_A	15 %	20%		

During the parameter estimation, the focus was inevitably given to the southern part of the model, where there are many observations in the karstic aquifer that receives water from a large part of the model. The final values for the hydraulic conductivities of the karstic aquifer differed a lot from the initial ones, while for the other parameters the initial values were relatively close to the ones estimates with UCODE 2014.

Finally, it should be mentioned that, as seen in Table 11, the hydraulic parameters reached very high values, which are not unrealistic for aquifers of such nature. The high values required have are also related to the way the simulation is done by MODFLOW 2005, i.e. MODFLOW is a finite differences code that is better used in porous aquifers and trying to simulate a karstic system with porous aquifer principles definitely requires higher hydraulic conductivities to produce realistic results.

3.8 Comparative results of the two models

In order to identify which model has managed to better represent the natural system, a straight comparison of the observed and simulated results is made. The comparison is not only based on the hydraulic heads that are simulated each time, but also to more qualitative results (e.g. the water table in the alluvial aquifer) that the models produce.

3.8.1 Observed vs. simulated hydraulic heads

The hydraulic heads that are simulated with the CHD model are systematically underestimated (Figure 3-6). The lower heads cannot be related to the pumping for irrigation since this parameter is not used in the parameter estimation process. In addition, this specific parameter is not used in either parameter estimation process. Using the hydraulic parameters of the karstic aquifer (i.e. the ones with the highest sensitivities) did not improved the residuals in the model. The largest residuals can be seen in the alluvial aquifer where, due to the low sensitivity of the related parameters, a better simulation has not been achieved.

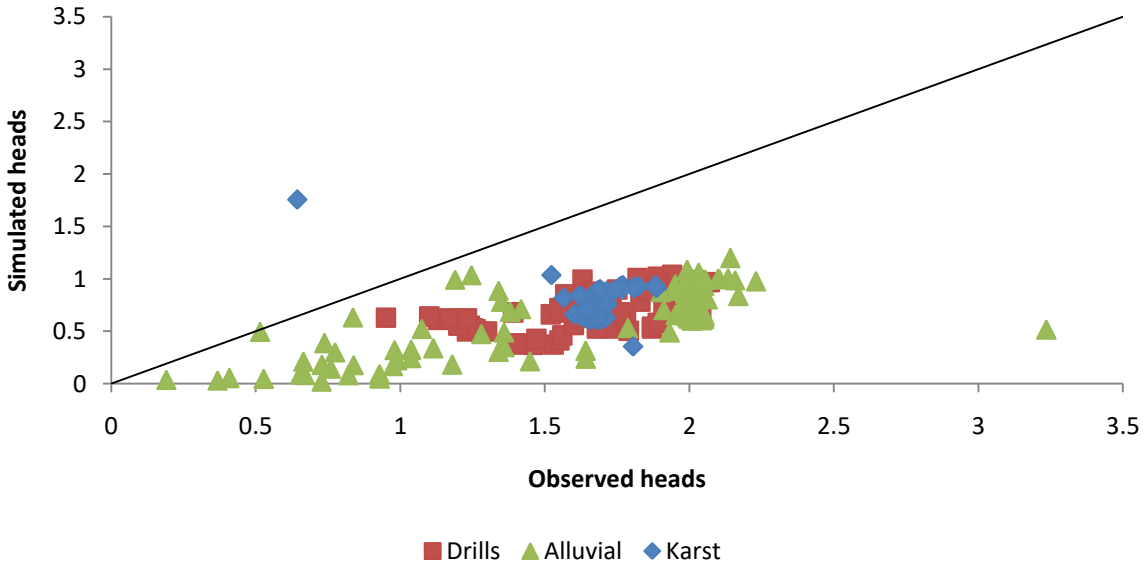

Figure 3-6: Observed vs. simulated heads graph of the CHD model using the final values of the parameter estimation.

Consequently, the CHD model is considered to not giving an acceptable representation of the natural system. Further efforts to calibrate the model were leading to parameters taking unrealistic values and were not successful to improve the final results (Figure 3-7).

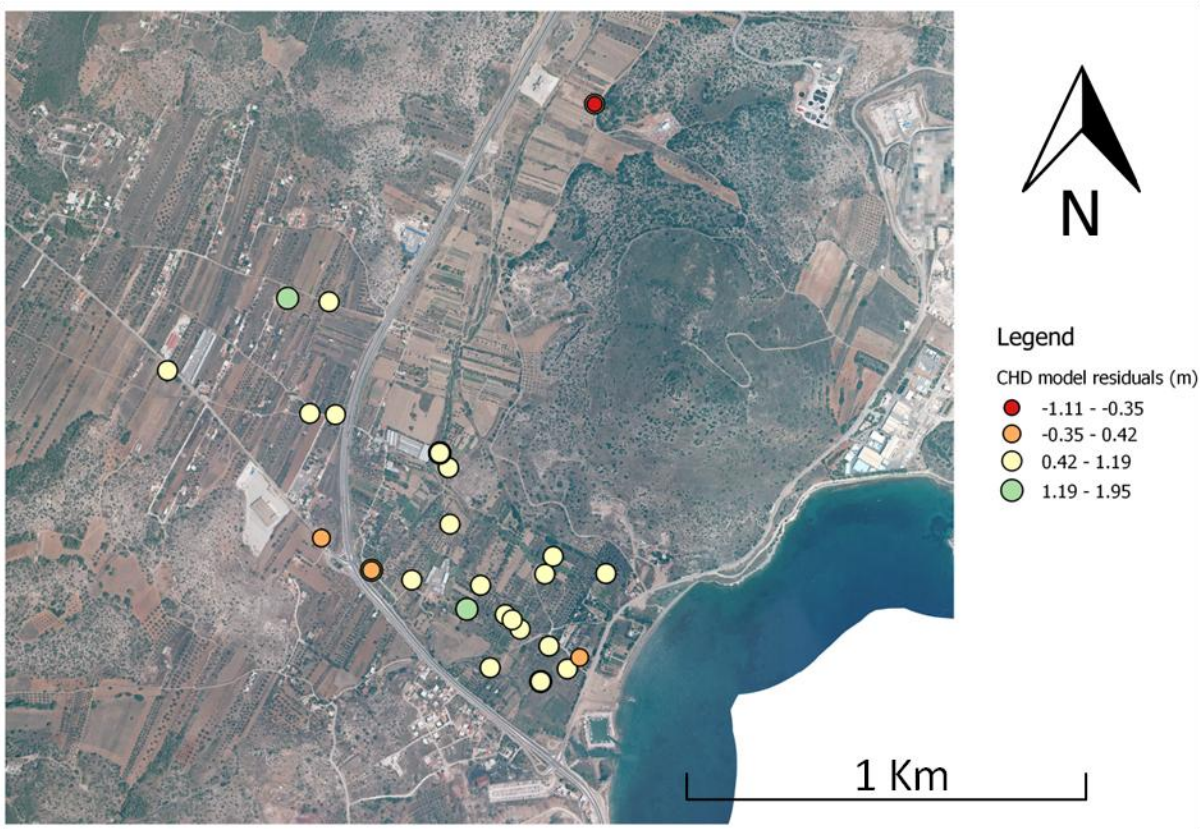

Figure 3-7: Map showing the residual values after CHD model calibration.

Looking at the results of the GHB model (Figure 3-8) there is a clear difference to the results produced by the CHD model. The simulation results are generally matching the observed hydraulic heads in an acceptable level. There are some locations (Drills) where the simulated heads are slightly underestimated and others (Alluvial) that have equally positive and negative residuals spread across the aquifer (Figure 3-9). Overall, the performance of the GHB model is considered to be sufficient and acceptable.

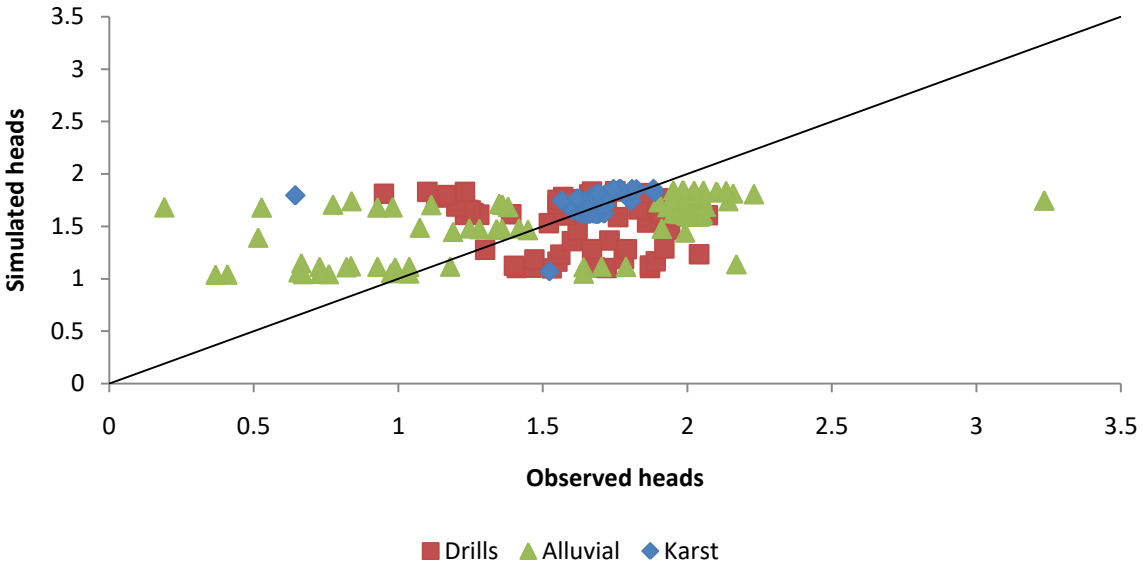

Figure 3-8: Observed vs. simulated heads graph of the GHB model using the final values of the parameter estimation.

The results of the GHB, when compared to the ones of CHD, are clearly much more representative of the natural system. A good indication of the discrepancy of the simulation is the sum of squared residuals (SSR), which for the GHB model is 34.9 m. This figure is considered to be very small taking into account the amount of observations (243 observations in total). As a general rule, the residuals are less than 1 meter in all cases except for a single observation (Figure 3-9).

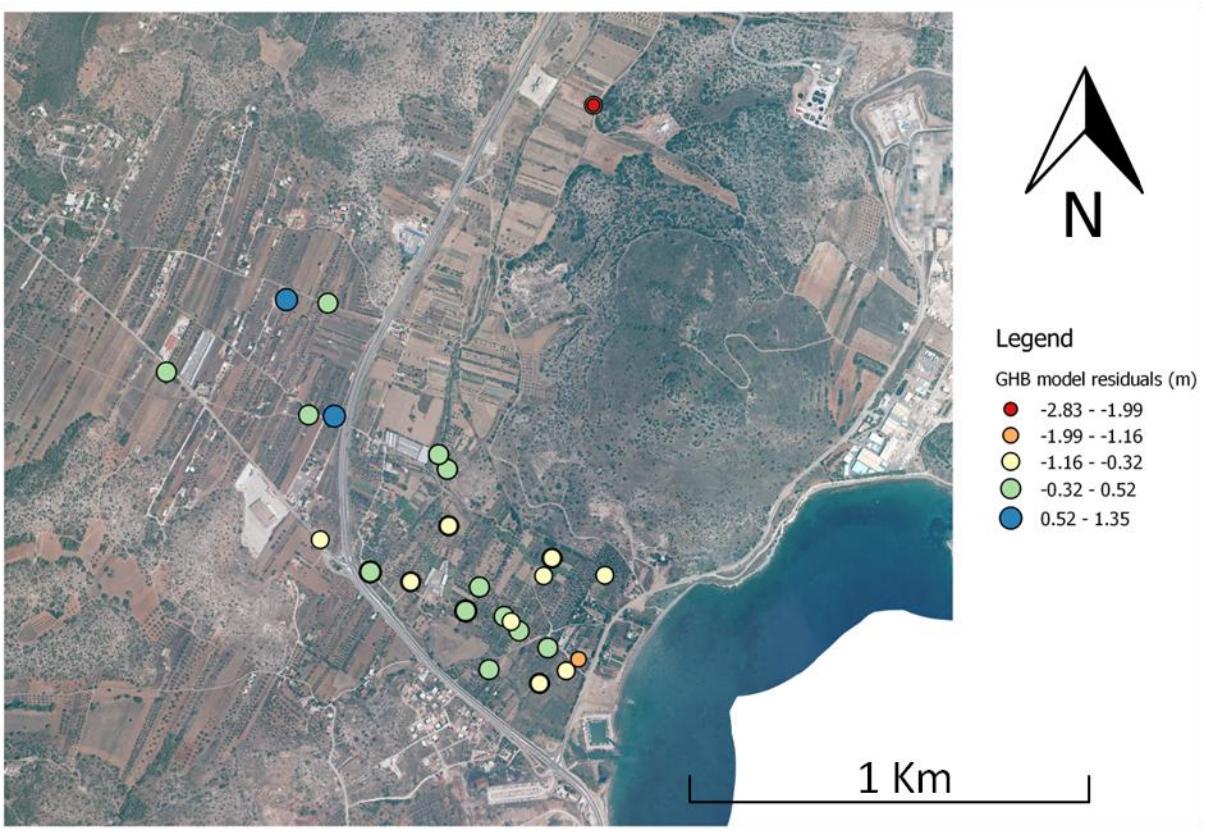

Figure 3-9: Map with the residual values after GHB model calibration.

Another aspect for the evaluation of the model performance is the water table that is produced by the model. A comparison of the water tables simulated by the two models and the water table produced by the field data is at Figure 3-10. The CHD model fails to reproduce the water table at a satisfactorily level, both in terms of absolute hydraulic heads and contour shape. The contour shape is explicitly mentioned because it corresponds to the aquifer hydraulic interconnection, so this is considered to be a very important result. The GHB model on the other hand has a much better performance in both of the aforementioned fields.

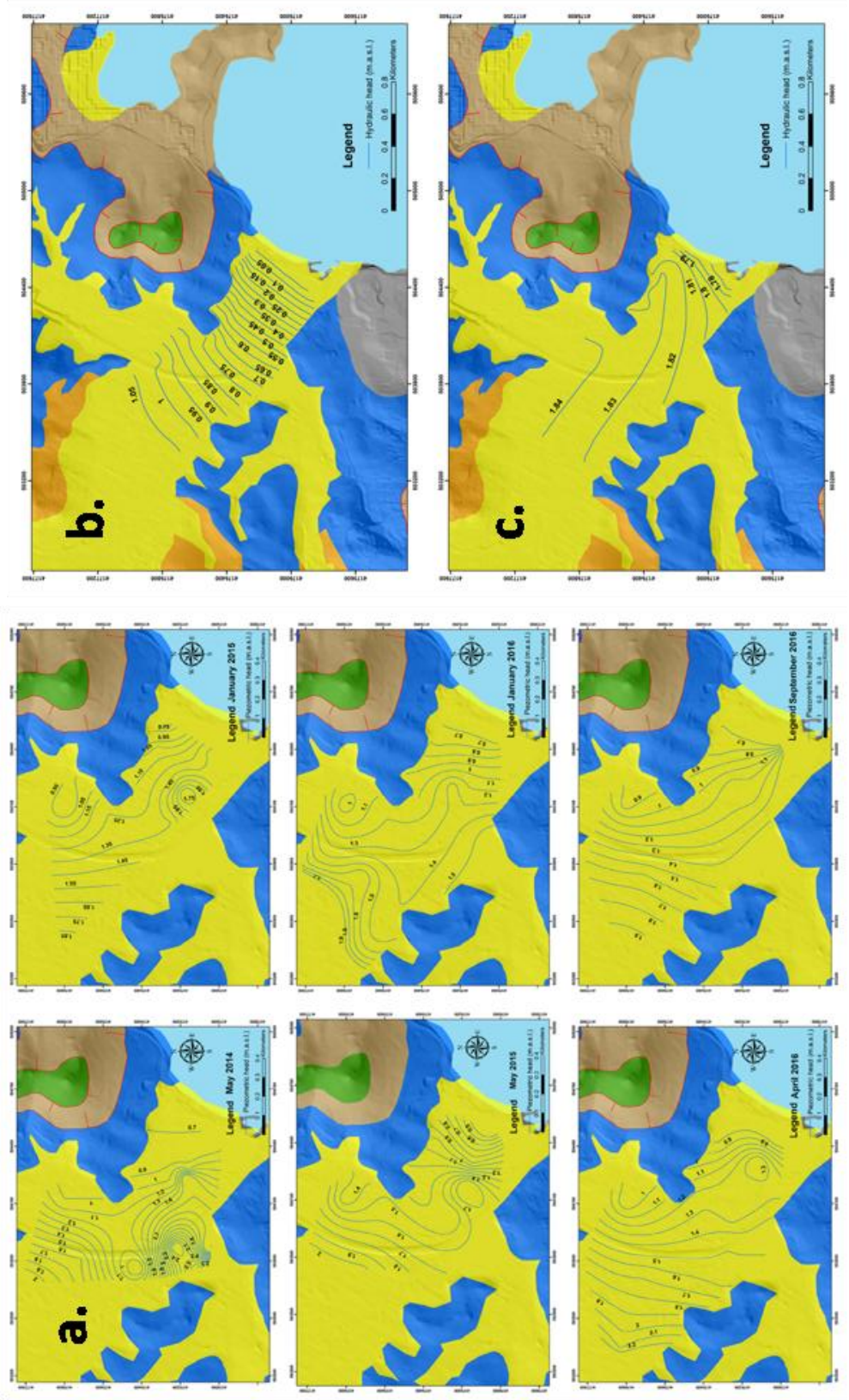

Figure 3-10: Comparison between the piezometric heads in a) the various field campaigns (Pouliaris et al., 2018), b) the CHD model and c) the GHB model. Both model results are at the end of the simulation period (December 2015).

3.8.2 Water budgets

The overall water budget of the model is important for realizing the fluxes that are exchanged between its components. The comparative graph of the water budgets for the two models is presented in Figure 3-11. The main inflow of both models is form the WEL package which represents the recharge for both aquifers. The water of the model is primarily discharged to the aquifer storage and the boundary condition representing the sea. A smaller amount is pumped out of the system and is used to cover the irrigation demand. Under this flow regime, in both cases there is no inflow from the boundary condition at the sea, which is thought to be representative for the study area.

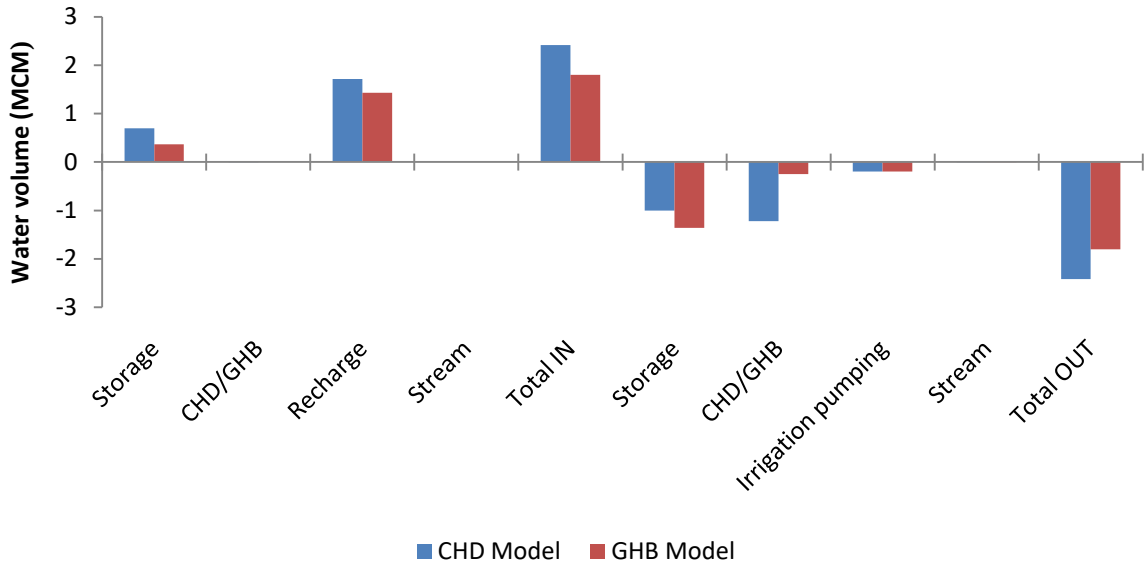

Figure 3-11: Comparison between the water budgets for both models. The components of the budget are the same, apart from the boundary representing the coast (CHD or GHB).

The differences that are recorded can be clearly assigned to the type of boundary condition used at the coast since this is the only difference between the two models. A reduced value in the GHB conductance is presumably the reason why there is a significant amount of water that is stored in the aquifer. In comparison, in the CHD model, corresponding amount of water is directed in the sea boundary and, finally, out of the model. Additionally, there is a slight difference to the amount of water that comes from recharge and this is a result of the parameter estimation process. This higher amount of recharge in the CHD model is not in line with the fact that the hydraulic heads are underestimated (as seen in §3.8.1), which also is an aspect of the fact of the CHD models' underperformance.

3.8.3 Response of the karstic aquifer as represented by the model

An interesting aspect of the model is how well the response of the karstic aquifer in Lavrio is simulated, given that the pumping test results showed that the behaviour of the aquifer when pumped was irregular. MODFLOW 2005 was not expected to precisely manage to simulate all the changes that were recorded by the pressure transducer, but a general trend of the water level fluctuation was aimed to be captured. The results (presented in Figures 3-12 and 3-13) are considered to be satisfactory.

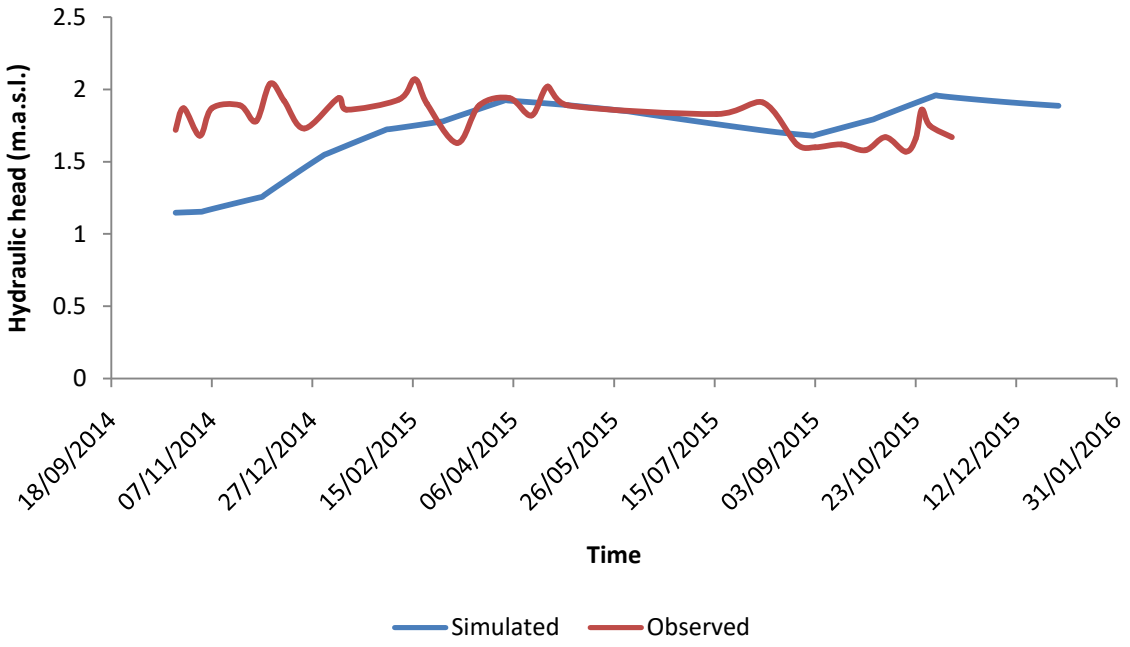

Figure 3-12: Comparison between the simulated and observed heads in the karstic aquifer (Konofagos drill).

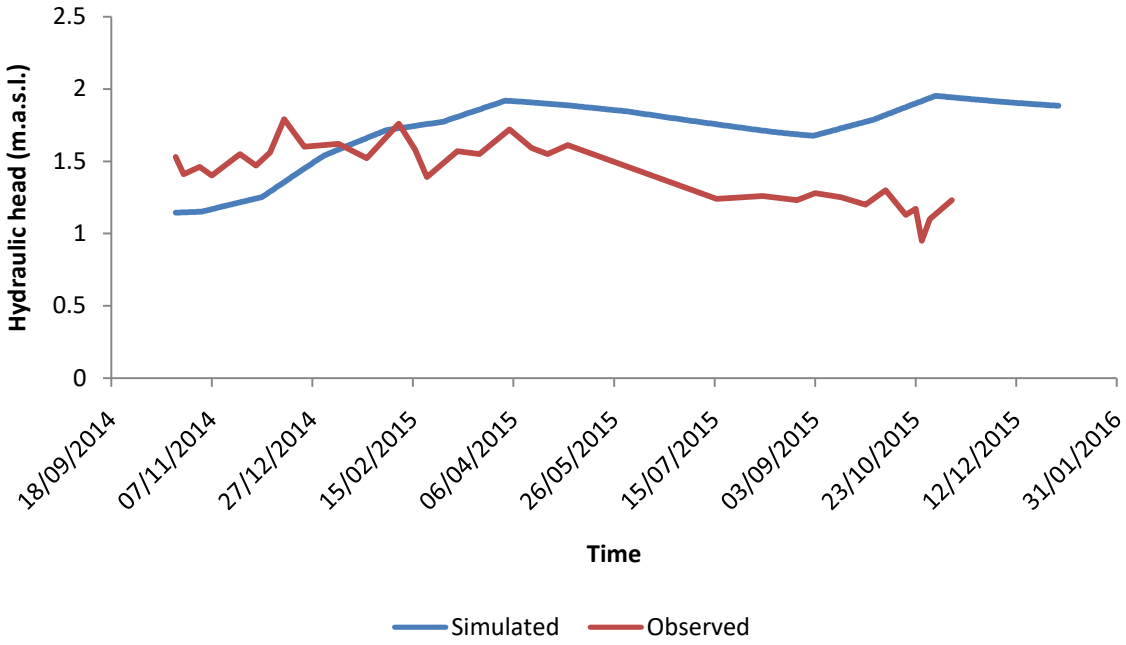

Figure 3-13: Comparison between the simulated and observed heads in the karstic aquifer (Eisodos drill).

Figures 3-12 and 3-13 present a comparison between the observed and simulated heads in the two monitoring points that are in the southern part of the basin. They are approximately 265 m away, both in the karstic aquifer, with Eisodos drill being downstream of Konofagos drill. In the Konofagos drill there is higher discrepancy in earlier times and less in the later times, while for the Eisodos drill this figure is reversed (i.e. heads in earlier times are better represented than the ones in later times). This difference can probably be assigned to the fact that changes in the natural karstic system take place much more rapidly than the changes simulated by MODFLOW, even when the values used for hydraulic conductivity are very high. This results at an artificial hysteresis, with the model needing more time to adapt to and produce the fluctuations that occur in the system. Overall, the discrepancies between the observed and simulated heads, but also between the two appoints, are rather small. It is concluded that, is such small scales, it is not straightforward to simulate the response of such aquifers using MODFLOW 2005, although for larger scales this might be more relevant.

3.8.4 Aquifer flux exchange

Through the modelling activities in Lavrio, interesting outcomes occurred regarding the hydraulic connection between the aquifer in the area. The exchange of the water between adjacent aquifers is

usually a major component of every water budget. However, it is usually difficult to quantify, so an approximation can be achieved only when all the other components of the water budget are known.

Having a well calibrated groundwater flow model can give an insight on that aspect. In the study area there is an exchange of water between the two aquifers (Figure 3-14) that takes place throughout the whole hydrological year. The largest amount of water flows from the karstic aquifer to the alluvial one, while there is also a small amount of water flowing the other way round. This figure represents the total exchange that can, however, vary spatially.

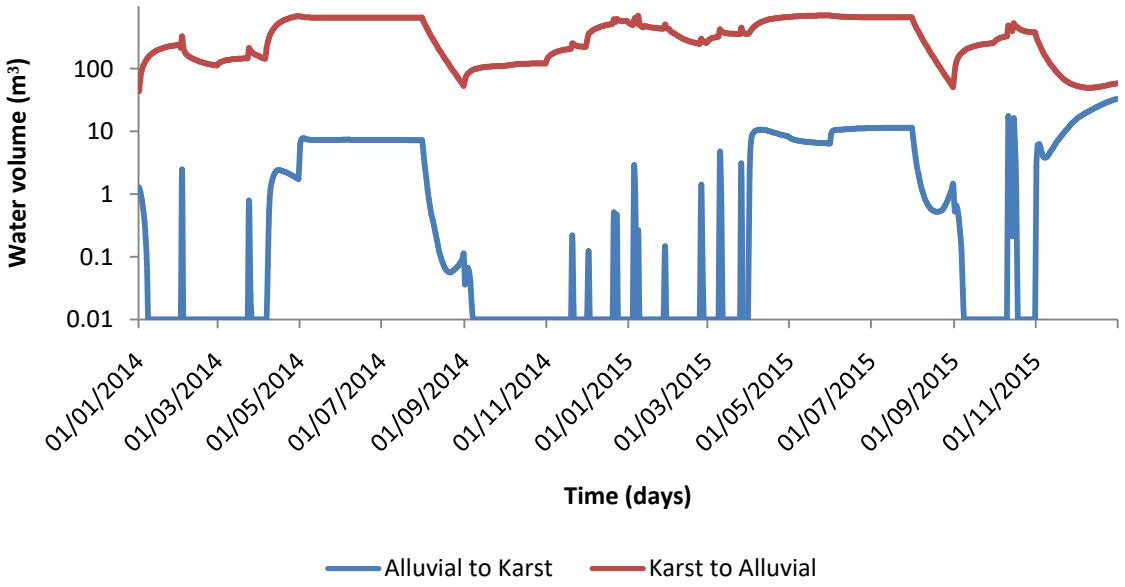

Figure 3-14: Exchange of groundwater between the karstic and alluvial aquifers in Lavrio.

The results presented above, although valid, could at a certain level be affected by the fact that both aqufier are in contact with the sea and that effect cannot be somehow accounted. Nevertheless, this would probably slightly affect the quantities that are exchanged and not the general flow regime.

4 Karst aquifer model

4.1 Idea for moving on to a karst implicit model

The primary idea for the further development of the model was to focus on the karstic aquifer and use the MODFLOWCFP code (Shoemaker et al., 2007) in order to simulate the processes that are related to karst. The base of that model was the model developed with MODFLOW 2005, so all the initial parameters used originally came from this previous work.

The layer that in the initial model was representing the karstic aquifer was further discretized into 6 layers in order to have some better insight into the flow regime within the aquifer. Field data about the characteristics of the fractures of that aquifer were acquired from outcrops in various locations in the study area and implemented into the model. The data gathered were the features of the joints of the marble formation (that hosts the karstic aquifer) has, including plane orientations, aperture, filling etc. This information was later used in the model as input values for the linear elements that represent the conduits in the model.

4.2 The MODFLOW CFP code: conduit flow process

The rising interest in focusing at the processes that take place within a karstic aquifer have led to the need for a code that treats the secondary porosity implicitly. The understanding of the flow in fractures/conduits has also led to the development of different concepts when modelling such systems (Figure 4-1). MODFLOW CFP has the advantage of being able to simulate a network of discrete conduits that are either connected with each other or totally isolated. Additionally, there is also the option to simulate a preferential flow layer that could either represent the unsaturated flow, especially in the case there is an epikarstic layer present, or any other preferential flow path.

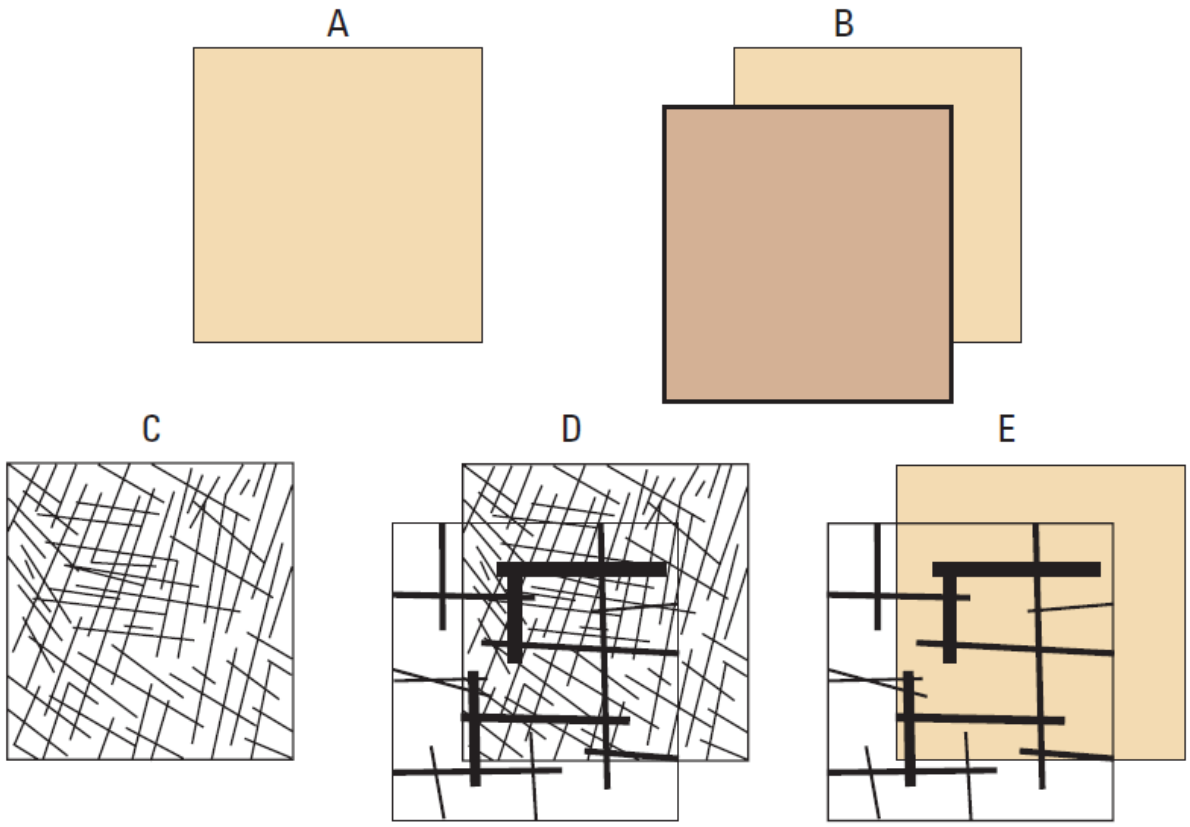

Figure 4-1: A variety of approaches can be use to model a karstic aquifer (A single continuum, B double continuum, C discrete fractures, D discrete multiple fracture networks, E discrete conduit coupled to single continuum, Shoemaker et al., 2007).

An important aspect of the karstic aquifers is that the flow, especially in the conduits, can change between laminar and turbulent conditions. MODFLOW CFP can also account for that by using a lower and upper Reynolds number to trigger the transition from one flow state to the other. For that reason, Hagen-Poiseuille equation is used for laminar flow conditions, while for the turbulent flow the Darcy-Weisbach equation is applied.

4.3 Karstic model structure

As mentioned above, the base of the karstic model is the previous flow model that has been developed with MODFLOW 2005. A series of modification had to be made in order to be able to focus on the karstic aquifer in higher detail.

The first step was to divide the layer into 6 distinct layers. Since the total thickness of the layer in the previous model is 60 m, in the karstic model the decision was made for all layers to have equal thickness of 10 m. The amount of layers chosen to be simulated is considered to be able to

reproduce the complexity of the flow in the karstic layer. The topography of the model was taken into account so that the new model layers follow it, in order to not have a straight bottom in each layer. In the end, the layers have the same thickness and similar topographies.

The zones with the different hydraulic conductivities were also used in the same way as in the parent model. For each one of the model layers there was a new conductivity zone introduced that was similar to the zones used in the parent model. This was slightly altered for some layers that were smaller in extend than others. Additionally, the same zones were used to implement vertical hydraulic conductivity parameters values. This is a major differentiation from the initial model, were the value of the vertical hydraulic conductivity was fixed to an order of magnitude lower than the horizontal hydraulic conductivity in each zone. This addition was necessary because, in the case of karstic aquifers, the vertical hydraulic conductivity is expected to have a large influence in the flow regime. Also, it is probable that the value of the vertical hydraulic conductivity is higher than the horizontal one because, in the natural system, the flow is primarily in the vertical direction (Figure 4-2) and the higher vertical conductivity values basically represent the rapid infiltration rates of those systems. This vertical flow can be enhanced when an epikarstic zone is present, or can be decreased if there is a soil horizon covering the karstic formation.

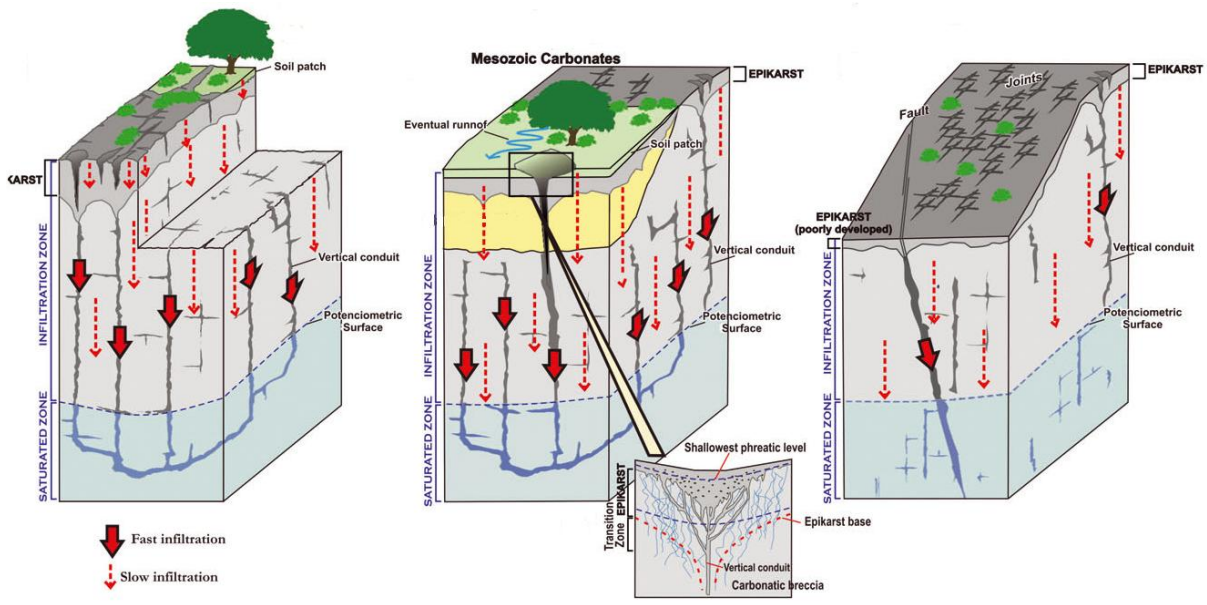

Figure 4-2: Conceptual model of the flow in karstic aquifers (Guardiola-Albert et al., 2014, with modifications).

Although the karstic model is based on the already existing MODFLOW model, changes in the initial parameter values had to be made, since at this version of the model they are representing just the

matrix conductivity and not a combination of the matrix and fracture conductivity. The change in the structure of the model (dividing the single layer to 6 layers) was another reason that imposes the lowering of the initial parameter values, because starting with a high value would probably lead to numerical instabilities. The additions made were related to the fractures and their geometrical characteristics, as they were recorded during the activities performed in the field.

4.4 Model driven geological investigation

When building such a model, one of the major inputs is definitely data related to the geometrical characteristics of the fractures. This is a type of data that are very rarely available and, even if there is some data availability, very often they are just presented in a qualitative way (e.g. rose diagrams with general trends). Since in the case of Lavrio there was no dataset available, a series of fracture characteristics measurements were performed in the field in various locations (Figure 4-3). The specific sites were chosen in order to have a representation of the fractures of the formation that is as representative as possible.

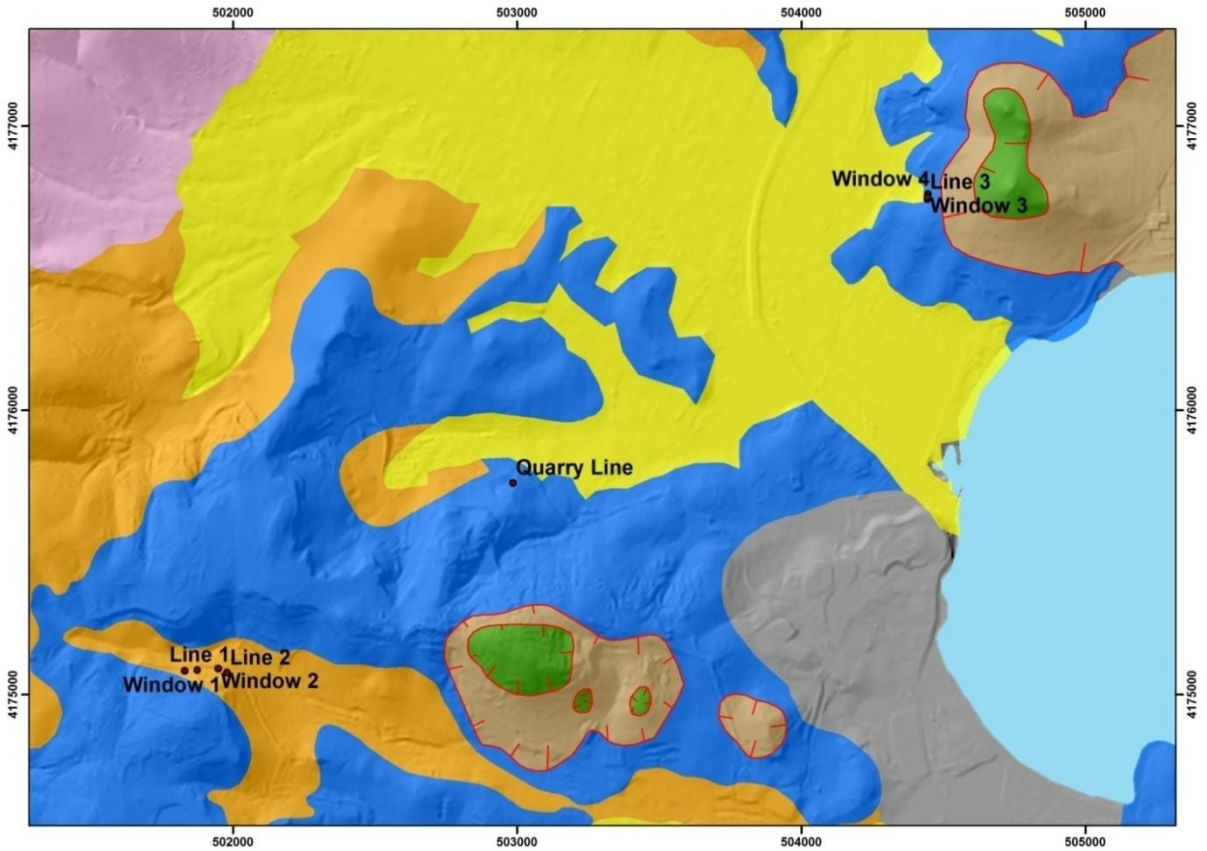

Figure 4-3: Map with the locations of the sites where the various field surveys were performed.

The methods used for the collection of fracture data were scan line surveys and fracture mapping. The implementation of these methods is done in outcrops of fractured rocks where different attributes are measured. The two methods use common principals in general, with the difference being that on one case (scan line surveys) the fracture characteristics are measured in along a measurement tape while, in the other (fracture mapping), the measurements are taken within a smaller part of the outcrop (usually called "window"). The properties that are measured are the following (Table 12):

Table 12: Data that was taken in the field when using the scan line survey and fracture mapping methodologies.

Property	Scan line survey	Fracture mapping	Details
Distance (in m)	✓	×	Distance from the beginning of the line
Dip/strike (in degrees)	✓	✓	Orientation of the fracture
Aperture (in mm)	✓	✓	Distance between the two walls of the fracture
Filling	✓	✓	Composition of the filling of the fracture, if any (usually either soil or $CaCO_3$)
Length (in m)	✓	✓	Length of the fracture (estimated in many occasions)
Nature	✓	✓	Primarily joint or conduit
Termination	✓	✓	Whether the fracture terminates in the outcrop/window
Truncation	×	✓	Choice of the minimum length to account for a fracture

4.4.1 Scan line surveys

In the scan line survey (Figure 4-4) the fractures are measured across a line that is placed in the outcrop. The distance from the start, along with information for each fracture (strike, dip, aperture, filling, nature and termination) is recorded. The line should be as straight as possible in order to have a more accurate representation of the fractures in one direction, which is the orientation of the line. The advantage is that a sufficient set of data regarding the fractures, at a relatively large extend, can be collected with this method. The disadvantages are that, in many cases, the length of the fractures has to be estimated because the surveyor cannot reach the top end of the fracture. Also, the

fractures that can be recorded are the ones that are crossing the line, excluding in that way fractures that are not vertical or with high dip values.

Figure 4-4: Scan line survey taken at an outcrop south of the city of Lavrio.The length of fractures with high angles had to be estimated because it was not easy to measure them due to the height of the outcrop.

4.4.2 Window mapping

In the window mapping (Figure 4-5) the method followed is slightly different than the scan line survey. First, a sample window is defined and this is where the fractures are going to be measured. The window ideally should be representative of the fracture spatial distribution. The area that the window has to cover can vary, although for practical reasons it would be good to have more than 1 m^2, and it should also be related to the density of the fractures. The characteristics of the fractures are also recorded (strike, dip, aperture, filling, length that is included in the window, nature, termination and truncation) in a similar way to the scan line survey. With this method the disadvantage is that the area covered is still relatively small compared to the whole formation and the area that this method can be performed is limited but the height the surveyor can reach. On the

other hand, the fact that the measurements are covering an area and not a line can give better information about the different families of fractures that exist in the formation.

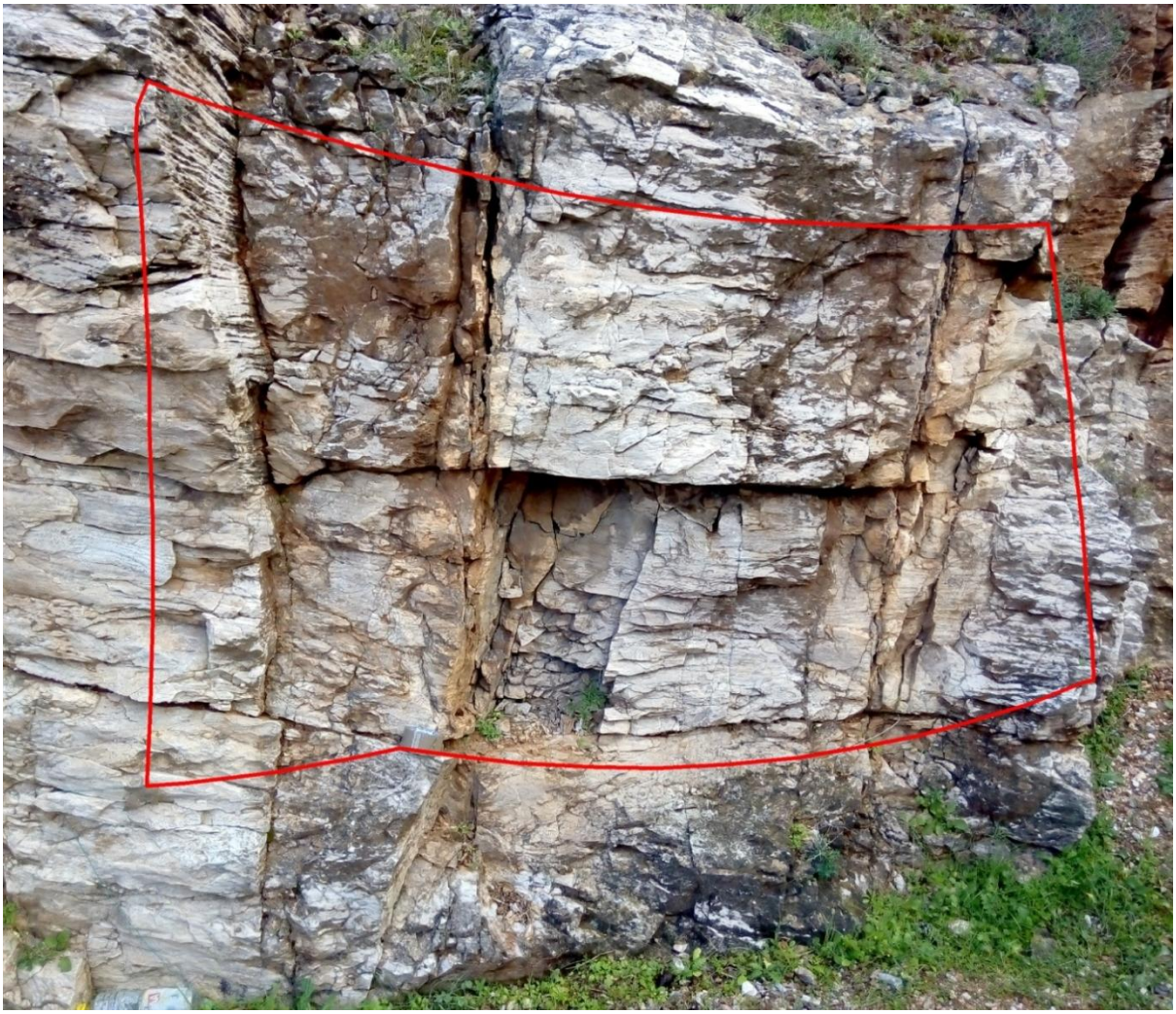

Figure 4-5: Fracture mapping in a window at an outcrop by the main road. The area that was used is highlighted.

In conclusion, both methods have advantages and disadvantages when compared with each other, so the combination of the two is probably the best way to perform such surveys. When the methods are combined the results can definitely be more reliable and trustworthy. It should be mentioned thought that the two methods share a common disadvantage, that being that they are biased by the orientation of the outcrop and, as such, any fractures that have a plane parallel to the outcrop cannot be recorded. To avoid missing important information, such surveys have to be performed in as many different locations, with different orientation as possible.

4.4.3 Fracture data acquired

The data that is specifically required by the CFP package depends on the module that is used. The appropriateness of each module for simulating an aquifer is certainly site specific, while it depends on the process that the modeller needs to simulate and the availability of data in each case. The modules can be used individually or in combination, if the data needed for either of them is available and the conceptual model can justify this choice.

CFP has two available modules that can be used for the simulation of the karstic aquifer. The first one is simulating a preferential flow layer, which could be applicable in the case of an epikarstic zone with significant hydrological processes taking place. The data needs of that module are limited to the temperature of the groundwater, so it can theoretically be applied in every case. In the case of Lavrio though, the epikarstic zone is not expected to have high impact on the processes taking place in the subsurface. The second available module is far more demanding in data that is not just related to the physical parameters of the fracture but also to the geometrical features (Table 13). While the geometry of, at least, the large cavities could be ideally taken from speleological studies, the physical parameters can be very difficult to acquire or estimate. The evaluation of the pumping test data (§ 2.4.4) has certainly been a starting point when the hydraulic conductivity parameters of the karstic model were implemented. Other parameters, such as the conduit wall permeability, had to be approximated. Overall, the building of the model was done taking into account the fracture characteristics that were taken from the scan line surveys and the fracture mapping, the results of the previous model and the data evaluation of the pumping tests.

To be able to make a model application for the area of Lavrio, certain simplifications in the initial model were made. The most significant of all is that the cell size had to be increased to 100 m X 100 m grid, something which aided the convergence of the code and substantially reduce the running time of the model. Another important change was in relation with the alluvial aquifer, for which the simplifications was that the pumping from that aquifer was neglected. The recharge, however, was included because to keep the main hydrogeological concept unchanged.

Table 13: Parameters and respected values used in the CFP package of MODFLOW.

Pipe property	Data source	Value	Details
Diameter (m)	Field measurements	Varied (depending on the location)	Mean diameter of the pipes
Tortuosity (m)	Approximation	1	The measure of how straight the pipe is
Roughness height (m)	Approximation	0	The measure of how smooth the inner walls of the pipe are
Lower Reynolds number (-)	Shoemaker et al., 2007	2000	The number at which the flow transits from turbulent to laminar
Higher Reynolds number (-)	Shoemaker et al., 2007	12000	The number at which the flow transits from laminar to turbulent
Wall permeability (m/d)	Estimation	5	Conductance factor that controls the exchange of water between the matrix and the conduit

4.4.4 Overview of the characteristics of fractures

The orientation data recorded from the fractures (Figure 4-6 a and b) show that the mean pole azimuth of the 119 fractures, for which measurements were taken, is 61.35°, while the mean dip is 31.04°. These attributes can also be seen in the pole projection showing that most fractures are dipping towards SSW directions. There is also a large number of fractures that have are dipping with very low angles (up to 10°) that at some occasions dip towards EES and on others at WWN. These results show that there are some general trends on the fracture directions in the karstic aquifer in Lavrio, making this a valuable piece of information for the understanding of the general subsurface flow directions.

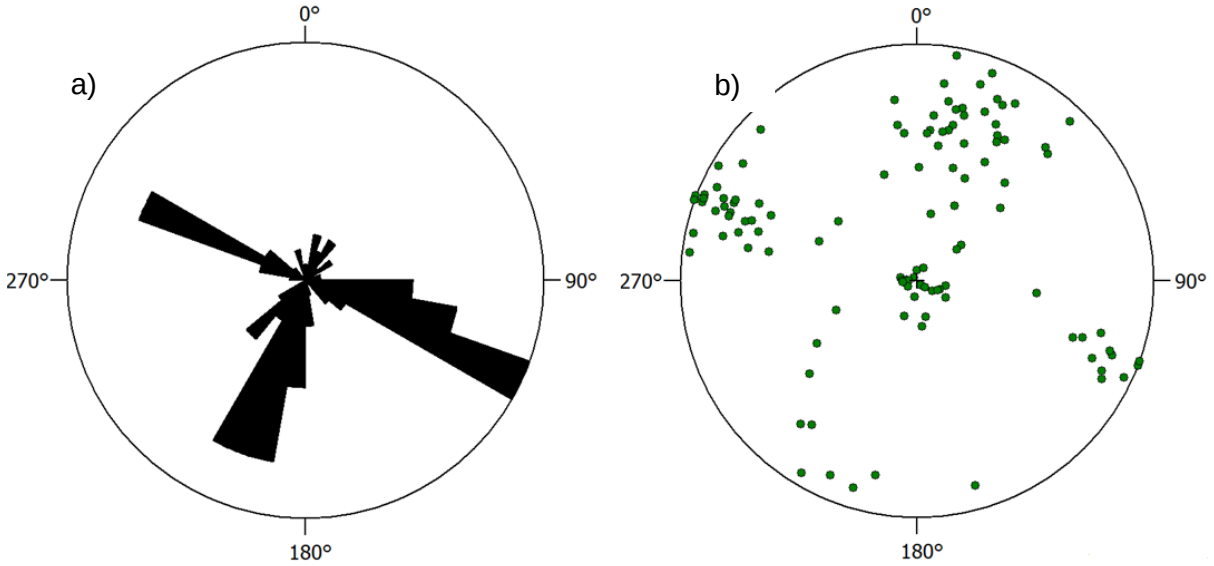

Figure 4-6: Lower hemisphere rose diagram (a) and pole projection (b) for the sum of fracture data that was taken in Lavrio.

4.5 Fracture implementation into the model

Process of introducing the fractures to the model is certainly of major importance because the simulation is closely related to it. In general, the data can be implemented in MODFLOW CFP as linear features. To have a representation of a planar element, such as a fracture, a series of “conduit” objects have to be used (Figure 4-7). To be able to use that concept, the model needs to be modified in order to be able to combine the data that have been recorded in the field and the data that is required by the model. A common example is the diameter of the conduit, where for a conduit that represents a cavity in the formation, a large diameter is applicable (with a value of some meters), while when using this feature to represent a fracture, diameters are expected to be small (having a maximum value of a few millimetres).

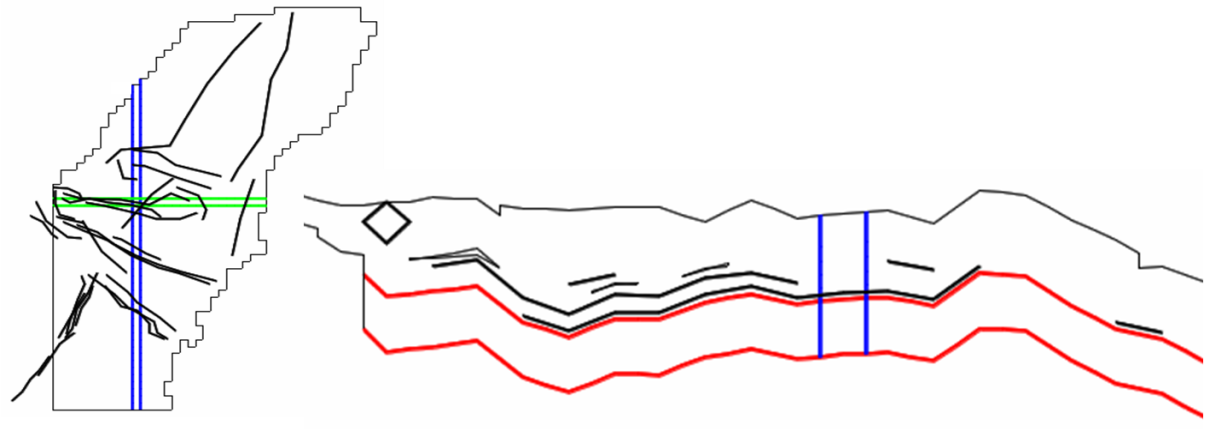

Figure 4-7: Fracture representation in the model. The lines represent the "conduits" that are placed at a sequenced of cells in order to represent a fracture.

To be able to import the fractures, a certain equation is used to transform the measurements that are taken in the field to three - dimensional information. This equation is called the scalar equation of a plane (Eq. 5) and when used the spatial extent of the plane of the fracture is reproduced:

$$Elevation = Z_0 - \left(\frac{1}{\sin(Dip)}\right) * (\sin(Azimuth) * \cos(Dip) * (X - X_0) + \cos(Azimuth) * \cos(Dip) * (Y - Y_0)) \quad \text{Eq. 5}$$

where *Elevation* is the final elevation at where the fracture is, X_0, $Y_0$and $Z_0$the coordinates and altitude where the measurement is taken, *Azimuth* and *Dip* the characteristics of the fracture.

For this equation, the coordinates of the measurement point, along with the elevation and the strike/dip of the fracture are required. When this information is imported into the model user interface, the locations that are crossed by the fracture are automatically shown. Sequentially, a series of linear features are drawn into the areas that are highlighted and the information about the fractures is implemented for each one.

4.6 Fracture CFP characteristics

The characteristics of the fractures were grouped while recorded in the field, so the fracture "families" that are created are not filtered later with respect to their characteristics. The grouping is expected to be more representative of the formation itself, using a geological approach, rather than a statistical approach. Finally, the grouping was also done so that points that are in close proximity are teamed to form one group (Table 14).

Table 14: Characteristics of the fracture families, as recorded in the field.

Class	Family	Azimuth	Dip	No of fractures
Quarry	1st	5.33	-5.33	6
//	2nd	122.33	-64.44	9
L3, W3, W4	1st	102.33	-66.27	15
L1, L2, W1, W2	1st	21.62	-84.62	21
//	2nd	202.22	-83.78	9
//	3rd	18.29	-70.86	8

As mentioned above, there is a certain bias when taking such measurements that is related to the orientation of the outcrop (Figure 4-8). To avoid this bias in the model, the choice of the locations where the surveys were made was done in order to be able to measure in outcrops with orientation that was as different as possible.

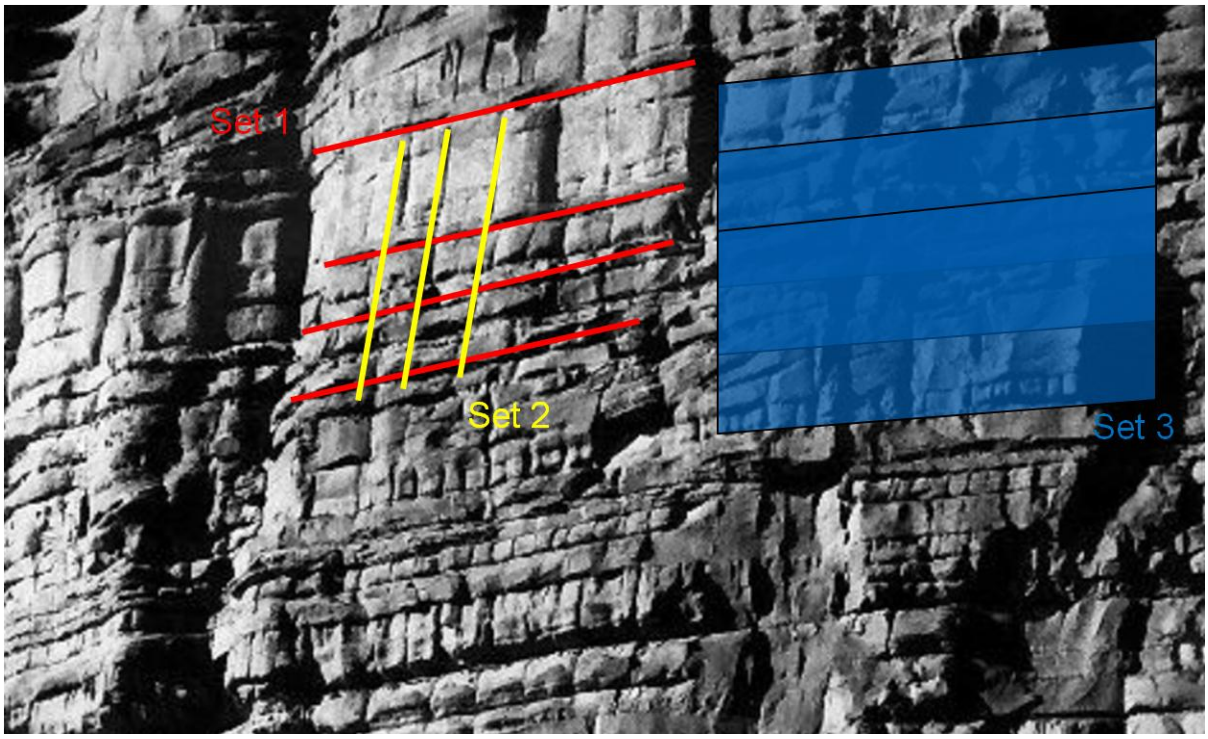

Figure 4-8: Representation of a fracture aquifer in the field. Sets 1 and 2 are easy to track and measure on the outcrop, while the features of Set 3 cannot be recorded because it is parallel to the orientation of the outcrop.

4.7 Sensitivity analysis of the karstic model

The sensitivity analysis of the model was performed, as in the parent model, in sequential steps. The aim, specifically for the karstic model, is to identify the parameters that are important for the model, starting from the ones that are common with the parent model and moving on to the parameters that characterize the flow in the karstic system. For the purpose of using those parameters, minor changes were made in order to get a better representation of the hydraulic heads in the karstic aquifer, since the initial residuals were much higher (when the single layer was divided in six) than the ones in the parent model. The tool used for that sensitivity analysis was once more the UCODE 2014 code.

The same process was followed when the vertical hydraulic conductivities were explicitly introduced in the model. This was done because it was expected the vertical conductivity of the layers was going to have a major impact on the result, reflecting the fact that the direction that the water primarily flows is vertical.

Finally, the sensitivity analysis of the CFP specific parameters was performed. The aim is to identify the most important parameters and have a better understanding of the characteristics that need to be clear when an application of MODFLOW CFP is required.

4.7.1 Sensitivity analysis of the initial model parameters

In the first sensitivity analysis was the base for the first minor changes in the model. All the parameters used were included in that step. Results showed that the SY_K_S was by far the most sensitive parameter in the model (Figure 4-9). HK_K5_S, HK_K6_S and HK_K4_S followed, with small differences from GHB_N_4S and HK_K3_S.

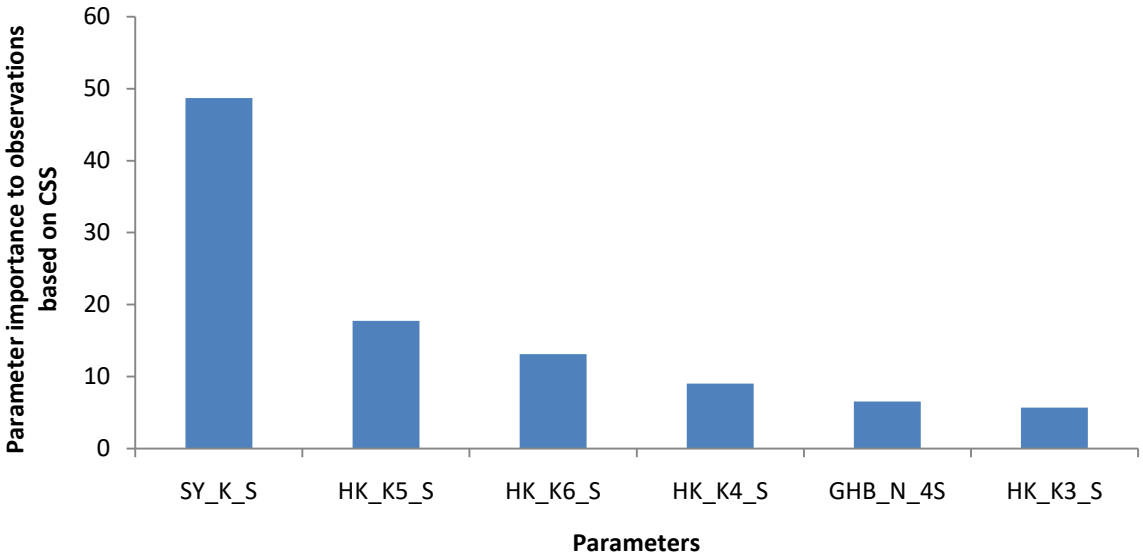

Figure 4-9: CSS for the parameters of the parent model. Each zone used in the previous model was also included for each layer of the karstic model.

The same analysis showed that there are certain pairs of parameters that are highly correlated but, in this case, it does not create any problems since the parameters that are highly correlated do not have high sensitivities, so they are not going to be used in the initial parameter estimation.

4.7.2 Parameter estimation of the initial model parameters

As mentioned above, a first step of parameter estimation was introduced in order to lower the residuals and be able to produce more trustworthy results when proceeding to the sensitivity analysis that included the parameters related to the conduits.

In that step, the parameters with the highest CSS, as presented above, are used. In the first run, HK_K6_S and SY_K_S were estimated and this already had a major impact on the residuals. Following, the second run included HK_K4_S, HK_K5_S and HK_K6_S, while in the last run the parameter with the highest CSS (SY_K_S) was once more used. The parameter estimation was not further used because at that point the results (Table 15) produced by the model were considered to be sufficient for moving on the sensitivity analysis of the CFP related parameters.

Table 15: Parameter estimation using the parameters of the initial model.

Parameter	Starting Value	Estimated value	Initial SSWR	Final SSWR
HK_K6_sout	0.005	0.03027	6991500	5587900
SY_K_south	0.08	0.1328		
HK_K4_sout	0.005	$1 * E^{-07}$		
HK_K5_sout	0.005	$0.7978 * E^{-05}$		

4.7.3 Sensitivity analysis using vertical conductivities

The second sensitivity analysis included the vertical conductivity parameters for each one of the karstic layers, along with the parameters that were used in the first parameter estimation (Figure 4-10). This was aiming to both reduce the running times and, at the same time, use only the parameters that were important in the previous step.

As expected, the vertical hydraulic conductivity parameters showed high sensitivities compared to the parameters of the initial model. In fact, only HK_K6_S shows a significant CSS, similar to VK_K5N and VK_K6M. The highest CSS was recorded for VK_K3N, VK_K4M and VK_K5M. All the other parameters followed.

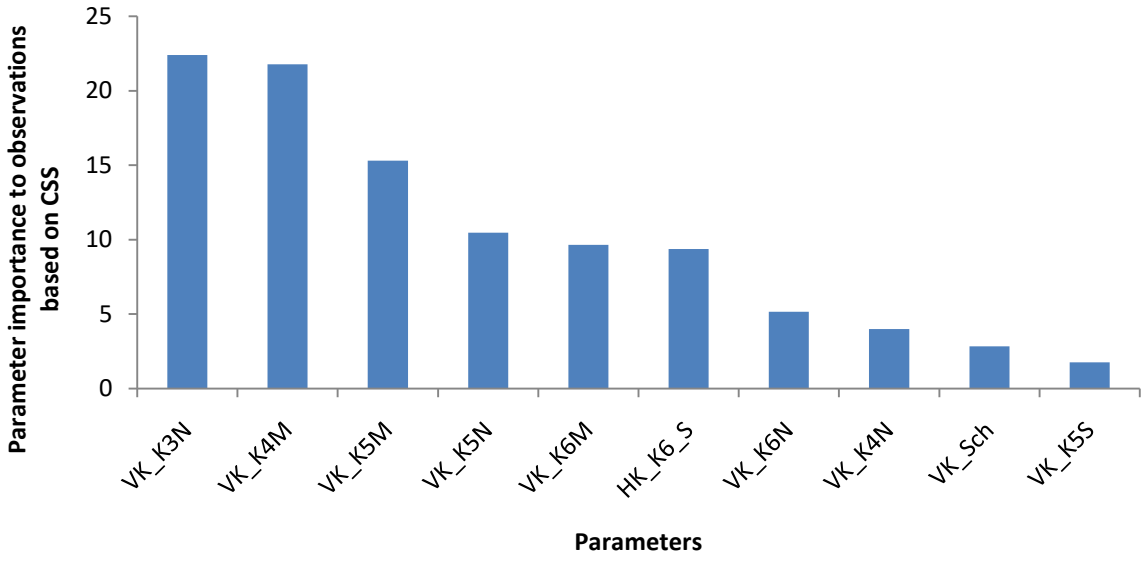

Figure 4-10: CSS graph of the sensitivity analysis that included the vertical conductivities.

With respect to correlation coefficients, there are some parameters that show very high correlation (Table 16), but, in general, there are not many parameter pairs that cannot be simultaneously used in the same parameter estimation run.

Table 16: Correlation coefficients for the parameter pairs that have the highest coefficient values.

Parameter 1	Parameter 2	Correlation coefficient
VK_K3N	VK_K4M	-0.99
VK_K3S	VK_K4S	-0.96
VK_K5N	VK_K6N	-0.97

4.7.4 Parameter estimation using vertical conductivities

An additional effort was made to further increase the accuracy of the simulated hydraulic heads but this time the parameters used in the parameter estimation process were VK_K3N, VK_K5N and VK_K5M (Table 17). The simulated results were further improved, so the next step of having a sensitivity analysis that included the CFP related parameters was initiated.

Table 17: Parameter estimation using the vertical hydraulic conductivities.

Parameter	Starting Value	Estimated value	Initial SSR	Final SSR
VK_K3N	$5 * E^{-06}$	$0.1485 * E^{-03}$	27413000	18707000
VK_K5N	$5 * E^{-06}$	$0.2389 * E^{-02}$		
VK_K5M	$1 * E^{-05}$	$0.1745 * E^{-02}$		

4.7.5 Sensitivity analysis of the CFP module

For the sensitivity of the CFP related parameters the choice was that they are going to be tested in comparison with the most sensitive parameters of the previous sensitivity analyses (i.e. the one that included the vertical hydraulic conductivities). The aim was to have a holistic approach for all the parameters and their relative sensitivity.

The CSS graph for that sensitivity analysis (Figure 4-11) shows that the pipe diameter (Diam) is without a doubt the most important parameter affecting the hydraulic heads in the model. Tortuosity (Tort), VK_K4M and the conductance of the conduits' walls (cond_CFP) come after the diameter, with small changes among them. Surprisingly, SY_K_S, which was the parameter with by

far the highest CSS in the first sensitivity, has very low CSS in this sensitivity. The rest of the parameters do not show any sensitivity.

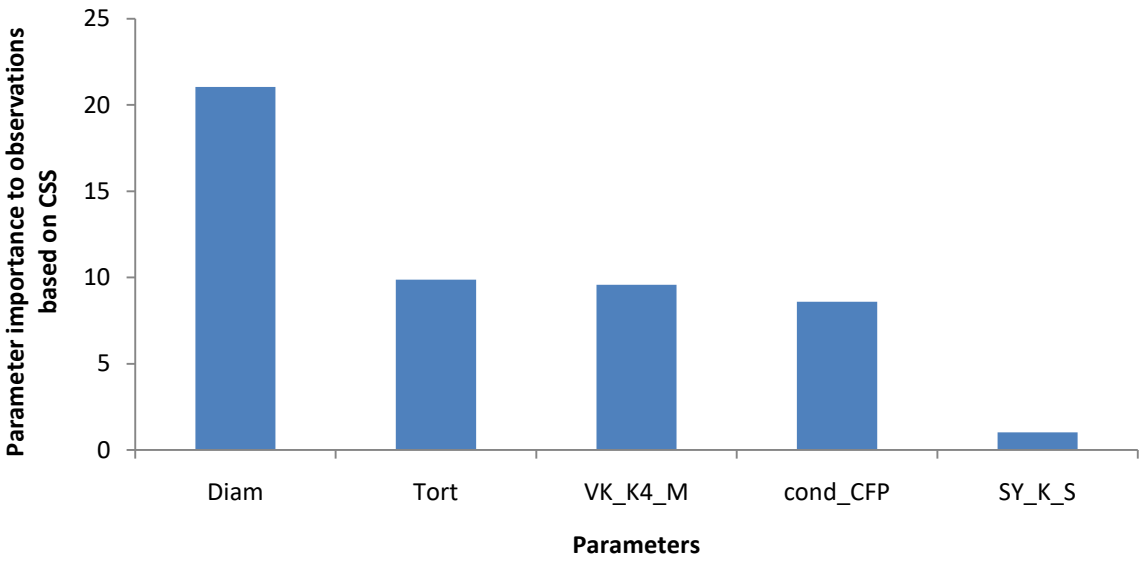

Figure 4-11: Sensitivity analysis results of the parameters related to the CFP module, along with the most sensitive parameters from the previous analyses.

Regarding the correlation coefficients, the only pair of parameters that has really high correlation is tortuosity and the wall conductance of the conduits, which have a -0.99 correlation coefficient. This could potentially cause problems in parameter estimation, but performing parameter estimation using the CFP related parameters would take the scope of the present study too far.

4.8 Results and comparison of the three sensitivity analyses

The comparison of the sensitivity analyses of the various model leads to some interesting conclusions, regarding not only the modelling of the karstic system in Lavrio but more general the way karstic systems are simulated.

The first outcome is that the CFP related parameters have a very high influence to the simulated results. This is, of course, what was expected of a karstic model, but the important part is that by far the most crucial parameter is the diameter of the conduits. This parameter is definitely very difficult to have in a large extent of the aquifer. The method used in the present study may be a good approximation to the karstic conduit network developed in an aquifer, but it would still depend on the availability of suitable locations for recording the information related to the fractures. The case

studies where the use of that specific methodology may be the most applicable are the ones where good knowledge about the development of caves is available. A mapped network of caves could be easily introduced into such a model and the results of the simulation could be highly valuable. However, the calibration of such models would still require hydraulic head measurements from such aquifers, which may or may not be easy to have, especially when these caves are under any kind of protection scheme.

Another important aspect of those models that was initially underestimated is how sensitive the model was in the vertical conductivity values. In general, the vertical conductivity is underrepresented in traditional groundwater flow models, where in many cases it is considered to be a default fraction of the horizontal hydraulic conductivity (usually 10 %), although this might be found to vary slightly. This approximation is probably valid in granular aquifers under normal conditions but apparently this is not the case for karstic aquifers. The fact that the unsaturated zone is very thick, as is the case in Lavrio, and the existence of the vertical preferential flow paths are probably the reasons why this high sensitivity of these parameters is noticed.

There is also a controversy in the combination of the flow in karstic aquifers and having the more conventional matrix (as it is used in MODFLOW) approach. This is linked to the models' structure and the reasons why MODFLOW has been initially developed by USGS. The introduction of many conduits in such a system might cause problems in the numerical simulation of the system, resulting in instabilities that could prevent the model from solving successfully the flow equation. For that reason, the best way to approach such systems may be to exclude smaller conduits/fractures and either consider them to be negligible or use bulk hydraulic conductivity values that account for both the matrix and the small fractures. However, this simplification, in combination with the fact that there is already a restriction originating from the cell size used in the model, limits the amount of detail that can be included into the model. In such cases, the simulation of larger conduits (cave networks) may already be sufficient to represent the affection these networks can have to general groundwater flow regime. Finally, building a spatially distributed model can, in most cases, be a better way to simulate karstic aquifers than using lumped models, which may be better at matching observed and simulated parameter values, but give no information about the flow conditions in the aquifer.

5 Concluding remarks

The concluding remarks of the present study can be summarized as follows:

For the lack of background data, a primary investigation was performed in the aquifer systems of Lavrio. Results show that there is a deficit in the water demand coming from the qualitative depletion of the groundwater resources in the area. The characteristics of the two main aquifers in the area (alluvial and karstic) have been investigated and have provided the input for the modelling activities that followed.

The climate of the area is characterized as semi arid. This, in addition to the fact that the regional geology is largely consisted of formations with no hydrogeological interest (schists), has led to the overexploitation of the aquifers and the deterioration of the groundwater quality due to seawater intrusion. At present, the exploitation of the aquifers is minor but the groundwater quality is still poor. The lack of surface water is also an aspect of that same problem, leading the population to import water for using for all needs (fresh water supply, agriculture etc.), having an effect also in the local economy.

The hydrogeological boundaries of the two aquifers have been defined, with the case of the karstic aquifer having significant importance for the water balance of the area. The two main aquifers are hydraulically connected, with the connection not being straightforward and varying in space and time. In most areas, the karstic aquifer, having a much larger extent and groundwater potential, feeds the alluvial one. This process is most probably also the reason why there is still saline water found in the alluvial aquifer, although the hydraulic gradient is always positive in the aquifer. Both aquifers finally discharge to the adjacent sea.

Due to its importance for the local system, there was some special focus on the karstic aquifer. A set of pumping test data was re-evaluated to acquire information about the hydraulic properties of the aquifer. The response of the aquifer to the test, but also to the various rain events, was irregular. The reason for that is that the karstification degree of the formation is high and the water flows in preferential flow paths that are not linear.

The characteristics of the alluvial aquifer have been delineated with the use of geophysical and drilling techniques. An estimation of the amount of rainwater that reaches the aquifer as recharge has provided information about the volumes of water that are accumulating in the aquifers.

The chemical imprint of the groundwater (major ions and isotopes) is also highly affected by the process of seawater intrusion in both aquifers. The high concentrations of seawater related ions (mainly Cl^-) are the main reason for the deterioration of groundwater quality.

All the data collected either from the literature review, available databases or in the field formed the input for the regional groundwater flow numerical model that was developed. The model involved both aquifers in Lavrio and all the information about the geometry was implemented. The boundary conditions used included all the hydrological processes taking place at the hydrosystem.

The sensitivity analysis of the models, which was based on statistical methods, showed that the most important components of the system are the recharge and the storage capacity of the karstic aquifer, along with the amount of water that is pumped from the alluvial aquifer for irrigation purposes. These parameters were primarily used in the parameter estimation process to calibrate the model and evaluate the results.

The developed model was also used to test the performance of various boundary conditions and how well they represent the coast. Subsidiary models were developed, differing only in that aspect. Results show that when head dependent boundary conditions are used the model manages to simulate the system dynamics much more adequately than when using specified head boundaries.

The model, although using a traditional MODFLOW approach also for the karstic aquifer, manages to simulate the response of the karstic aquifer at a satisfactory level. An insight is also given to the hydraulic connection of the two aquifers, where it is concluded that the karstic aquifer primarily feeds the alluvial one, although this general figure can change locally.

For the purpose of focusing on the processes taking place in the karstic aquifer, the previously developed model formed that base for moving on to a karst explicit model. Apart from that, the aim was also to highlight which parameters are the most important when developing such models. Alterations that aimed to refine the parent model and make it appropriate for use were performed.

The model was also fed with data about the characteristics of the fractures in Lavrio. The data were collected in the field using two different methods. Various features of the fractures were recorded in many locations and used. The geometry of the fractures was also introduced in the model, so the representation of the karstic processes is adequate in the model.

A series of sensitivity analyses were performed in the model for the karstic aquifer. The aim was to highlight the most important parameters that are crucial for the model. The diameters of the conduits used in the model, along with the vertical hydraulic conductivities were the parameters that had the highest sensitivities. According to that, the data that is crucial for such models can be collected when similar modelling applications are developed.

References

Abusaada M, Sauter M (2013): Studying the flow dynamics of a karst aquifer system with an equivalent porous medium model, Groundwater, Vol. 51, No. 4, pp. 641-650

Alexakis D (2002): The effect of geological and anthropogenic factors on the quality and chemical composition of groundwater in East Attica. Ph.D. thesis, National and Kapodistrian University of Athens, Athens, Greece (in Greek)

Alexakis D (2011): Diagnosis of stream sediment quality and assessment of toxic element contamination sources in East Attica, Greece. Environ Earth Sci 63:1369–1383

Allen R, Pereira L, Raes D, Smith M (1998): Crop evapotranspiration— guidelines for computing crop water requirements, FAO Irrigation and Drainage, Paper No. 56, FAO, Rome, 300

Amir N, Kafri U, Herut B, Shalev E (2013): Numerical simulation of submarine groundwater flow in the coastal aquifer at the palmahim area, the Mediterranean coast of Israel, Water Resour Manage, 27:4005–4020, DOI 10.1007/s11269-013-0392-2

Andreo B, Vías J, Durán JJ, Jiménez P, López-Geta JA, Carrasco F (2008): Methodology for groundwater recharge assessment in carbonate aquifers: application to pilot sites in southern Spain, Hydrogeology Journal, 16: 911–925 DOI 10.1007/s10040-008-0274-5

Apostolopoulos G, Kallioras A, Pavlopoulos K, Stathopoulou K, Vlassopoulou A (2014): Reconnaissance geophysical survey for the detection of salinization and stratigraphy in Thorikos valley, Attica, Greece, 20th European Meeting of Environmental and Geophysics of the Near Surface Geoscience Division of EAGE, Athens, Greece, 14-18 September 2014

Aquilina L, Ladouche B, Dörflige N (2005): Recharge processes in karstic systems investigated through the correlation of chemical and isotopic composition of rain and spring-waters, Applied Geochemistry, 20, pp. 2189–2206, doi:10.1016/j.apgeochem.2005.07.011

Avdis V (1990): A reinterpretation of the geology of the Atticocycladic Massif (Greece). Geol Bull Turk 33:83–94

Bajocco S, De Angelis A, Salvati L (2012):A satellite-based green index as a proxy for vegetation cover quality in a Mediterranean region. Ecol Ind 23:578–587

Bakker M., Schaars F., Hughes J.D., Langevin C.D., Dausman A.M. (2013): Documentation of the seawater intrusion (SWI2) package for MODFLOW: U.S. Geological Survey Techniques and Methods, book 6, chap. A46, 47 p., http://pubs.usgs.gov/tm/6a46/

Barbieri M, Boschetti T, Petitta M, Tallini M (2005): Stable isotope (2H, 18O and 87Sr/86Sr) and hydrochemistry monitoring for groundwater hydrodynamics analysis in a karst aquifer

(Gran Sasso, Central Italy), Applied Geochemistry, 20, pp. 2063–2081, doi:10.1016/j.apgeochem.2005.07.008

Barker JA (1988): A generalized radial flow model for hydraulic tests in fractured rock. Water Resour Res 24(10):1796–1804

Baziotis IP (2008): Petrology and geochemistry of the metamorphic formations of Attica. Ph.D. Thesis, National Technical University of Athens, Athens, Greece (in Greek)

Baziotis I, Mposkos E (2011): Origin of metabasites from upper tectonic unit of the Lavrion area (SE Attica, Greece): geochemical implications for dual origin with distinct provenance of blueschist and greenschist's protoliths. Lithos 126:161–173

Baziotis I, Proyer A, Mposkos E (2009): High-pressure/low-temperature metamorphism of basalts in Lavrion (Greece): implications for the preservation of peak metamorphic assemblages in blueschists and greenschists. Eur J Mineral 21:133–148

Berger A, Schneider DA, Grasemann B, Stockli D (2013): Footwall mineralization during Late Miocene extension along the West Cycladic Detachment System, Lavrion, Greece. Terra Nova, 25(3):181–191

Binet S, Joigneaux E, Pauwels H, Albéric P, Fléhoc C, Bruand A (2017): Water exchange, mixing and transient storage between a saturated karstic conduit and the surrounding aquifer: Groundwater flow modeling and inputs from stable water isotopes, Journal of Hydrology, 544, pp. 278–289, http://dx.doi.org/10.1016/j.jhydrol.2016.11.042

Chalikakis K, Plagnes V, Guerin R, Valois R, Bosch FP (2011): Contribution of geophysical methods to karst-system exploration: an overview, Hydrogeology Journal, 19: 1169–1180, DOI 10.1007/s10040-011-0746-x

Chang CM, Yeh HD (2010): Spectral approach to seawater intrusion in heterogeneous coastal aquifers, Hydrology and Earth System Sciences, 14, pp 719 – 727, doi:10.5194/hess-14-719-2010

Chow V T (1959): Open-channel hydraulics, Mc Graw-Hill, New York

Cobaner M, Yurtal R, Dogan A, Motz LH (2012): Three dimensional simulation of seawater intrusion in coastal aquifers: A case study in the Goksu Deltaic Plain, Journal of Hydrology, 464–465, pp. 262–280

COMSOL(2018): Introduction to COMSOL Multiphysics, Vesrion COMSOL 5.4, COMSOL AB

Custodio E. (2010): Coastal aquifers of Europe: an overview, Hydrogeology Journal, 18, pp 269-280, DOI 10.1007/s10040-009-0496-1

Daskalaki P, Voudouris K (2008): Groundwater quality of porous aquifers in Greece: a synoptic review. Environ Geol 54:505–513. https ://doi.org/10.1007/s0025 4-007-0843-2

Datta B., Vennalakanti H., Dhar A. (2009): Modeling and control of saltwater intrusion in a coastal aquifer of Andhra Pradesh, India, Journal of Hydro-Environment Research, 3, pp 148 – 159, https://doi.org/10.1016/j.jher.2009.09.002

De Filippis G., Foglia L., Giudici M., Mehl S., Margiotta S., Negri S.L. (2016): Seawater intrusion in karstic, coastal aquifers: Current challenges and future scenarios in the Taranto area (southern Italy), Science of the Total Environment, 573, pp 1340 – 1351, https://doi.org/10.1016/j.scitotenv.2016.07.005

De Filippis G., Foglia L., Giudici M., Mehl S., Margiotta S., Negri S.L. (2017): Effects of different boundary conditions on the simulation of groundwater flow in a multi-layered coastal aquifer system (Taranto Gulf, southern Italy), Hydrogeology Journal, DOI 10.1007/s10040-017-1589-x

Diersch HJG (2005): FeFlow finite element subsurface flow and transport simulation system. Reference manual, Berlin, Germany: WASY GmbH

El Yaouti F, El Mandour A, Khattach D, Kaufmann O (2008): Modelling groundwater flow and advective contaminant transport in the Bou-Areg unconfined aquifer (NE Morocco), Journal of Hydro-environment Research 2, 192-209, doi:10.1016/j.jher.2008.08.003

Fleury P, Plagnes V, Bakalowicz M (2007): Modelling of the functioning of karst aquifers with a reservoir model: Application to Fontaine de Vaucluse (South of France), Journal of Hydrology, 345, pp. 38–49, doi:10.1016/j.jhydrol.2007.07.014

Ford D, Williams P (2007): Karst hydrogeology and geomorphology. Wiley, Chichester

Gat JR (1971): Comments on the stable isotope method in regional groundwater investigations. Water Resour Res 7(4):980–993

Geyer T, Birk S, Reimann T, Dörfliger N, Sauter M (2013): Differentiated characterization of karst aquifers: some contributions, Carbonates Evaporites, 28:41–46, DOI 10.1007/s13146-013-0150-9

Gossel W, Sefelnasr A, Wycisk R (2010): Modelling of paleo-saltwater intrusion in the northern part of the Nubian Aquifer System, Northeast Africa, Hydrogeology Journal, 18: 1447–1463, DOI 10.1007/s10040-010-0597-x

Guardiola-Albert C, Martos-Rosillo S, Pardo-Iguzquiza E, Duran Valsero JJ, Pedrera A, Jimenez-Gavilan P, Linan Baena C (2014): Comparison of recharge estimation methods during a wet period in a karst aquifer, Groundwater, doi: 10.1111/gwat.12310

Hanson RT, Schmid W, Faunt CC, Lear J, Lockwood B (2014): Integrated hydrologic model of Pajaro Valley, Santa Cruz and Monterey Counties. U.S. Geological Survey Scientific Investigations Report 2014–5111, California.https ://doi.org/10.3133/sir20 14511 1

Harbaugh AW (2005): MODFLOW-2005, The U.S. Geological Survey modular ground-water model—the Ground-Water Flow Process: U.S. Geological Survey Techniques and Methods 6-A16, variously p

Hartmann A, Wagener T, Rimmer A, Lange J, Brielmann H, Weiler M (2013): Testing the realism of model structures to identify karst system processes using water quality and quantity signatures, Water Resources Research, Vol. 49, 3345–3358, doi:10.1002/wrcr.20229

Hartmann A, Gleeson T, Rosolem R, Pianosi F, Wada Y, Wagener T (2015): A large-scale simulation model to assess karstic groundwater recharge over Europe and the Mediterranean, Geosci. Model Dev., 8, pp. 1729–1746, doi:10.5194/gmd-8-1729-2015

Healy RW, Cook PG (2002): Using groundwater levels to estimate recharge. Hydrogeol J 10:91–109. https ://doi.org/10.1007/s10040-001-0178-0

Hill MC, Tiedman CR (2007): Effective groundwater model calibration, 978 John Wiley & Sons Inc., Hoboken, New Jersey

IAEA (2016): Helliniko airport data. http://www-naweb .iaea.org/napc/ih/IHS_resou rces_gnip.html. Accessed 10 Oct 2016

IGME (2003): Koropi-Plaka sheet, Geological map of Greece, 1:50.000, Athens

IGME (2007): Lavrio sheet, Geological map of Greece, 1:50.000, Athens

Javadi A, Hussain M, Sherif M, Farmani R (2015): Multi-objective Optimization of Different Management Scenarios to Control Seawater Intrusion in Coastal Aquifers, Water ResourcesManagement, 29, pp 1843-1857, DOI 10.1007/s11269-015-0914-1

Jeannin PY, Eichenberger U, Sinreich M, Vouillamoz J, Malard A, Weber E (2013): KARSYS: a pragmatic approach to karst hydrogeological system conceptualisation. Assessment of groundwater reserves and resources in Switzerland, Environ Earth Sci, 69:999–1013, DOI 10.1007/s12665-012-1983-6

Kacimov AR, Sherif MM (2006): Sharp interface, one-dimensional seawater intrusion into a confined aquifer with controlled pumping: Analytical solution, Water Resources Research, 42, W06501, doi:10.1029/2005WR004551

Kakavogiannis E (2005:) Metals worked and forgiven; the organizingand exploitation of ore deposits at Lavreotiki from the Atheniandemocracy, Ministry of Culture (in Greek)

Kallioras A, Pliakas F, Diamantis I (2010): Simulation of groundwater flow in a sedimentary aquifer system subjected to overexploitation, Water Air Soil Pollut, 211:177–201, DOI 10.1007/s11270-009-0291-6

Kargas G, Kerkides P, Poulovassilis A (2012): Infiltration of rain water in semi-arid areas under three land surface treatments. Soil Tillage Res 120:15–24

Kaufmann G(2016): Modelling karst aquifer evolution in fractured, porous rocks, Journal of Hydrology, 543, pp. 796–807, http://dx.doi.org/10.1016/j.jhydrol.2016.10.049

Kolditz O, Shao H, Wang W, Bauer S (2015): Thermo-Hydro-Mechanical-Chemical Processes in Fractured Porous Media: Modelling and Benchmarking – Closed-Form Solutions, DOI: 10.1007/978-3-319-11894-9, ISBN: 978-3-319-11893-2, Springer International Publishing

Koumantakis I, Panagopoulos A, Markantonis K, Papaioannou N, Vasileiou E, Tsoutsos I (2000): Technical report on hydrogeological conditions. In: Environmental restoration of the Lavrion Technical and Cultural Park (LTCP), National Technical University of Athens, Greece (in Greek)

Kourakos G, Mantoglou A (2015): An efficient simulation-optimization coupling for management of coastal aquifers, Hydrogeology Journal, 23, pp 1167 – 1179, DOI 10.1007/s10040-015-1293-7

Koussis AD, Mazi K, Destouni G (2012): Analytical single-potential, 1000 sharp-interface solutions for regional seawater intrusion in sloping unconfined coastal aquifers, with pumping and recharge, Journal of Hydrology, 416 – 417, pp 1 – 11, doi:10.1016/j.jhydrol.2011.11.012

Langevin CD, Thorne DT Jr, Dausman AM, Sukop MC, Guo W (2008): SEAWAT Version 4: A Computer Program for Simulation of Multi-Species Solute and Heat Transport: U.S. Geological Survey Techniques and Methods Book 6, Chapter A22, 39 p.

Langevin CD, Zygnerski M (2013): Effect of Sea-Level Rise on Salt Water Intrusion near a Coastal Well Field in Southeastern Florida, Groundwater, 51 (5), pp 781 – 803, doi: 10.1111/j.1745- 6584.2012.01008.x

Levanon E, Yechieli Y, Gvirtzman H, Shalev E (2017): Tide-induced fluctuations of salinity and groundwater level in unconfined aquifers – Field measurements and numerical model, Journal of Hydrology, 551, pp. 665–675, http://dx.doi.org/10.1016/j.jhydrol.2016.12.045

Liati A, Skarpelis N, Pe-Piper G (2009): Late Miocene magmatic activity in the Attic-Cycladic Belt of the Aegean (Lavrion, SE Attica, Greece): implications for the geodynamic evolution and timing of ore deposition. Geol Mag 146(5):732–742

Liati A, Skarpelis N, Fanning MC (2013): Late Permian-Early Triassic igneous activity in the Attic Cycladic Belt (Attica): new geochronological data and geodynamic implications. Tectonophysics595–596:140–147

Liedl R, Sauter M, Hückinghaus D, Clemens T, Teutsch G (2003): Simulation of the development of karst aquifers using a coupled continuum pipe flow model, Water Resources Research, Vol. 39, No. 3, 1057, doi:10.1029/2001WR001206

Lin J, Snodsmith B, Zheng C, Wu J (2009): A modeling study of seawater intrusion in Alabama Gulf Coast, USA, Environmental Geology, 59, pp 119 – 130, DOI 10.1007/s00254-008-1288-y

Lu C, Werner AD, Simmons CT, Luo J (2015): A Correction on Coastal Heads for Groundwater Flow Models, Groundwater, 53 (1), pp 164 – 170, doi: 10.1111/gwat.12172

Malard A, Jeannin PY, Vouillamoz J, Weber E (2015): An integrated approach for catchment delineation and conduit-network modeling in karst aquifers: application to a site in the Swiss tabular Jura, Hydrogeology Journal, 23: 1341–1357, DOI 10.1007/s10040-015-1287-5

Mantoglou A (2003): Pumping management of coastal aquifers using analytical models of saltwater intrusion, Water Resources Research, 39 (12), doi:10.1029/2002WR001891

Marinos G, Petrascheck WE (1956): Geologic map of the Laurium metalliferous area. Institute of Geology and Subsurface Research, Athens

Matiatos I (2010): Hydrogeological and isotopic investigations at regions of the Argolis peninsula. Ph.D. thesis, National and Kapodistrian University of Athens, Athens, Greece (in Greek)

Mayaud C, Walker P, Hergarten S, Birk S (2015): Nonlinear flow process: A new package to compute nonlinear flow in MODFLOW, Groundwater, Vol. 53, No. 4, pp. 645–650, doi: 10.1111/gwat.12243

McDonald MG, Harbaugh AW (1988): A modular three-dimentional finite-difference ground-water flow modelTechniques of Water-Resources Investigations, Book 6, Chapter A1, variously p

Montiel D, Dimova N, Andreo B, Prieto J, García-Orellana J, Rodellas V (2018): Assessing submarine groundwater discharge (SGD) and nitrate fluxes in highly heterogeneous coastal karst aquifers: Challenges and solutions, Journal of Hydrology, 557, pp. 222–242, https://doi.org/10.1016/j.jhydrol.2017.12.036

Moussoulis E, Mallinis G, Koutsias N, Zacharias I (2015): Modelling surface runoff to evaluate the effects of wildfires in multiple semi-arid, shrubland-dominated catchments, Hydrol. Process. 29, pp. 4427–4441, DOI: 10.1002/hyp.10509

Nastos PT, Politi N, Kapsomenakis J (2013): Spatial and temporal variability of the Aridity Index in Greece. Atmos Res 119:140–152

Oehlmann S, Geyer T, Licha T, Birk S (2013): Influence of aquifer heterogeneity on karst hydraulics and catchment delineation employing distributive modeling approaches, Hydrol. Earth Syst. Sci., 17, 4729–4742, doi:10.5194/hess-17-4729-2013

Panagopoulos G(2012): Application of MODFLOW for simulating groundwater flow in the Trifilia karst aquifer, Greece, Environ Earth Sci, 67:1877–1889, DOI 10.1007/s12665-012-1630-2

Paparrizos S, Maris F, Matzarakis A (2014): Estimation and comparison of potential evaportanspiration based on daily and monthly data from Sperchios valley in central Greece, Global NEST Journal, Vol 16, No 2, pp 204-217

Pavlopoulos K (1997): Geomorphological evolution of southern Attica, GAIA No 2, National and Kapodistrian University of Athens, Athens, Greece (in Greek, with extensive summary in English)

Petalas C, Pisinaras V, Gemitzi A, Tsihrintzis VA, Ouzounis K (2009): Current conditions of saltwater intrusion in the coastal Rhodope aquifer system, northeastern Greece. Desalination 237:22–41,https ://doi.org/10.1016/j.desal .2007.12.020

Photiades A, Carras N (2001): Stratigraphy and geological structure of the Lavrion area Attica, Greece). Bull Geol Soc Greece 34(1):103–109

Poeter EP, Hill MC, Banta ER, Mehl S, Christensen S (2005): UCODE_2005 and Six Other Computer Codes for Universal Sensitivity Analysis, Calibration, and Uncertainty Evaluation: U.S. Geological Survey Techniques and Methods 6-A11, 283p.

Poeter EP, Hill MC, Lu D, Tiedeman CR, Mehl S (2014):UCODE_2014, with new capabilities to define parameters unique to predictions, calculate weights using simulated values, estimate parameters with SVD, evaluate uncertainty with MCMC, and more: Integrated Groundwater Modeling Center Report Number GWMI 2014-02

Pouliaris C, Perdikaki M, Foglia L, Schüth C, Kallioras A (2018): Hydrodynamic analysis of a Mediterranean aquifer system with the use of hydrochemical and isotopical analysis as supporting tools, Environmental Earth Sciences, 77:237, https://doi.org/10.1007/s12665-018-7418-2

Praamsma T, Novakowski K, Kyser K, Hall K (2009): Using stable isotopes and hydraulic head data to investigate groundwater recharge and discharge in a fractured rock aquifer, Journal of Hydrology, 366,pp. 35–45, doi:10.1016/j.jhydrol.2008.12.011

Qahman K, Larabi A (2006): Evaluation and numerical modeling of seawater intrusion in the Gaza aquifer (Palestine), Hydrogeology Journal, 14, pp 713 – 728, https://doi.org/10.1007/s10040-005-1047 003-2

Reilly TE, Harbaugh AW (2004): Guidelines for evaluating ground-water flow models: U.S. Geological Survey Scientific Investigations Report 2004-5038, 30 p.

Romanazzi A, Gentile F, Polemio M (2015): Modelling and management of a Mediterranean karstic coastal aquifer under the effects of seawater intrusion and climate change, Environmental EarthSciences, 74, pp 115 – 128, DOI 10.1007/s12665-015-4423-6

Rozos E, Koutsoyiannis D(2006): A multicell karstic aquifer model with alternative flow equations, Journal of Hydrology, 325, pp. 340–355, doi:10.1016/j.jhydrol.2005.10.021

Sefelnasr A, Sherif M(2014): Impacts of seawater rise on seawater intrusion in the Nile Delta aquifer, Egypt, Groundwater, Vol. 52, No. 2, pp. 264–276, doi: 10.1111/gwat.12058

Scanlon BR, Healy RW, Cook PG (2002): Choosing appropriate techniques for quantifying groundwater recharge, Hydrogeol J, 10:18–39, https ://doi.org/10.1007/s1004 0-00101 76-2

Scheffer C, Vanderhaeghe O, Lanari P, Tarantola A, Ponthus L, Photiades A, France L (2015): Syn- to post-orogenic exhumation of metamorphic nappes: structure and thermobarometry of the western Attic-Cycladic metamorphic complex (Lavrion, Greece). J Geodyn 96:147–193

Shoemaker BW (2004): Important Observations and Parameters for a Salt Water Intrusion Model, Groundwater, 42 (6), pp 829 – 840

Shoemaker W.B., Kuniansky E.L., Birk S., Bauer S., Swain E.D. (2007): Documentation of a Conduit Flow Process (CFP) for MODFLOW-2005: U.S. Geological Survey Techniques and Methods, Book 6, Chapter A24, 50 p.

Siarkos I, Latinopoulos P (2016): Modeling seawater intrusion in overexploited aquifers in the absence of sufficient data: application to the aquifer of Nea Moudania, northern Greece. Hydrogeol J 24:2123–2141. https ://doi.org/10.1007/s1004 0-016-1455-2

Skarpelis N (2007): The Lavrion deposit (SE Attica, Greece): geology, mineralogy and minor elements chemistry. Neues Jahrbuch Mineralogie Abhandlungen 183(3):227–249

Skarpelis N, Argyraki A (2009): Geology and origin of the supergene ore at the Lavrion Pb–Ag–Zn deposit, Attica, Greece. Resour Geol 59(1):1–14

Skarpelis N, Tsikouras B, Pe-Piper G (2008): The Miocene igneous rocks in the Basal Unit of Lavrion (SE Attica, Greece): petrology and geodynamic implications. Geol Mag 145(1):1–15

Stamatis G, Voudouris K, Karefilakis F (2001): Groundwater pollution by heavy metals in historical mining area of Lavrio, Attica Greece. Water Air Soil Pollut 128:61–83

Sun A, Painter S, Green R (2005): Modeling Barton Springs Segment of the Edwards Aquifer using MODFLOW-DCM. In: Beck, B.F. (Ed.), Sinkholes and the Engineering and Environmental Impacts of Karst, Amer. Soc. Civil Engineers, Geotech. Spec. Publ., No. 144, pp. 163–177.

Szymkiewicz A, Gumuła-Kawęcka A, Šimůnek J, Leterme B, Beegum S, Jaworska-Szulc B, Pruszkowska-Caceres M, Gorczewska-Langner W, Angulo-Jaramillo R, Jacques D (2018): Simulations of freshwater lens recharge and salt/freshwater interfaces using the HYDRUS and SWI2 packages for MODFLOW, Journal of Hydrology and Hydromechanics, 66 (2), pp 246-256, DOI: 10.2478/johh-2018-1071 0005

Tsokas GN, Stampolidis A, Angelopoulos AD, Kilias S (1998): Analysis of potential field anomalies in Lavrion mining area, Greece. Geophysics 63(6):1965–1970

Voudouris KS, Lambrakis N, Papatheothorou G, Daskalaki P (1997): An Application of Factor Analysis for the Study of the Hydrogeologicai Conditions in Plio-Pieistocene Aquifers of NW Achaia (NW Peloponnesus, Greece), Mathematical Geology, 29, 1, pp 43-59

Voudouris P, Melfos V, Spry PG, Bonsall T, Tarkian M, Economou-Eliopoulos M (2008): Mineralogical and fluid intrusion constraints on the evolution of the Plaka intrusion related ore system, Lavrion, Greece. Mineral Petrol 93:79–110

Worthington SRH(2009): Diagnostic hydrogeologic characteristics of a karst aquifer (Kentucky, USA), Hydrogeol J, 17: 1665–1678, DOI 10.1007/s10040-009-0489-0

Xu Z, Hu BX, Ming Y (2018): Numerical modeling and sensitivity analysis of seawater intrusion in a dual-permeability coastal karst aquifer with conduit networks, Hydrol. Earth Syst. Sci., 22, pp. 221–239, https://doi.org/10.5194/hess-22-221-2